



AUJUS

Auburn University Journal of Undergraduate Scholarship

Spring 2015 Volume 4

New for 2015:
Research
Highlights

Mentor of the Year:
Dr. Alan Wilson

AJJUS cover artwork by Amanda Butcher, a junior in the Graphic Design Program.

Amanda said, “This photo was taken by shining a Mag-Lite flashlight through a colander onto a wall. The circular forms were intended to convey a sense of motion or instability. Also, the overall form made me think of a giant arachnid, which not only had a biological appeal, but also could relate to the word ‘chimerical.’”

Table of Contents

2 | About the Editors

4 | AUJUS Advisory Board

5 | Letter from the Editors-in-Chief

6 | Mentor of the Year: Dr. Alan Wilson

Research Articles

8 | Medroxyprogesterone Acetate Reduced Cellular Proliferation of the Luminal and Glandular Epithelium in the Developing Canine Uterus

Katharyn Brennan, Robyn Wilborn, Meghan Davolt, Anne Wiley, Dori Miller, Paul Cooke, Aime Johnson, Bruce Smith, and Frank Bartol

14 | Detection of Pathogens from Biopsy by Use of Sortase Activity

Andrew Clark, Jiansheng Huang, and Peter Panizzi

21 | Diindolylmethane Inhibits the Activity of P-glycoprotein in 17-71 Canine B-Cell Lymphoid Tumor Cells

Ala Mansour, Kodye Abbott, Patrick Flannery, Elaine Coleman, Amit Tiwari, and Satyanarayana Pondugula

27 | Evaluating the Novel Role of Tryptophan 438 in Active Turnover of *Mycobacterium tuberculosis* Catalase-Peroxidase

Ethan McCurdy, Lauren Barr, Olive Njuma, Elizabeth Ndontsa, and Douglas Goodwin

33 | Password Storage in Databases: Best Practices

Robert Sanek

Research Highlights

40 | Brief summaries of student engagement in research

59 | About the Authors

61 | Call for AUJUS Submissions

About the Editors



Caroline Barr is a senior from Huntsville, Alabama pursuing a Bachelor of Arts in English with a minor in Journalism and is planning to pursue a MFA in Creative Writing following her graduation in May 2015. She plans on a future career in the publishing industry as an editor because she enjoys exploring the versatility of language in both academic research and creative writing projects. She serves as Copy Editor for the Glomerata and Director of Programs for the English Club, spent a summer studying abroad in London, and has had her creative work published in Auburn University's literary magazine, *The Circle*.



Connor Dobson is a junior pursuing a Bachelor of Science in Chemical Engineering with a specialty in Biomedical Engineering. He has been a cooperative education student in the Innovations Department at Noramco, Inc., in Athens, Georgia, a Johnson & Johnson site. His research interests include drug delivery and novel medical technologies. Under the guidance of Dr. Robert Arnold in the Harrison School of Pharmacy, Connor researches nanocomposite drug delivery systems for cancer therapy and diagnosis. He is also the founder and president of the Auburn chapter of the Biomedical Engineering Society. He plans to pursue a doctorate in Chemical Engineering.



Andrew Hill is a senior pursuing Bachelors of Science in both Physics and Computer Science. His research interests include network and distributed computing and computation on large data sets. He works as an undergraduate research assistant in the Auburn Parallel Architecture and System Laboratory (PASL) under the direction of Dr. Weikuan Yu. He is a member of the Phi Kappa Phi and Sigma Pi Sigma honor societies. In his free time, he enjoys reading, hiking, and drinking maté. In the future, he hopes to receive a doctorate in computer science.



Patrick Michael is a senior from Lexington, Kentucky pursuing a Bachelor of Science in Physics with a Pre-Medicine Concentration and minors in German and Economics. He will be attending medical school this fall after graduating in May 2015. He has been involved with promoting undergraduate research on Auburn's campus as the founder and first director of the SGA Undergraduate Research Board, inspired by his own experience with research in labs at the University of Kentucky Markey Cancer Center and the University of Chicago Department of Radiology. He is currently working towards completion of an Honors Thesis in the Auburn University Department of Physics.



Rachel Pipan is a senior pursuing a Bachelor of Arts in Public Relations with a minor in Business. Upon graduation in May 2015, Rachel begin a master's degree in Strategic Communication at American University in Fall 2015. Rachel's future goals include becoming the communications director for a nonprofit organization that seeks to empower women across the globe and using her public relations skills to increase the number of U.S. women who run for political office. She currently serves as the Communications Assistant for the Office of Undergraduate Research. Her hobbies include reading, hiking, and cooking for friends.



Ellen Rankins is a junior pursuing a Bachelor of Science in Animal Sciences – Equine Science. Her research focus is on equine movement under the guidance of Drs. Wagner and Weimar. Within the College of Agriculture, she is an officer and active member in both Agriculture Ambassadors and Block and Bridle. During her spare time, she can be found volunteering and teaching at Storybook Farm, a therapeutic riding center, where she is dedicated to bringing "Hope on Horseback" to their special riders.

AUJUS Advisory Board

Bonnie MacEwan

Dean
Libraries

Brian Thurow

Associate Professor
Aerospace Engineering

Dafni Greene

Advisor
Student Affairs

Ross Heck

Professor
Graphic Design

David Carter

Associate Professor
History

Donald Connor

Professor
Poultry Science

Dean Schwartz

Associate Professor
Anatomy, Physiology, and Pharmacy

Onikia Brown

Assistant Professor
Nutrition and Dietetics

Raymond Henry

Professor and Associate Dean for Research
College of Science and Mathematics

Frank Bartol

Professor and Associate Dean for Research and
Graduate Studies
College of Veterinary Medicine

AUJUS Editors-in-Chief

Margaret J. Marshall

Director of University Writing

Lorraine W. Wolf

Director of Undergraduate Research

AUJUS Production Team

Matthew M. Werner

Communications & Marketing
Specialist
Office of University Writing

Whitney Rains

Administrative Support
Associate
Office of University Writing

Betsy Dean

Communications & Marketing
Intern
Office of University Writing

Letter from the Editors-in-Chief

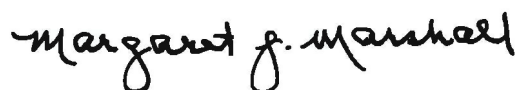
Experienced scholars understand that research is incomplete if it is not subjected to rigorous review by experts in the field and then made public. The *Auburn University Journal of Undergraduate Scholarship (AUJUS)* provides an opportunity for undergraduate students in any discipline to present their work for review and to share their work with a broad audience.

A publication such as this requires the support of the many faculty members who mentor undergraduates throughout the research process, the reviewers who read and comment on submissions, the student authors who revise and thereby improve the presentation of their work, the student associate editors who manage this process, and the graphic design team who produces the final layout and journal design. We are thankful to have the support of all these people and of the *AUJUS* Advisory Board who together help make *AUJUS* a yearly publication. We believe the selected articles clearly demonstrate that undergraduate students can make original and important scholarly contributions to their disciplines. We also believe that the student authors who submitted their work gain a deeper understanding of the research process.

This fourth edition of *AUJUS* showcases only a small fraction of the research done by undergraduate students and their faculty mentors, but it represents the extraordinary potential of Auburn students and their intellectual accomplishments. This year, we introduce a new feature, Research Highlights, that captures student research more broadly through short, non-technical summaries of their student work. For our upcoming fifth edition, we will be allowing submissions at any time during the academic year, with online publication as soon as the approximately eight-week review and revision process is complete. Once each year, we will print a subset of those articles and highlights previously accepted. As in the past, we welcome students of all disciplines to contribute their original research and creative scholarship for consideration. Those interested in serving as student associate editors or submissions reviewers are encouraged to contact us. We look forward to seeing what these new features and processes will teach us.



Lorraine W. Wolf
Director of Undergraduate Research
Professor of Geophysics



Margaret J. Marshall
Director of University Writing
Professor of English

Mentor of the Year: Dr. Alan Wilson



Dr. Alan Wilson

Fostering Undergraduate Research and Creative Scholarship, a prestigious award that rewards outstanding mentors of undergraduates. His record of excellent mentorship began when he pursued his master's degree in Fisheries and Wildlife at Michigan State University. "We had three undergraduates in my lab when I began my master's degree," said Wilson. "It was exciting to see them enthusiastic about the research and we continued to host three students every summer." Wilson's knack for undergraduate mentorship was evident – two of his original undergraduate research assistants went on to get master's degrees, and one will be graduating with a Ph.D. in aquatic ecology this year. "Some students have a spark," Wilson said. "With the right encouragement, it becomes a big fire."

Wilson has worked to fan that fire ever since, working with undergraduates during his Ph.D. program at Georgia Tech, his postdoc at the University of Michigan, and in his faculty position at Auburn University. While at Auburn University, he led a Research Experience for Undergraduates (REU) in aquatic ecology that was funded by the National Science Foundation. The focus of his research was to find ecosystem-friendly ways to reduce the number of algal blooms, which can negatively impact water quality. "I love seeing undergraduates be successful in the lab and head toward their careers," said Wilson. "Undergraduates bring energy to the lab – their exuberance is great."

Working with undergraduates is not without its challenges. "Some undergraduates are not a good fit,"

"Advisors should be more than class registration codes taped to a door," thought Dr. Alan Wilson as he walked past his advisor's office as an undergraduate student. Originally a pre-med student, Wilson had little guidance from mentors or advisors when he chose classes, or when he switched his major to ecology, much less advice on starting undergraduate research. His own dedication to undergraduates stems from a simple premise – he wants them to have more mentorship than he did at their age. "I didn't want to be a similar bad advisor to my students," said Wilson. "I work to engage undergraduates in research as best I can."

Wilson, who shares a joint appointment as an Associate Professor in Fisheries and Allied Aquacultures and Biological Sciences, was the 2014 recipient of the Provost's Award for Faculty Excellence in

Although I have moved on from Auburn University, my time there will persist in my mind as one of the best times of my life due to the professional growth and development, relationships, and unforgettable memories, due in no small part to the dedication, gregarious personality, and guidance of Dr. Wilson. His efforts have built something that will outlast the confines of that time and place. He has endowed 11 students the tools they need to be professional ecologists, and in doing so, developed a community of friends and future colleagues who will be environmental leaders across the country.

– Michael Moore
Auburn University



Dr. Alan Wilson (left) and Rachel Zitomer (right) set up a field experiment to see how the amount of nutrient fertilizer influenced the effect of fish consumers on phytoplankton primary producers.

said Wilson. “But students should know that not every research experience will work out, and it is good if not better, to learn about what you don’t want to do now. Going outside and getting into a pond isn’t for everybody.” Wilson’s lab, by his own admission, requires a lot of hard work and a willingness to get your hands dirty. “The best students, by far, were the pre-vet and animal sciences students. They dove right into the work,” said Wilson. For his REU, Wilson sought to find undergraduates early in their academic career. “That means I work with freshmen and sophomores, which is definitely more work because they don’t know much about research methods yet,” said Wilson. “However, because they’re so young, they could also fall in love with the research and work in the lab for years.” Wilson likes to bring undergraduates to research early because he believes it gives them valuable skills. “I would be a better researcher now if I had done undergraduate research,” said Wilson. “I know that.”

When seeking mentorship as an undergraduate, Dr. Wilson was met with a closed door. His undergraduate researchers have quite a different experience – they go to the lab, pull on their boots, and join Dr. Wilson in a pond to do their research. “At the end of the day, I’m glad I get to work with students,” said Wilson. “But we need to get better about engaging all undergraduates in research. We all need to do better.”

Wilson’s dedication to undergraduates was rewarded last year when he won the Provost’s award for undergraduate mentorship. “I suspect this will be the most meaningful award I’ll get while working at Auburn University,” said Wilson. “It’s important to me, but it also shows that Auburn University cares about people who care about engaging undergraduates in research.”

Wilson is now on leave from Auburn, working at the National Science Foundation on a temporary appointment as a program director for the Population and Community Ecology program. “Now I get to see the other side of hosting REUs,” said Wilson. “After I finish my appointment, I will be able to help my colleagues at Auburn and other schools navigate the process of finding funding for their own undergraduate research projects,” said Wilson.

Medroxyprogesterone Acetate Reduced Cellular Proliferation of the Luminal and Glandular Epithelium in the Developing Canine Uterus

Katharyn Brennan, Robyn Wilborn, Meghan Davolt, Anne Wiley, Dori Miller, Paul Cooke, Aime Johnson, Bruce Smith, and Frank Bartol

ABSTRACT

The uterine gland knockout (UGKO) phenotype was produced in both sheep and mice by strategic administration of progestins to neonates from birth (Postnatal Day = PND 0). Adult UGKO animals lack uterine glands and cannot support pregnancy. Induction of the UGKO phenotype in dogs would provide a means of inducing sterility non-surgically. In the dog, uterine gland development begins during the first week of neonatal life and progesterone receptors are present in uterine tissue at this time. The objectives of this study were to determine the effects of neonatal progestin treatment on canine uterine gland development. Seven mixed breed puppies were given either medroxyprogesterone acetate (MPA; $n=3$) (10mg/kg body weight, i.m.) or an equal volume of sterile saline ($n=4$) at PND 5 and again once birth weight had tripled. Gland penetration measurements were obtained from uterine cross-sections which were stained

with Hematoxylin and imaged using the Aperio® Imaging system. Additionally, uterine cross-sections were stained with POPO-1 to visualize cell nuclei and immunohistochemically stained for cytokeratin 8 (CK8), an epithelial marker, and proliferating cell nuclear antigen (PCNA), a marker of cell proliferation. Primary antibodies were localized using fluorochrome-labeled secondary antibodies in order to produce target-specific signals at defined emission wavelengths. Images were obtained using the Nuance FX® multispectral imaging system and spectrally unmixed images were analyzed using Cell Profiler™ and Cell Profiler Analyst™. Quantitative data were subjected to analyses of variance. No effects of treatment on uterine gland penetration depth were identified. However, a treatment by cell-compartment interaction was detected ($P < 0.01$) for PCNA labeling index, with the luminal and glandular epithelium experiencing reductions in cell proliferation. While uterine gland development

was not completely abolished, MPA significantly reduced cell proliferation within glandular and luminal epithelial cells, indicating that manipulation of uterine development in the canine may be possible with further investigation.

INTRODUCTION

Millions of companion animals are euthanized each year (Olson, 1993) and companion animal overpopulation poses a threat to the quality of life for animals as well as the health of humans (Fournier, 2005). Currently the most effective means of population control is sterilization surgery (Kutzler, 2006). Surgery can be costly, inconvenient, requires specialized and sterilized equipment, and comes with a certain degree of morbidity and, less commonly, mortality. Thus, discovering a method to induce sterility non-surgically in companion animals is an area of great interest.

Uterine gland development, or adenogenesis, in the dog

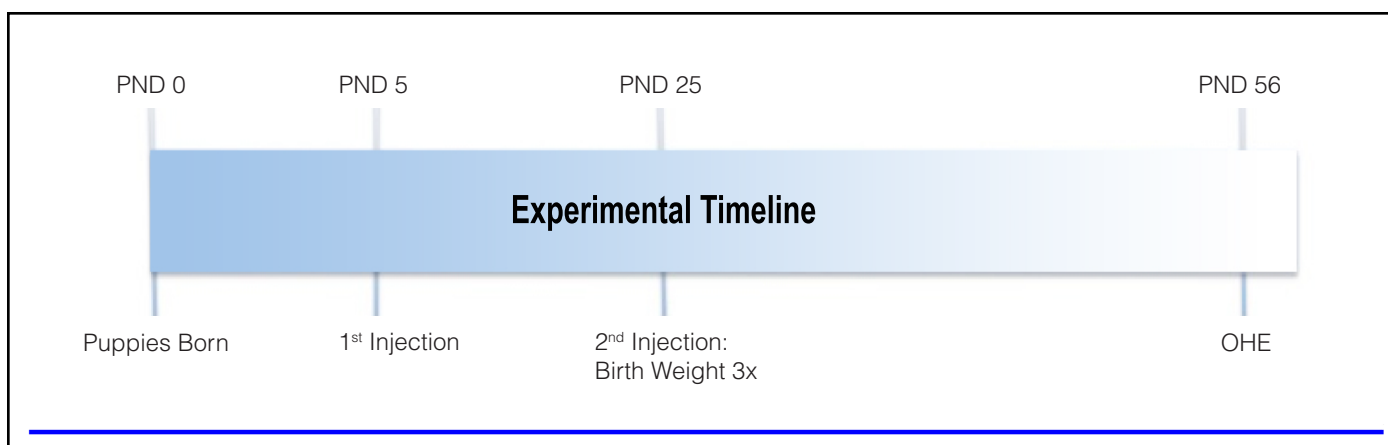


Figure 1. Experimental timeline. The first MPA injection (10 mg/kg BW, i.m.) was given on postnatal day (PND) 5 (PND 0 = birth). The second injection was given when birth weight tripled (mean of PND 25 for all puppies). Animals underwent ovariectomy (OHE) on PND 56.

begins within the first week of life and is complete by 6 weeks of age (Cooke, 2012). During the pre-pubertal time period, there should be no endogenous steroid hormones (i.e., estrogen or progesterone) in circulation. Exposure of neonatal sheep and mice to progesterone or progesterone-like compounds (collectively called progestins) has been successfully used to induce the uterine gland knockout (UGKO) phenotype (Bartol, 1999; Cooke, 2012). Uterine glands secrete critical substances that support fetal growth during pregnancy (Gray, 2001) and adult UGKO animals cannot support pregnancy due to their aglandular phenotype (Bartol, 1999; Cooke, 2012). Developing a UGKO phenotype in the dog would potentially provide the means to induce sterility without the need for surgery.

The presence of progesterone and estrogen receptors have been

demonstrated in the canine uterus at seven days of age (when uterine gland development begins in this species) and these receptors continue to be expressed until six weeks of age (Cooke, 2012). Medroxyprogesterone acetate (MPA) is a synthetic progestin that is bioactive in the dog (Beijerink, 2007). Previous research looking at MPA exposure in the female dog has been focused on studying long-term effects of MPA exposure as a means to control reproductive cyclicity in adult females (Von Berky, 1993). However, there is very little information regarding the use of MPA in juvenile dogs. Although previous MPA studies in dogs did not examine neonatal exposure, they did provide critical dosage information to help ensure that deleterious effects were not observed later in the puppies from this experiment (Smith, 1993).

Given that uterine gland development in the dog begins

within the first week of life and given that MPA has been shown to act as a bioactive progestin in the dog, the objective of this experiment was to determine the effects of neonatal MPA treatment on uterine gland development and cell proliferation in the canine uterus. It was hypothesized that neonatal MPA treatment during a critical developmental time period would alter normal uterine development and specifically would inhibit the development of uterine glands. Changes in uterine histology with respect to uterine glands and cell proliferation were analyzed to determine the effects of MPA treatment in neonatal canine uterine tissue.

METHODS

Animals, MPA Administration, and Assay

Seven mixed breed puppies from three litters were used in this study. There were three MPA-treated animals and four

controls. Beginning at PND 5, puppies were given either MPA (10mg/kg body weight, i.m.) or an equal volume of sterile saline. Because neonatal puppies grow at an exponential rate, the MPA dose was repeated once birth weight had tripled (between 2-3 weeks of age) (Figure 1). Following ovariectomy (OHE) at PND 56, puppies were monitored for 10 days under the care of a veterinarian and then adopted out to permanent homes.

Serial blood samples of 1-1.5 mL were obtained via jugular venipuncture on PND 5 prior to treatment (baseline) and then subsequently 14, 20, 28, 42 and 49 days post-treatment to determine serum MPA concentration. Serum samples were stored at -80°F and then serum levels of MPA were measured by a conventional radioimmunoassay (RIA) method using commercial kits (Immunometrics Ltd.; London, UK). Serum samples were diluted with 0.9% NaCl at a ratio of 1:10 prior to assay. The RIA method is an extraction type RIA and utilizes tritium-labeled (3H)-MPA as a tracer and the specific anti-MPA polyclonal antibody produced in New Zealand rabbits. MPA in serum samples was extracted with diethyl ether. The solvent containing the extracted MPA was evaporated to dryness and reconstituted with the assay buffer. The residue was dissolved and incubated with tracer and antibody overnight. Bound and free steroids were separated

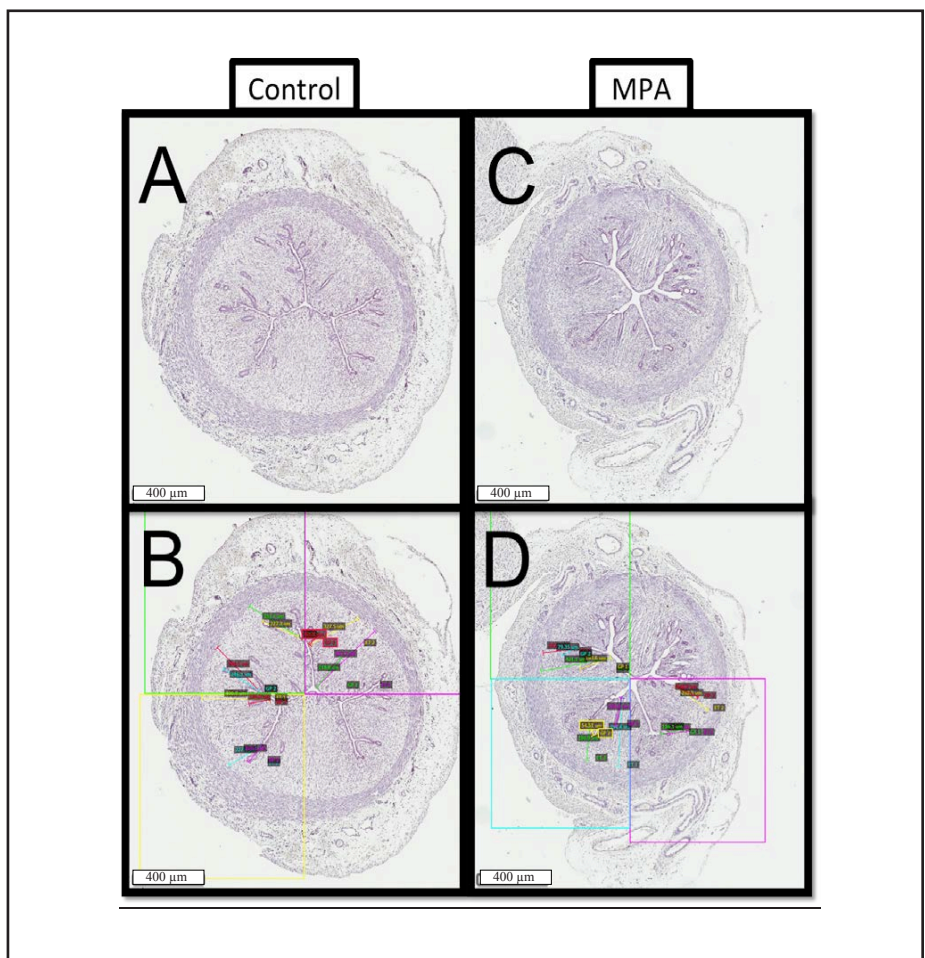


Figure 2. Uterine cross-sections obtained via OHE on PND 56, stained with hematoxylin and imaged using the Aperio® imaging system. Shown are representative tissues from control (left; panels A, B) and MPA-treated (right; panels C, D) females. Boxes B & D illustrate how data for gland penetration were obtained; note quadrant divisions and the multi-colored lines inside of each quadrant showing measurement sets.

using dextran-coated charcoal suspension. The linear range for the standard curve was 20 to 1300 pmol/L and the sensitivity of the assay was found to be 70 pmol/L. The assay is monitored using four internal quality control samples (Pools 1, 2, 3 & 4 with MPA concentrations in the range of 900, 1600, 2700 and 5100 pmol/L, respectively) included in each assay. The intra- and inter-assay coefficients of variations were less than 10% in

these assays for all four quality control samples used.

Tissue Processing & Gland Penetration Measurements

Uterine tissues were collected at the time of OHE, fixed in 4% paraformaldehyde, and embedded in Paraplast-plus® (VWR International, LLC; Radner, PA). Tissues were sectioned at 6µm, deparaffinized with Hemo-De® (Scientific Safety Solvents; Keller, Texas), mounted

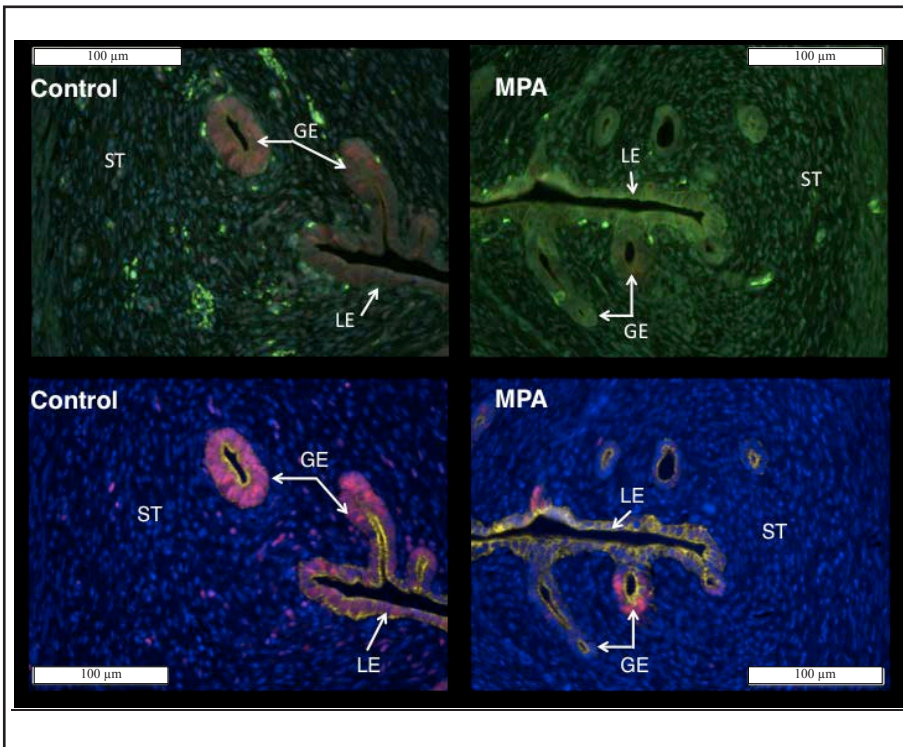


Figure 3. Raw (top) and spectrally unmixed (bottom) images of canine uterine tissue obtained from control (left) and MPA-treated (right) females. In the spectrally unmixed images nuclei are blue (POPO-1), epithelium (luminal = LE, glandular = GE) is yellow (CK8, A568), and nuclear PCNA is red (A594). Note that PCNA-specific signal occurs more frequently in control as compared to MPA-treated tissue.

on VWR Superfrost® Plus slides (VWR International, LLC; Radner, PA), rehydrated through a graded series of alcohol rinses to de-ionized water, and stained with hematoxylin. Uterine cross-sections were imaged using the Aperio® Imaging system. Gland penetration depth was determined by measuring gland penetration as a function of stromal compartment depth. Measurements were organized by dividing uterine cross-sections into four quadrants, beginning at the mesometrium and continuing systematically in a clock-wise direction around the tissue section (Figure 2). Two sets of measurements were

taken per quadrant with fourteen total sets of measurements obtained per animal. All data were subjected to analyses of variance using GLM procedures (Statistical Analysis Software, SAS; Cary, NC).

Immunohistochemical (IHC) staining

Mounted tissue sections were subjected to heat induced antigen retrieval in a citrate buffer solution (pH 6.0). After cooling, a blocking solution of 10% non-immune goat serum (1:10 v/v; diluted in PBS) was applied at room temperature for 20 minutes in a humidity chamber. Primary antibodies

were applied simultaneously and sections were allowed to sit at room temperature for one hour. Anti-proliferating Cell Nuclear Antigen (PCNA), specific for an auxiliary protein of DNA polymerase delta, mouse monoclonal-IgG2a (Santa Cruz Biotechnology; Santa Cruz, CA) was applied at a 1:50 v/v dilution. Guinea Pig polyclonal anti-Cytokeratin 8 (CK8; Fitzgerald Industries Intl; Acton, MA) was applied at a 1:250 v/v dilution. Primary antibodies were diluted in 10% goat serum/PBS solution. AlexaFluor®-labeled fluorescent secondary antibodies (ThermoFisher Scientific; Waltham, MA), A594 (goat anti-mouse IgG2a, 1:400 v/v) and A568 (goat anti-guinea pig CK8, 1:400 v/v) were applied and incubated for one hour. POPO™-1 iodide was applied as a nuclear counterstain (1:10 1mM/200uL, Invitrogen Corporation; Carlsbad, CA) and incubated for 20 minutes at room temperature. Coverslips were mounted using VectaShield® Mounting Medium for fluorescence (Vector Laboratories, INC; Burlingame, CA) and slides were stored overnight in a dark humid chamber at 4°C.

Multispectral Imaging (MSI)

Slides were imaged using the Nuance FX MSI system (Perkin Elmer; Hopkinton, MA). Images were obtained at 40X magnification. Image data was collected from 420 – 720 nm at 10 nm wavelength increments.

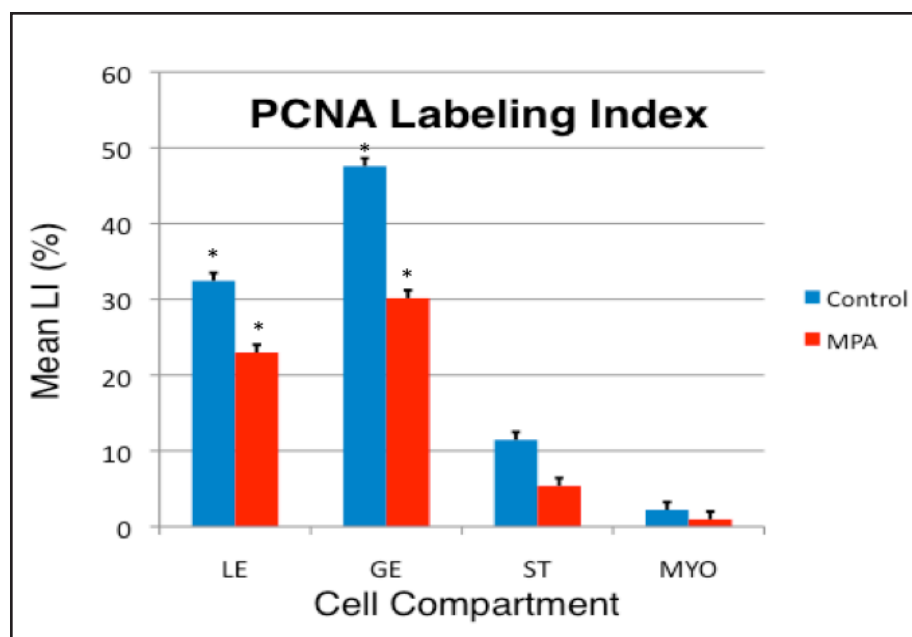


Figure 4. PCNA Labeling Index (LI) data for control (blue bars) and MPA-treated (red bars) tissues. Data are expressed as percent PCNA-positive cells for luminal epithelium (LE), glandular epithelium (GE), endometrial stroma (ST), and myometrium (MYO). A treatment by cell compartment interaction (* = $P < 0.01$) was identified indicating that effects of MPA on reduction of PCNA LI were more pronounced in some cell compartments, as illustrated.

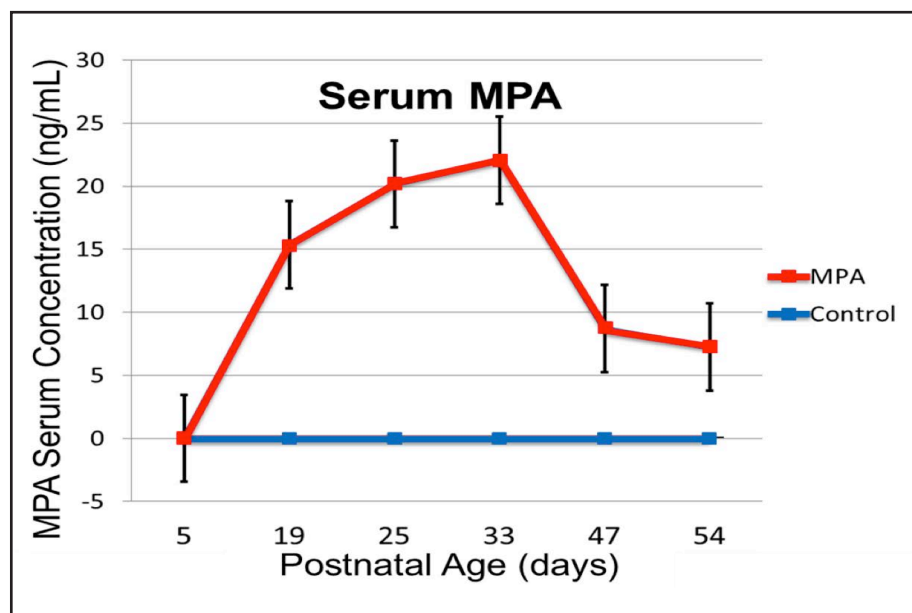


Figure 5. MPA serum concentrations (ng/mL) as a function of age in MPA-treated (red line) as compared to control females (blue line). In treated animals, serum MPA concentrations increased after the first injection at PND 5, reached peak levels one week after the booster injection was given when the birth weight had tripled at PND 25 ± 1 , and remained elevated for the duration of the experimental period.

Acquiring a spectral library allowed the images to be digitally unmixed according to the specific emission wavelengths for each fluorescent label. Spectrally unmixed images were analyzed using Cell Profiler™ and Cell Profiler Analyst™ (www.cellprofiler.org) (Figure 3). Data were collected after constructing a CellProfiler™ “pipeline” that could identify nuclei, distinguish PCNA-positive versus PCNA-negative nuclei, and collect data according to cell compartment (luminal epithelium = LE, glandular epithelium = GE, stroma = ST, myometrium = MYO).

RESULTS

When uterine characteristics were compared between control and MPA-treated females, several differences were noted. Cellular arrangements visibly differed between control and MPA-treated females (Figure 2). However, only a few of these parameters were supported by statistical differences. When gland penetration depth was examined, there was no effect of treatment (mean gland penetration depth for control animals was $153.5 \pm 46.2 \mu\text{m}$ and for MPA treated animals was $113.0 \pm 12.7 \mu\text{m}$).

When the four uterine cell compartments were compared, it was determined that glandular epithelium and luminal epithelium were affected by treatment. A treatment by cell-compartment interaction

was detected ($P < 0.01$) for PCNA labeling index, indicating compartment-specific changes in cell proliferation associated with MPA exposure (Figure 4). Specifically, cell proliferation within glandular epithelium and luminal epithelium was significantly reduced in the MPA-treated animals as compared to the controls.

Measurements of MPA concentrations in peripheral circulation confirmed adequate absorption of the drug at the dosage and volume administered. Compared to controls, circulating MPA levels were elevated at the first time point post-treatment and remained elevated through the end of the experimental period in treated animals (Figure 5).

DISCUSSION

While differences due to treatment were not as profound as those previously reported in uterine tissue of other species, important changes were observed. In sheep, cattle, and mice, a similar experimental design successfully induced the UGKO phenotype; this model did not achieve the same effect in the dog. In each of the previous UGKO animal models, the critical window for progestin exposure was highly specific and determined within those studies. In the dog, the critical window for progestin exposure has not yet been determined; defining this time period should be explored further.

Due to the exponential growth rate in neonatal puppies, there was some concern that the MPA would be metabolized before their bodies could respond to the treatment. The ability to measure detectable concentrations of MPA in systemic circulation throughout the study was essential to confirm that puppies absorbed the medication and to provide assurance that MPA was in systemic circulation throughout the study period (Figure 5).

The extent to which MPA acts as a progestin in the neonatal canine uterus is unclear. It has been shown to bind promiscuously with glucocorticoid receptors in the adult canine (Selman, 1996). Therefore, it is possible that MPA preferentially bound glucocorticoid receptors and did not elicit as robust a response as if it had bound preferentially with progesterone receptors. Alternatively, it is also possible that glucocorticoid signaling pathways could provide the means to induce a UGKO phenotype in the dog.

Establishing non-surgical methods of sterilization for companion animals has many benefits including reducing morbidity and the high costs associated with OHE surgery. Neonatal progestin exposure as implemented here did not induce a UGKO phenotype, but did reduce endometrial cell proliferation as reflected by labeling index for PCNA (Figure 4). MPA was shown to be

anti-proliferative in the neonatal canine uterus and these results align with the observations of UGKO phenotypes in previous studies, just to a lesser extent. Results indicate that uterine gland development in dogs may be abolished with identification of appropriate anti-adenogenic conditions. Alternate signaling pathways such as the glucocorticoid receptor should also be explored to determine if there is a more efficient treatment to accomplish these goals in the female dog.

ACKNOWLEDGMENTS

Supported in part by grants from the Morris Animal Foundation (to Paul S. Cooke and Frank F. Bartol), NSF-EPS-1158862 (to Frank F. Bartol), and the Scott-Ritchey Research Center Interdepartmental Research Grants Program (to Robyn R. Wilborn).

The authors would also like to thank Steve Waters for the care of the animals in this study as well as Dr. Narendar Kumar for performing the MPA assays.

REFERENCES

[Click here to view references at the end of the journal.](#)

Detection of Pathogens from Biopsy by Use of Sortase Activity

Andrew Clark, Jiansheng Huang, and Peter Panizzi

ABSTRACT

Sortase A is a transpeptidase expressed by *Staphylococcus aureus* (*S. aureus*) that covalently attaches with bacterial proteins encoded in a LPXTG motif to the pathogen surface. Sortase A functionally coats the pathogen with needed receptors and ligands that promote virulence of *S. aureus*. Although the majority of nosocomial infections are caused by *S. aureus*, there remain challenges in the clinical detection of the pathogen due to the non-specific methods used to diagnose these invasive infections. The development of pathogen-specific, non-invasive probes that target particular bacteria would provide a more effective alternative to diagnosing and monitoring clearance of *S. aureus* infections. Here we test whether a Förster resonance energy transfer (FRET) substrate containing a central LPXTG motif could be used to determine the presence or absence of the enzyme produced by dangerous pathogens in tissue biopsy samples. Initially, we expressed recombinant sortase A

and compared the activity of our recombinant (sortase A)-His₆ with previous kinetic parameters for the enzyme. Analysis indicated our (sortase A)-His₆ had a K_m of 10 μ M for the LPXTG-containing FRET substrate, DABCYL-LPETG-EDANS and its phenotypic enhancement in the presence of calcium ions. In a prelude to our *in vivo* experiments, we tested sortase A activity of lysates from several *S. aureus* strains to correlate the relative concentrations of sortase A produced by each *S. aureus* strain, namely Tager 104, RF122, and Xen29. As proof-of-principle for its use as a clinical diagnostic tool, an intramuscular infection of *S. aureus* Xen29 was established in albino C57BL/6 mice and tissue biopsies were performed. We determined the relative sortase A activity of whole tissue extracts isolated from the spleen, kidneys, and infection site of these animals and compared our results to control uninfected tissue. Our findings suggest that sortase A activity can be used as an indicator of the presence of *S. aureus* from tissue, which implies significant diagnostic potential.

INTRODUCTION

Staphylococcus aureus (*S. aureus*) is a virulent, Gram-positive bacterium that is known as a leading cause of many types of dangerous infections and is responsible for the majority of hospital-acquired infections in the United States (Dantes, 2013). Among the most dangerous of these infections is bacterial endocarditis, an infection of the heart valve leaflets that ultimately leads to valve insufficiency, compromising cardiac function. *S. aureus* endocarditis makes up 30-40% of diagnosed cases with about a 20% fatality rate, even with intravenous antibiotic therapy (Baddour, 2005). With the increased prevalence of multi-drug resistant strains of *S. aureus*, new clinical strategies are being developed to both treat these infections and to diagnose these pathogens before irreversible damage to the patient occurs. This reality underscores the need for rapid and reliable techniques to improve patient care by implementation of effective treatment protocols, which should increase patient survival.

Currently, bacterial endocarditis is diagnosed using primarily transesophageal echocardiogram, which requires a hospital stay and usually multiple imaging sessions (Baddour, 2005). The results of this technique are less than definitive, lack specificity for any given pathogen, and are subject to artifacts caused by respiratory and cardiac motion. Combined, these challenges limit the early detection of hallmark bacterial-fibrin-platelet vegetations, delaying life-saving surgical intervention. Newer molecular imaging approaches hold the promise of identifying the casual pathogens *in vivo*. Detection of *S. aureus* virulence factors could one day prove to be a more reliable alternative as they provide an advantage of discriminating the casual strain of the infection, thus directing appropriate therapy. Of interest here, *S. aureus* and other Gram-positive pathogens produce a transpeptidase that switches the carboxyl glycine (Gly) on proteins bearing a LPXTG-motif for the penta-Gly residues found on the bacterial cell wall (Mazmanian, 2002). This enzyme is called sortase A and is not similar to any known mammalian protein. Previous studies have shown that these sortase A-mediated covalent attachments are necessary for the pathogenicity of *S. aureus* and for avoidance of host immune response during infections (Maresso, 2008). As sortase A is specific to Gram-positive microbes, such a substrate could be used to confirm the presence of such virulent organisms if the assays were sensitive enough to be performed

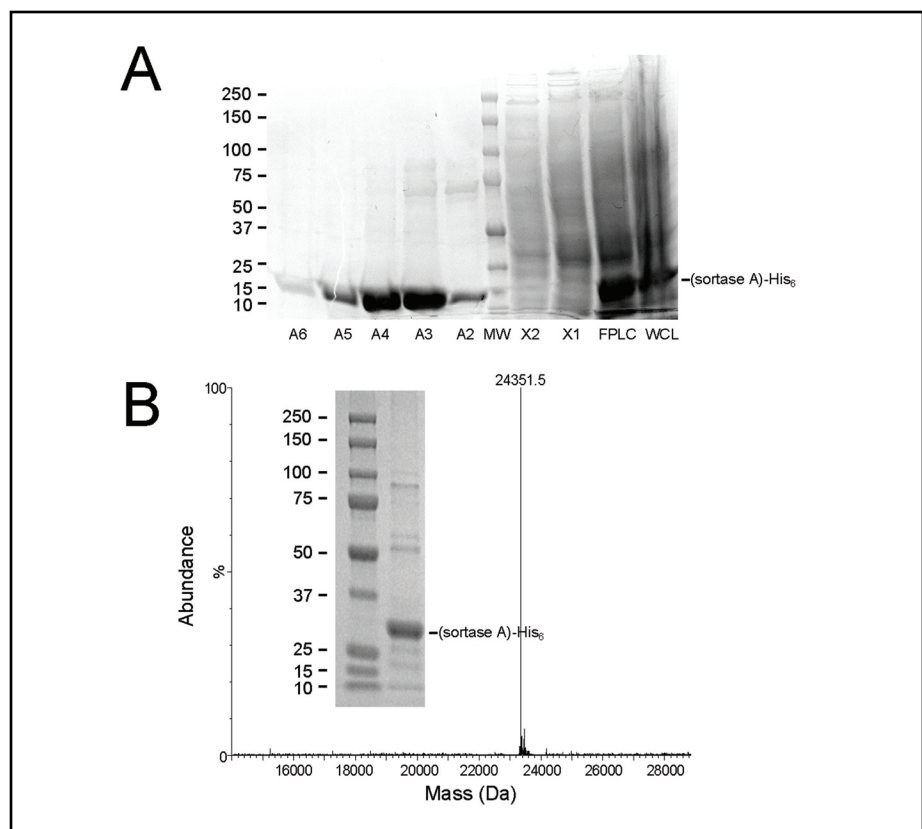


Figure 1. Purification and characterization of recombinant (sortase A)-His₆. **A:** The SDS-PAGE gel showing FPLC fractions obtained from chromatographic purification of recombinant (sortase A)-His₆ by nickel affinity chromatography. This total protein stained 4-10% polyacrylamide gradient gel shows a central protein molecular weight marker used to verify the molecular weight of the proteins present in the 0.5 mL eluted fractions (namely A2, A3, A4, A5, and A6) followed by samples from the column wash steps (X1 and X2), the column load (Pre FPLC), and whole cell lysate post sonication (WC). **B:** MALDI-TOF mass spectrometric analysis of our purified (sortase A)-His₆ with a resultant MW of 24,351.5 for the major protein shown in the insert.

in complex protein mixtures found in homogenates of tissue biopsies (Spirig, 2011). Here, we show that a LPXTG-containing Förster resonance energy transfer (FRET) substrate that is specific for the sortase A enzyme can be used as a specific reporter for the detection and tracking the progression of *S. aureus* infections.

MATERIALS AND METHODS

Animals

For this study, 4 albino C57BL/6 mice were purchased from The Jackson Laboratories (Bar Harbor, ME). Mice were housed at the Auburn University College of Veterinary Medicine with *ad libitum* access to alfalfa-free chow and water. All procedures were designed in accordance with the Guide for the Care and

Use of Laboratory Animals of the National Institutes of Health and approved by the Institutional Animal Care and Use Committee of Auburn University.

Expression and Purification of (Sortase A)-His₆

Sortase A was originally cloned from *Staphylococcus aureus* strain N315 genomic DNA (Kobashigawa, 2009). The pGBMCS-SortA plasmid (Addgene #21931) were encoded for a fusion protein of sortase A with a carboxyl-terminal His-tag (Kobashigawa et al., 2009). The pGBMCS-SortA plasmid was transformed into *Escherichia coli* Rosetta II (DE3) pLysS competent cells (Novagen) and selected for positive clones via the presence of an ampicillin resistance gene. Three colonies were used to inoculate a Luria broth (250mL) culture with carbenicillin (100μg/ml). The overnight culture was diluted 50-fold into fresh media and shaken at 225 rpm at 37°C until the optical density (OD_{600nm}) reached 0.5 absorbance units. At that point, the culture was induced by the addition of isopropyl β-D-1-thiogalactopyranoside to a final concentration of 500 μM for a duration of 3 hours. Cells were harvested by centrifuge using a JA-30I Avanti centrifuge (Beckman-Coulter Inc.) at 4200 rpm for 30 minutes at 4°C. The pellets were resuspended in 50 mM 4-(2-hydroxyethyl)-1-piperazineethanesulfonic acid (HEPES), 400 mM NaCl, 1 mg/ml polyethylene glycol 8000, 10 mM imidazole, 10% glycerol, 1 mM

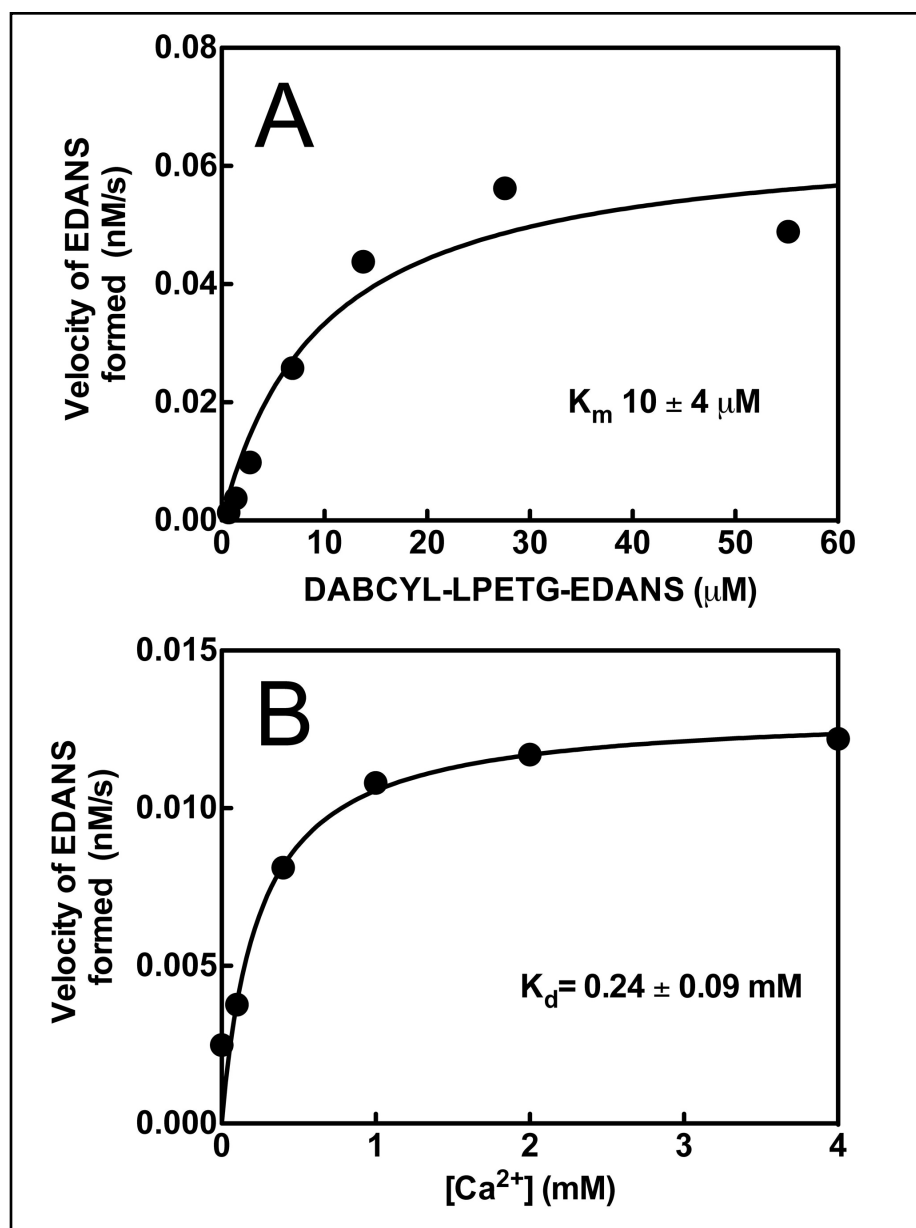


Figure 2. Kinetic analysis of purified (sortase A)-His₆. **A:** Michealis-Menten plot used to determine our purified sortase A kinetic parameters (K_m of 10.07 μM and V_{max} of 0.068 nM/s) for cleavage of the FRET substrate (DABCYL-LPETG-EDANS). **B:** The apparent dissociation constant for calcium (Ca^{2+}) binding to the sortase enzyme obtained by fitting the quadratic binding equation to the dependency of molar rate of substrate hydrolysis (K_d of 0.24 mM) over a range of Ca^{2+} concentrations, which is in good agreement with the previous literature values (Naik, 2006).

phenylmethylsulfonyl fluoride, pH 7.4. The cells were lysed using three rounds of sonication with Vibra-cell sonicator (Sonics) on ice with constant temperature monitoring. Post sonication

cellular debris was removed by centrifugation at 18,000 rpm for 20 minutes in Oak Ridge tubes followed by filtration of the supernatant through a 0.8-micron syringe filter.

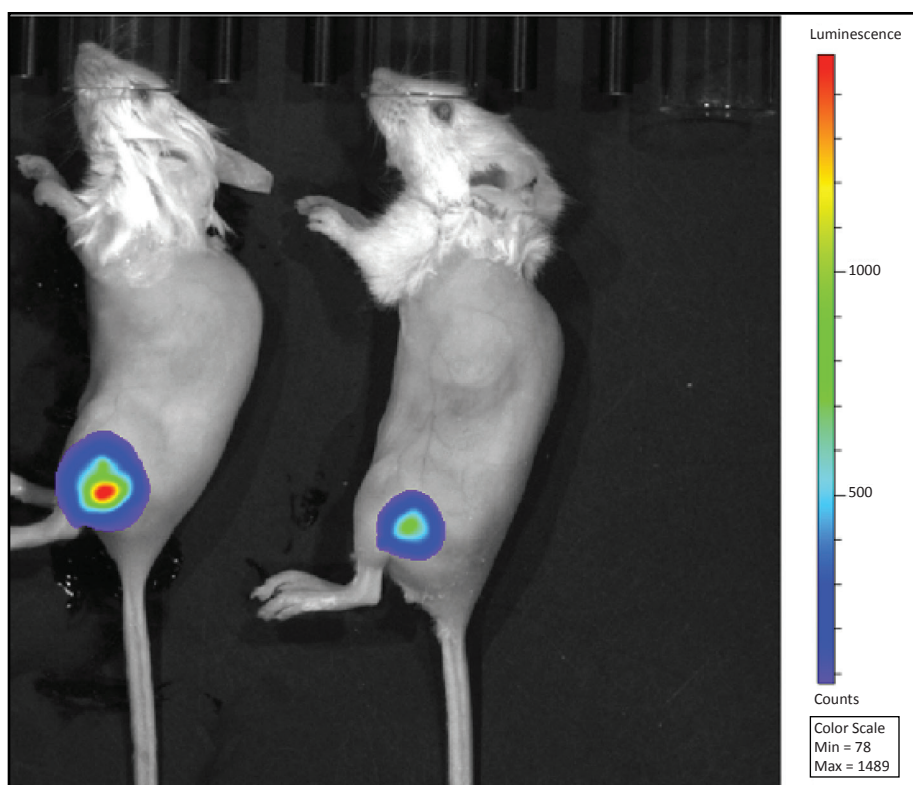


Figure 3. Intramuscular infections examined by bioluminescence imaging using the IVIS Lumina XRMS system. Specifically, the image shows mice (reference mouse numbers M109 and M110) at 5 days post intramuscular infection with bioluminescent Xen29. M110 on the left was used for organ isolation and tissue biopsy for relative sortase A presence.

To purify the (sortase A)-His₆, the filtered supernatant was loaded onto a HisTrap column using fast protein liquid chromatography (FPLC) using an AKTA Purifier UPC10 (GE Biosciences). The column had been equilibrated with 50 mM HEPES, 400 mM NaCl, 40 mM imidazole, pH 7.4 and a linear gradient up to 100 mM HEPES, 500 mM NaCl, 1 M imidazole, 10% glycerol, pH 7.4. Purified (sortase A)-His₆ was pooled by absorbance signal and dialyzed against 50 mM Tris-HCl, 150 mM NaCl, pH 8. SDS-PAGE followed by GelCode blue staining (Pierce) for total protein content was used to determine the purity of the recombinant (sortase A)-His₆. The (sortase A)-His₆ concentration

was determined by absorbance at $\lambda_{280\text{ nm}}$ with a calculated molar absorption coefficient of 24,410 M⁻¹ cm⁻¹ (Pace, 1995).

MALDI-TOF mass spectrometry analysis of Sortase A

Matrix-assisted laser desorption/ionization time-of-flight (MALDI-TOF) mass spectrometry was used to determine the molecular weight of (sortase A)-His₆ after purification. Protein samples were diluted to optimal concentration and spotted onto a 96-well plate using a sandwiched method where the protein solution was diluted 1 to 1 with sinapinic acid matrix (30 mg matrix in 1 ml of 33% acetonitrile, 0.1% TFA, freshly

prepared) were air dried at room temperature, and rinsed with H₂O and dried prior to sinapinic acid matrix addition (1 μ L) to allow for crystal growth. The spectra were acquired using a MALDI-TOF (Microflex, Burkholder Daltonics) with FlexControl (version 3.3) and data analysis by FlexAnalysis software (version 3.3). Mass calibration used insulin and BSA for instrument and for external spectrum. Laser power and voltages were tuned so an optimum signal to noise ratio was achieved. MALDI spectrum was calibrated against external standard, smooth and subtracted background. MPO parent and cleaved fragments with and without heme were identified in the MALDI spectrum range from 10,000 to 150,000 Da.

Characterization of Sortase A using an LPXTG-containing FRET substrate

Michaelis-Menten substrate dependency from sortase A was determined for the FRET substrate, namely DABCYL-LPETG-EDANS (Anaspec). Energy transfer was detected using λ_{ex} 350 nm, and λ_{em} 490 nm using Varioskan Flash microplate reader (Thermo Scientific). Sortase A activity was assayed over a range of DABCYL-LPETG-EDANS concentrations from 2.5-75 μ M using a Spectramax 340PC (Molecular Devices Inc.). The reactions contained (sortase A)-His₆ (7 μ M) in 50 mM Tris-HCl, 150 mM NaCl, pH 8 supplemented with 5 mM CaCl₂. The dependency of (sortase A)-His₆ concentrations (1-20 μ M) was also determined

at a constant DABCYL-LPETG-EDANS concentration of 50 μ M. Fluorescence was converted to molar concentrations of product using a standard curve of the EDANS.

Whole Cell Lysate Assays

To determine whether the DABCYL-LPETG-EDANS FRET substrate can be used to detect sortase A activity in lysates of staphylococcal strains, the bacteria was plated from isolation of individual colonies in blood agar medium and grown overnight at 37 °C. Several colonies were used to inoculate a liquid culture of brain heart broth (Research Products International) and incubated overnight at 37° C with shaking at 225 rpm. After growth, the OD_{600nm} was measured to determine the approximate CFU / mL and when the OD_{600nm} reached 0.6 absorbance units, the cells were recovered by centrifugation. As sortase A is an intracellular protein, samples were lysed by treatment with 30 μ g/ml of lysostaphin for 10 min at 37° C added to them and were put through 3 freeze/thaw cycles. After lysing, the lysates were assayed with 50 μ M FRET substrate and 5 mM Ca²⁺ in the Varioskan plate reader. The *Staphylococcus aureus* strains tested included RF122 and Tager 104, and the *Streptococcus pyogenes* strain tested was clinical isolate Alab49. Untransformed Rosetta II *E. coli* was also assayed to act as a Gram-negative control for sortase A activity in bacterial lysates.

Mouse Model of Infection and Tissue Assays

To determine whether tissue biopsy can also be used to monitor mice injected with *S. aureus* Xen29 (10⁶ cfu / ml) to induce intramuscular infections so the levels of sortase A *in vivo* could be tested, the infections were allowed to develop over the course of 1 week, and the mice were imaged using an IVIS Lumina XRMS imaging system to confirm the presence of bioluminescent Xen29. The mice were then sacrificed and organs harvested. The samples were weighed, suspended in 50 μ L of lysis buffer (50 mM TRIS, 10 mM EDTA, pH 8), and homogenized using a Pro Scientific PRO200 tissue homogenizer. Samples from each of the homogenates were streaked onto Blood Agar (BD BBL stacker plate) blood agar plates and incubated overnight at 37 °C to confirm the presence of Xen29. After growth, the plates were imaged using a Fujifilm LAS-1000 to confirm the presence of the bioluminescent Xen29. The homogenates that displayed Xen29 presence were then lysed using 30 μ g/ml lysostaphin and cells lysed by three rounds of freezing in liquid nitrogen and thawing at 37° C. Sortase A activity was assayed with the Horiba Fluoromax 4 using the FRET substrate at 50 μ M final concentration.

RESULTS

Sortase A Characterization

The purified (sortase A)-His₆ was found to have a concentration of

2.3 mg/ml and a molecular weight of approximately 27 kDa (Figure 1A). MALDI-TOF Mass spectrometry was used to determine that the molecular weight of (sortase A)-His₆ was 24351.5 Da, which matches with the estimated value 24351.3 Da computed from the amino acid sequence (Figure 1B). Michaelis-Menten plots were generated to determine the kinetic parameters of our recombinant sortase A enzyme by varying the FRET used to initiate the reactions. The hyperbolic dependency of the rate of molar product with increasing FRET substrate was fit with an apparent K_m value of 10 μ M and a V_{max} of 0.07 nM/s (Figure 2A). It is well known that sortase A can recognize and cleave LPXTG motif and then catalyze the formation of an amide bond between the carboxyl group of threonine and the amino group of cell-wall cross-bridges of bacteria. DABCYL-LPETG-EDANS substrate (Anaspec) was used to measure and monitor sortase A activity through FRET assay by use of spectrofluorometer. Maximal velocity (0.07 \pm 0.01 nM/s) and K_m (10 \pm 4 mM) for this FRET probe was obtained by fitting with Michaelis-Menten equation in Prism 5.0. Furthermore, our results also show that sortase A activity was enhanced by increasing concentration of Ca²⁺. The K_D for calcium binding obtained by fitting of the quadratic binding equation to the dependency of sortase A activity was determined as 0.24 mM (Figure 2B).

Table 1. FRET assay was used to measure the sortase A activity in the samples, the approximate relative concentrations of sortase A was calculated in the whole cell lysates of T104, RF122, and Alab49.

| Bacterial Strain | Sortase A Concentration (μM) |
|------------------|---|
| RF122 | 0.680 |
| T104 | 1.760 |
| Alab49 | 0.961 |

Table 2. FRET assay was used to measure the sortase A activity in the samples. The calculated concentrations of sortase A in the homogenates from infection site, spleen, and kidney of M110 is shown. The concentrations have been normalized to the mass of the tissue samples.

| Tissue Type | Sortase A Concentration in Tissue ($\mu\text{M}/\text{mg}$) |
|----------------|---|
| Infection Site | 0.0165 |
| Spleen | 0.0032 |
| Kidney | 0.0069 |

Whole Cell Lysate Assay

Of the *S. aureus* strains tested, both the lysates of RF122 and T104 displayed significant sortase A activity. The *S. pyogenes* strain Alab49 also showed strong activity, and the relative amounts of sortase A present in these strains can be seen in Table 1. The *E. coli* lysate showed no observable activity when tested. Appropriate tissue was isolated from the control mouse to verify the specificity of the enzyme-substrate pair under the reaction condition used.

Tissue Homogenate Assay

The IVIS images of M110 showed bioluminescence signal at the injection site of the Xen29 (Figure 3). The plate streaks of homogenates of M110's spleen, kidneys, and the infection site all displayed significant

S. aureus growth and when imaged, the colonies displayed bioluminescence indicative of Xen29. When these homogenates were assayed, they all showed significant activity with the FRET substrate and the approximate levels of sortase A in each sample can be seen in Table 2. Plots of the assays can be seen in Figure 4.

DISCUSSION

Bacterial endocarditis caused by *S. aureus* that affects approximately 38,000 people in the United States each year (Bor, 2013). The current diagnostic methods used to identify this disease are often time consuming and indeterminate and the development of novel diagnostic techniques for the identification of bacterial endocarditis could lead to improved patient prognosis. The activity of the sortase A transpeptidase

could be used to develop such a technique by acting as a target for FRET based fluorescent probes.

The activity seen in both the whole cell lysate assays and the assays of the tissue samples show that sortase A is produced in detectable amounts during the bacterial growth, both in culture and *in vivo*. Our results suggest that FRET based substrates provide a reliable method for detecting the presence of sortase A, which is found in several clinically important Gram-positive species such as *S. aureus*, *Streptococcus pyogenes*, *Bacillus anthracis*, and *Enterococci faecium* (Spirig, 2011). This method of sortase A detection thus can confirm the presence of these pathogens post infection and could be used to develop a rapid test to monitor antibiotic therapy and to remotely diagnose

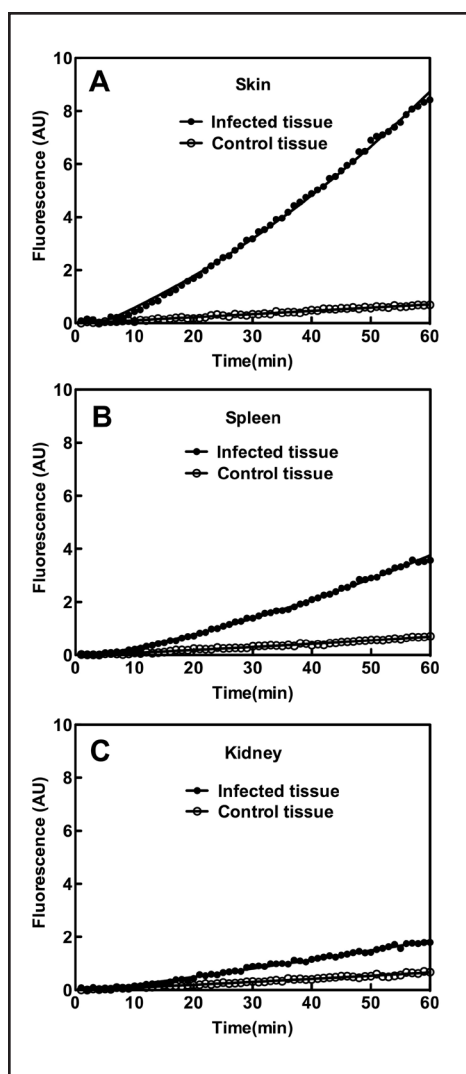


Figure 4. Plots of the tissue homogenate assays. The sortase A activity was measured in various samples (*E. coli*, skin biopsy sample, spleen, and kidney from mice injected with *S. aureus* Xen29) with 50 μ M of FRET substrate DABCYL-LPETG-EDANS using FRET assay over the course of 1 hour. The data was fit with second order polynomial in Prism 5.

organ involvement by tissue biopsy. This has several advantages over currently used techniques including blood-based PCR analysis, as our assays would require only a hand-held spectrofluorometer and may be used at the patient's bedside.

Our previous studies using near-infrared fluorescence analogs of prothrombin in a murine model of endocarditis proved that optical-based methods could be used to monitor the development and treatment of these dangerous infections (Panizzi, 2011). The current sortase A probe, namely DABCYL-LPETG-EDANS, has a FRET probe pairing that is not appropriate for use *in vivo*, as the energy transfer would occur in wavelengths obscured by blood and tissue auto-fluorescence due to hemoglobin (Stamatas, 2006). Yet, we show that sortase A-based activity in conjugating LPXTG bearing proteins to penta-Gly sites in the cell wall could provide a pathway to label bacterial growth in invasive infections with fluorescent tags. Development of a sortase A-based positron emission tomography (PET) reporter could be particularly useful in the diagnosis of infective endocarditis, as sortase A producing organisms such as *S. aureus* and streptococcal species account for the majority of infective endocarditis cases (Bor, 2013). In combination with imaging techniques such as PET, such a system could monitor an infection's progress and provide vital information in treatment effectiveness. However, the viability of this method remains to be studied.

Our study has shown that biopsies of infected tissue contain detectable amounts of sortase A; in the medical settings these tissue biopsies are routinely done and rather safe. As such, a diagnostic methodology based on maximizing information

obtained from tests of patient biopsies has great potential. Furthermore, it is possible that this protocol could be adapted to test for bacteremia in blood samples taken during suspected infections. Our assay would take minutes whereas cultivating organisms from blood would take days (Baddour, 2005). Thus, detecting sortase A presence in the blood or tissue using a FRET- or PET-based substrate would prove to be a more efficient method of diagnosis. Future studies will focus on testing the sensitivity of FRET substrates in detecting sortase A activity to determine the viability of this method for use in the clinic (Maresso, 2008).

ACKNOWLEDGMENTS

The authors would like to thank Dr. Yonnie Wu of the Auburn University Mass Spectroscopy facility in the Department of Chemistry and Biochemistry for collection of the MALDI-TOF data. This work is supported by the National Institutes of Health through grants provided by the National Heart, Lung, and Blood Institute, R00HL094533 (to Peter Panizzi) & R01HL114477 (to Peter Panizzi), the National Institute of Allergy and Infectious Diseases grant 2R44AI085840-02 (to Peter Panizzi), and funding from the Auburn Cellular and Molecular Biosciences Undergraduate Research Fellowship (to Andrew Clark).

REFERENCES

[Click here to view references at the end of the journal.](#)

Diindolylmethane Inhibits the Activity of P-glycoprotein in 17-71 Canine B-Cell Lymphoid Tumor Cells

Ala Mansour, Kodye Abbott, Patrick Flannery, Elaine Coleman, Amit Tiwari, and Satyanarayana Pondugula

ABSTRACT

B-cell lymphoma is the most common hematopoietic tumor in dogs and is usually treated with multiple chemotherapy drugs. However, relapses are often seen and chemoresistance is a significant concern in cases of relapses. Chemoresistance in B-cell lymphoma was shown to be associated with upregulation of the expression/activity of multidrug transporters, particularly P-glycoprotein (P-gp). The existing P-gp inhibitors have limited success mainly due to undesired toxicities. Novel and safer approaches are therefore crucial for overcoming chemoresistance by downregulating P-gp. Here, we studied whether 3,3'-diindolylmethane (DIM), a natural dietary supplement, affects the function of P-gp in the chemoresistant 17-71 canine B-cell lymphoid tumor cells. Cell viability, P-gp function, and P-gp gene expression were studied using ATP-based CellTiter-Glo luminescent cell viability assays, intracellular rhodamine 123 accumulation assays, and RT-PCR, respectively.

DIM, at its physiologically relevant concentrations, did not significantly affect the viability of either the chemoresistant 17-71 and chemosensitive GL-1 canine lymphoid tumor cells, suggesting that DIM is non-cytotoxic at physiologically relevant concentrations. P-gp specific inhibitor PSC-833 significantly increased the intracellular accumulation of P-gp substrate rhodamine 123 in 17-71 but not GL-1 cells, suggesting that 17-71, but not GL-1, expresses functional P-gp. Similar to PSC-833, DIM at its non-cytotoxic concentrations significantly increased the intracellular accumulation of rhodamine 123 in 17-71 cells, indicating that DIM inhibits the activity of P-gp in 17-71 cells. These results are consistent with our conclusion that DIM inhibits the function of P-gp in the chemoresistant canine 17-71 B-cell lymphoid tumor cells.

INTRODUCTION

Lymphoma is one of the most common cancers in dogs, accounting for up to 25% of all canine cancers

(Meuten, 2002). Notably, B-cell lymphoma accounts for about 85% of lymphomas (Ruslander, Gebhard, Tompkins, Grindem, & Page, 1997). Most untreated dogs diagnosed with B-cell lymphoma will only survive for 4-6 weeks (Meuten, 2002). B-cell lymphoma is usually treated with aggressive chemotherapy protocols involving a combination of chemotherapeutics, including vincristine (VCR) and doxorubicin (DOX). While these multi-agent chemotherapy regimens (Dervisis et al., 2007; Fahey et al., 2011; Flory et al., 2008; Griessmayr, Payne, Winter, Barber, & Shofer, 2009; Lori, Stein, & Thamm, 2010; Moore et al., 1999; Northrup et al., 2009; Rassnick et al., 2002; Rebhun et al., 2011) improve the survival time between 6 and 18 months (Lori et al., 2010), relapses are frequently seen. Most importantly, relapsed lymphoma often displays resistance to chemotherapy drugs, resulting in a poor prognosis. Due to high risk of cardiotoxicity, the lifetime cumulative dose of DOX must be limited (Banco, Grieco, Servida, & Giudice, 2011; MacDonald, 2009). Likewise, to

avoid potential gastrointestinal abnormalities, myelosuppression, and extravasation injury, the lifetime cumulative dose of VCR must also be limited (Banco et al., 2011; MacDonald, 2009). As such, novel therapeutic approaches are sought to combat chemoresistance as well as avoid the limiting threshold of the chemotherapy drugs.

Chemoresistance in a variety of cancers is associated with upregulation of expression/function of multidrug transporters (drug efflux pumps), such as P-glycoprotein (P-gp) (Borst, Evers, Kool, & Wijnholds, 2000; Chen et al., 2012; Marzac et al., 2011; Pondugula and Mani, 2013). Chemoresistance in canine B-cell lymphoma is also associated with P-gp upregulation (Fan, 2003; Lee, Hughes, Fine, & Page, 1996; Moore, Leveille, Reimann, Shu, & Arias, 1995; Steingold et al., 1998; Uozurmi, Nakaichi, Yamamoto, Une, & Taura 2005). Functionally, P-gp prevents the retention of cytotoxic drugs within tumor cells resulting in little or no cytotoxic effect. For example, P-gp can preclude the cytotoxic effect of VCR and DOX by exporting them from tumor cells (Borst et al., 2000; Okamura, Sakaeda, & Okumura, 2004; Sharom, 2008; Sodani, Patel, Kathawala, & Chen, 2012).

A common approach to avoiding chemoresistance and drug cytotoxicity involves the use of rationally designed combinatorial treatments. The dual employment of one of several pharmaceutical

P-gp inhibitors, such as verapamil, valsopodar, cyclosporine A, PSC-833, or Tariquidar (Baer et al., 2002; Daenen et al., 2004; Fox and Bates, 2007; Kolitz et al., 2004), along with anticancer agents is one conventional method of reversing chemoresistance (Dano, 1973; Tsuruo, Iida, Tsukagoshi, & Sakurai, 1981). However, such P-gp inhibitors have had limited success because of their undesired dose-dependent toxicity and unpredictable pharmacokinetic side effects (Thomas and Coley, 2003). Due to these restraints, the use of naturally occurring compounds as alternatives to these pharmaceutical P-gp inhibitors has been a topic of massive interest in cancer research.

3,3'-Diindolylmethane (DIM) is a natural health supplement and is the major active metabolite of indole-3-carbinol (I3C) (Anderton et al., 2004b), which is also a natural health supplement as well as a naturally occurring compound in cruciferous vegetables (Bonnesen, Eggleston, & Hayes, 2001). DIM is used to treat recurrent respiratory papillomatosis (Auborn, 2002; Wiatrak, 2003). The emerging evidence from several studies indicates that DIM could be used for both the treatment and prevention of a variety of human cancers, including prostate and breast cancers (Azmi et al., 2008; Biersack and Schobert, 2012; Chen et al., 2012). The aim of this study was to investigate whether DIM inhibits the function of P-gp in the chemoresistant canine B-cell lymphoid tumor cells.

MATERIALS AND METHODS

Cell Culture

17-71 and GL-1 canine B-cell lymphoid tumor cell lines were provided by Dr. Steven Suter, North Carolina State University. These lymphoid tumor cell lines are well characterized to reflect *in vivo* properties and widely used for B-cell lymphoma studies (Jamadar-Shroff, Papich, & Suter, 2009; Kojima, Fujino, Goto-Koshino, Ohno, & Tsujimoto, 2013; Matsuda et al., 2010; Uozurmi et al., 2005; Zandvliet, Teske, Chapuis, Fink-Gremmels, & Schrickx, 2013). 17-71 and GL-1 cell lines were grown in RPMI-1640 medium (Lonza, Walkersville, MD) containing 10% fetal bovine serum (HyClone, Logan, UT), 100 U/ml penicillin and 100 µg/ml streptomycin (Cellgro, Manassas, VA), 2 mM L-glutamine (Cellgro), and 1 mM sodium pyruvate (Cellgro). Both cell lines were cultured in a humidified incubator with an atmosphere of 5% CO₂ and 95% air at 37°C.

Chemicals

3,3'-Diindolylmethane (DIM), Dimethyl sulfoxide, Valsopodar (PSC-833), and Rhodamine 123 (R123) were purchased from Sigma-Aldrich (St Louis, MO). DIM, PSC-833, and R123 were reconstituted in DMSO to obtain stock solutions.

Cell Viability Assays

17-71 and GL-1 cells were plated into 96-well culture plates

Table 1. Forward (F) and Reverse (R) Primers Used for Quantitative RT-PCR of 18S rRNA and P-gp

| Gene/Primer Sequence | Amplified Segment (bp) | Gene Bank Accession No. | Reference |
|----------------------------------|------------------------|-------------------------|--|
| 18S rRNA | | | |
| F: 5' - GAGGTTCTGAAGACGATCAGA-3' | 315 | BK000964 | Pondugula, Tong, Wu, Cui, & Chen (2010) |
| R: 5' - TCGCTCCACCAACTAAGAAC-3' | | | |
| P-gp | | | |
| F: 5'- CCATCTGGAGGAGGAAATGA-3' | 227 | AF045016 | Greger, Gropp, Morel, Sauter, & Blum (2006); Gropp, Gregor, Morel, Sauter, & Blum (2006) |
| R: 5'- TGGAGACATCGTCTGTGAGC-3' | | | |

(PerkinElmer, Waltham, MA) at a density of 10,000 cells per well in a final volume of 100 μ l medium. The cells were then either untreated or treated with DMSO or DIM (25 to 100 μ M) for 24 h. The CellTiter-Glo luminescent cell viability assays (Promega, Madison, WI) were used to determine the number of viable cells by quantifying the ATP present, which indicates the presence of metabolically active cells. Luminescence was measured with a FLUOstar Optima plate reader (BMG Labtech, Cary, NC).

Intracellular Rhodamine 123 Accumulation Assays

The efflux activity of P-gp in the lymphoid tumor cells was determined by measuring the intracellular accumulation of the fluorescent P-gp probe rhodamine 123 (Harmsen et al., 2010; Ishikawa et al., 2010). The tumor cells were washed with Hank's Balanced Salt Solution (HBBS, without Ca^{2+} , Mg^{2+} and phenol red) and incubated at 37°C for 15 min with or without DMSO, DIM, or PSC-833 (P-gp specific inhibitor)

(Keller et al., 1992; Zandvliet et al., 2013) in HBBS. Rhodamine 123 (5 μ M) was added later to the cells in the presence or absence of DMSO, DIM, or PSC-833 and incubated for another 45 min. The cells were washed with ice-cold-HBBS and solubilized in Triton-HBBS. To determine the intracellular concentration of rhodamine 123, the fluorescence was measured using the Infinite microplate reader (TECAN, San Jose, CA) at an excitation wavelength of 485 nm and an emission wavelength of 538 nm.

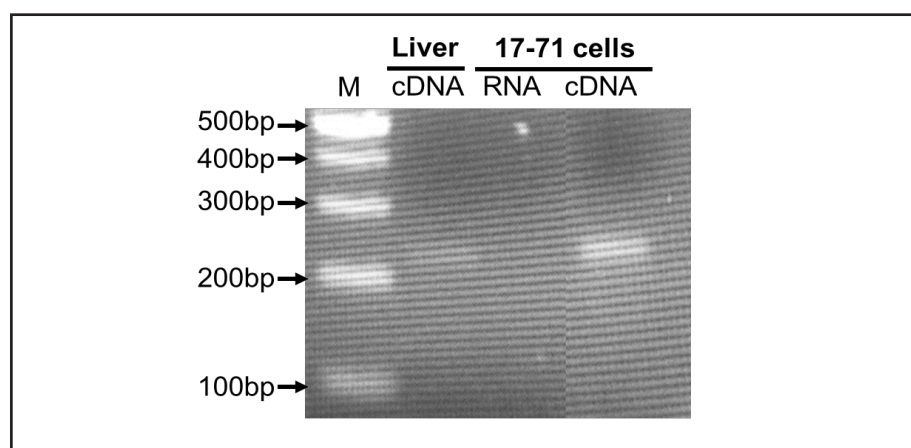


Figure 1. Detection of P-gp mRNA by RT-PCR in 17-71 cells. A single band was visualized for P-gp mRNA at the expected size in 17-71 cells as well as in positive control tissue dog liver. No signal was observed when RNA was used as negative control template. The identity of the band was verified by sequence analysis. M, 100-bp ladder.

RT-PCR analysis

Total RNA was extracted from 17-71 cells using the RNeasy Mini Kit (Qiagen, Valencia, CA). The quality and quantity of the total RNA was assessed using NanoVue Plus Spectrophotometer (GE Healthcare, Pittsburg, PA). Dog liver RNA was provided by Dr. Bruce Smith, Auburn University. Reverse transcription was performed with the QuantiTect Reverse Transcription Kit (Qiagen) to synthesize

complementary DNA (cDNA) from total RNA. This cDNA was subsequently used as a template for polymerase chain reaction (PCR). PCR was performed by using Taq PCR Master Mix Kit (Qiagen) and PCR Detection System (Bio-Rad; Hercules, CA) according to the manufacturer's protocol. Transcripts of the 18S small subunit ribosomal RNA (18S rRNA) housekeeping gene and P-gp were amplified using gene-specific primers (Table 1). Each of the 40 PCR cycles was conducted at 95°C for 30 s, 55°C for 30 s, and 72°C for 30 s. PCR products were electrophoresed on 2% agarose gel and detected by ethidium bromide to check the amplicon size. The specific bands were excised from agarose gels and the PCR products were purified using the gel extraction kit (Qiagen). Purified PCR product was sequenced by Auburn University gene sequencing facility. The sequences were then verified for their identity using the National Center for Biotechnology

Information's (NCBI's) Basic Local Alignment Search Tool (BLAST) program.

Data Presentation and Statistical Analysis

Cell viability data are expressed as percentage of DMSO treated cells (control), where control was set as 100% viability. The vehicle DMSO treatment did not significantly affect cell viability when compared to untreated cells. Data are shown as mean values from at least three independent experiments with bars indicating the standard deviation. The Student's t-test was used to determine statistical significance ($*p < 0.05$) of unpaired samples by comparing the viability of cells treated with DMSO to DIM. In accumulation assays, fluorescence intensity of the samples without R123 was considered as the background. Fluorescence intensity of all the samples with R123 was subtracted with the background fluorescence before data normalization. The efflux activity of P-gp is presented

as relative R123 accumulation by normalizing the fluorescence intensity of the samples with vehicle DMSO, DIM, or PSC-833 to the samples without the vehicle, DIM, or PSC-833. Statistical significance ($*p < 0.05$ vs control) was determined using unpaired Student's t-test.

RESULTS

P-gp Gene Expression in 17-71 Canine B-cell Lymphoid Tumor Cells

Other studies in our lab have shown that only 17-71, but not GL-1, cells are resistant to traditional chemotherapeutic drugs such as VCR and DOX, which are commonly used to treat canine B-cell lymphoma (Dervisis et al., 2007; Fahey et al., 2011; Flory et al., 2008; Griessmayr et al., 2009; Lori et al., 2010; Lymphoma, n.d.; Moore et al., 1999; Northrup et al., 2009; Rassnick et al., 2002; Rebhun et al., 2011). These observations led us to ask whether the chemoresistant 17-71 cells express P-gp, which is known to be associated with chemoresistance in canine B-cell lymphoma (Fan, 2003; Lee et al., 1996; Moore et al., 1995; Steingold et al., 1998; Uozurmi et al., 2005). Indeed, the transcript for P-gp was detected in 17-71 cells (Figure 1). Dog liver was used as a positive control for P-gp gene expression.

Effect of DIM on Viability of the Lymphoid Tumor Cells

Some dietary supplements are known to exert antitumorigenic properties by inducing selective

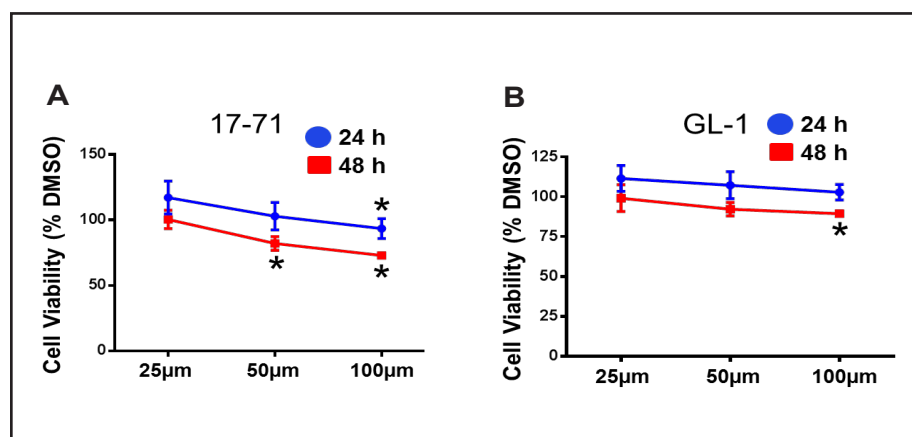


Figure 2. Effect of DIM on viability of canine B-cell lymphoid tumor cells. Cell viability was measured after treating 17-71 (A) and GL-1 (B) cells with vehicle DMSO or increasing concentrations of DIM as indicated for 24 or 48 h. Data are presented as mean \pm SD of three separate experiments ($*P < 0.05$ determined by Student's unpaired t-test).

cytotoxicity in tumor cells. Recently, DIM has been shown to exert antitumor actions in a variety of human cancer cells (Azmi et al., 2008; Biersack and Schobert, 2012; Chen et al., 2012). We studied the effect of DIM on viability of the lymphoid tumor cells. DIM was found to be non-cytotoxic to 17-71 cells at 25 μ M treatment for 24 or 48 h, although it was cytotoxic at higher concentrations (Figure 2A), suggesting that DIM is nontoxic at physiologically relevant concentrations (up to 20 μ M) (Anderton et al., 2004a; Anderton et al., 2004b; Fan, Meng, Saha, Sarkar, & Rosen, 2009; Moiseeva, Almeida, Jones, & Manson, 2007; Reed et al., 2006; Reed et al., 2008), but can inhibit the growth of the lymphoid tumor cells at supraphysiological concentrations. Similarly, DIM was found to be non-cytotoxic to GL-1 cells at its physiologically relevant concentrations (Figure 2B).

DIM is Not a Fluorescent Substrate

DIM, similar to DMSO, did not exhibit a noticeable intracellular fluorescence in 17-71 cells in intracellular substrate accumulation assays (Figure 3). In contrast, treatment with fluorescent dye R123, a substrate of P-gp, resulted in a significant increase in intracellular fluorescence (Figure 3). Together, these results suggest that only R123, but not DIM, behaves as a fluorescent substrate in our experimental conditions.

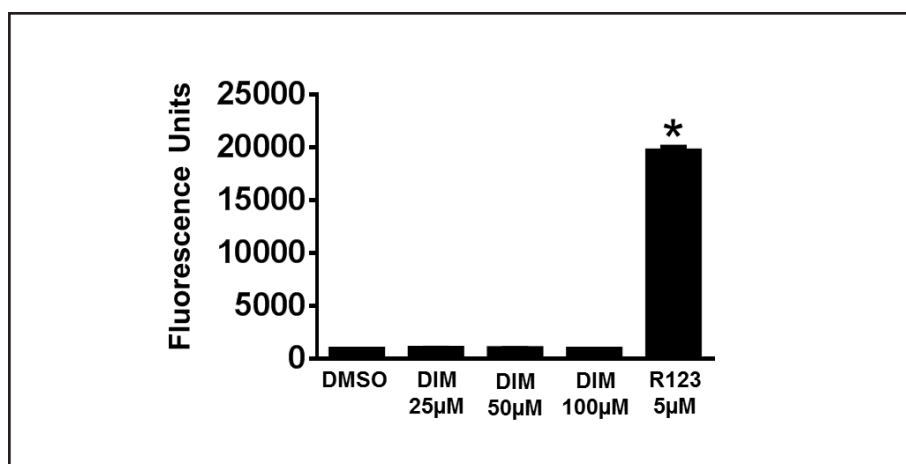


Figure 3. Effect of DIM on intracellular fluorescence in 17-71 cells. Intracellular fluorescence was measured in 17-71 cells after treating with DMSO, DIM, or R123 for 1 h. The data are presented as mean \pm SD of four independent observations (* $P < 0.05$).

Effect of DIM on the Efflux Activity of P-gp

Chemoresistance in a variety of cancers is associated with upregulation of expression/function of multidrug transporters, particularly P-gp (Borst et al., 2000; Chen, 2010; Marzac et al., 2011; Pondugula and Mani, 2013). It is known that some dietary supplements suppress chemoresistance by downregulating the expression/activity of multidrug transporters (Borst et al., 2000; Gelsomino et al., 2013; Kuan, Walker, Luo, & Chen, 2011; Okamura et al., 2004; Rahman, Veigas, Williams, & Fernandes, 2013; Sharom, 2008; Sodani et al., 2012). Chemoresistance in canine lymphoma was shown to be associated with P-glycoprotein (P-gp) (Fan, 2003; Lee et al., 1996; Moore et al., 1995; Steingold et al., 1998; Uozurmi et al., 2005). Recently, it was shown in DOX-resistant canine lymphoid tumor cells that Masitinib, a tyrosine kinase inhibitor, reversed DOX

resistance by inhibiting the function of P-gp (Zandvliet et al., 2013).

We tested whether DIM can inhibit the function of P-gp in the chemoresistant 17-71 lymphoid tumor cells. Intracellular accumulation of the fluorescent dye R123, a substrate of P-gp, was used to study the efflux activity of P-gp. Treatment of 17-71 cells with PSC-833, a prototypical inhibitor of P-gp, resulted in a significant increase in intracellular accumulation of P-gp substrate R123 (Figure 4A). This result suggests that the chemoresistant 17-71 cells functionally express P-gp. On the other hand, in the chemosensitive GL-1 cells, there was no change in R123 accumulation after PSC-833 treatment (Figure 4B), suggesting that GL-1 cells lack functional P-gp expression. The absence of functional P-gp system in GL-1 cells is in agreement with a previous report (Zandvliet et al., 2013) and is also consistent with lack of resistance towards VCR

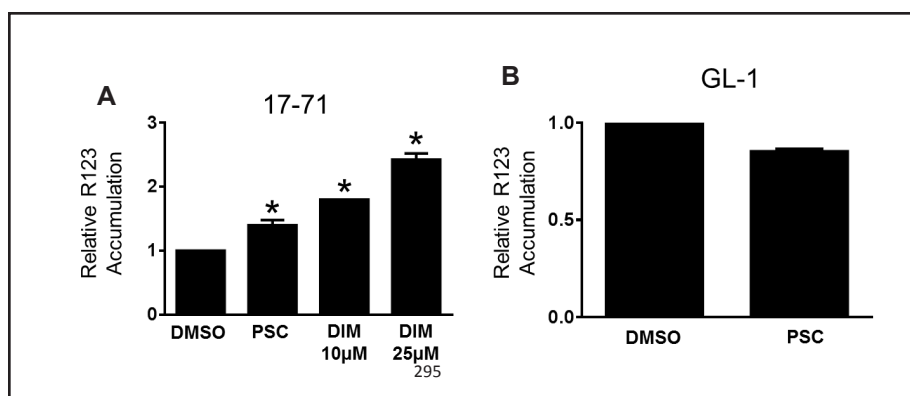


Figure 4. Effect of DIM on intracellular R123 accumulation in canine B-cell lymphoid tumor cells. R123 fluorescence was measured in 17-71 and GL-1 cells in the absence or presence of DMSO, DIM, or P-gp specific inhibitor PSC-833. Relative R123 accumulation was determined by normalizing the fluorescence in the absence or presence of DMSO, DIM, or PSC-833, as described in the methods. The data are presented as mean \pm SD of four independent experiments (* $P < 0.05$).

and DOX induced cytotoxicity in the other studies in our lab. Similar to PSC-833, DIM at its non-cytotoxic physiologically relevant concentrations, 10 and 25 μ M, considerably increased the intracellular accumulation of R123 in 17-71 cells, suggesting that DIM inhibits the efflux activity of P-gp in 17-71 cells.

DISCUSSION

To our knowledge, our study is the first to report DIM at its physiologically relevant concentrations could inhibit the activity of P-gp in any chemoresistant cancer cell line. This study identifies a natural dietary supplement that inhibits the efflux activity of P-gp in the chemoresistant canine lymphoid tumor cells.

DIM is not only a health supplement, but also the major active metabolite of I3C (Anderton et al., 2004b), which is also a health supplement and naturally occurring compound enriched in cruciferous vegetables such as broccoli, cabbage, and

cauliflower (Bonnesen et al., 2001). It is noteworthy that the acidic environment of the stomach fosters the non-enzymatic self-condensation of about 20% I3C to form DIM (Spande, 1979; Stresser, Williams, Griffin, & Bailey, 1995). Therefore, DIM could be taken as a direct supplement, indirectly in the form of I3C as a supplement, or through I3C-rich cruciferous vegetables.

While its therapeutic potential has been well emphasized, the plasma concentration of DIM is not fully evaluated. While DIM was being tested in several *in vitro* studies at concentrations ranging from 1-100 μ M, up to 20 μ M has been reported as physiological concentration of DIM as these concentrations would be comparable with serum or tissue concentrations achievable *in vivo* in humans/rodents (Anderton et al., 2004a; Anderton et al., 2004b; Fan et al., 2009; Moiseeva et al., 2007; Reed et al., 2006; Reed et al., 2008). Together, based on published *in vitro* and *in vivo* studies, our

results show that DIM can inhibit P-gp activity at its physiologically relevant concentrations.

The mechanism of DIM inhibition of P-gp is unknown, although it is possible that it can directly inhibit the activity of P-gp by serving as a substrate of P-gp, like other P-gp inhibitors such as PSC-833. The results of our research suggest that DIM can be administered in combinatorial chemotherapeutic treatment as a means to overcoming chemoresistance by blocking P-gp activity in chemoresistant lymphoid tumor cells. However, it remains to be determined whether DIM sensitizes the chemoresistant lymphoid tumor cells, including 17-71 cells, to chemotherapy drugs such as VCR and/or DOX. Our future studies will address these questions.

ACKNOWLEDGMENTS

The authors thank Dr. Steven Suter (North Carolina State University) for providing 17-71 and GL-1 cell lines, Dr. Bruce Smith (Auburn University) for providing dog liver total RNA, and Drs. Tao and Irwin for sharing the microplate reader. This work was supported by funding through Auburn University Start-up Funds, Scott-Ritchey Research Center Research Program Grant, and Auburn University Research Initiative in Cancer Grant to S.R. Pondugula.

REFERENCES

[Click here to view references at the end of the journal.](#)

Evaluating the Novel Role of Tryptophan 438 in Active Turnover of *Mycobacterium tuberculosis* Catalase-Peroxidase

Ethan McCurdy, Lauren Barr, Olive Njuma, Elizabeth Ndontsa, and Douglas Goodwin

ABSTRACT

Catalase-peroxidase (KatG) is an enzyme capable of utilizing both catalase and peroxidase activity to break down hydrogen peroxide. Catalase activity by the enzyme generally dominates, but peroxidatic electron donors have been shown to stimulate catalase activity, likely by rescuing catalase-inactive intermediates resulting from off-pathway electron transfer. To investigate tryptophan 438 as a potential conduit for this misdirected transfer, a variant form of the enzyme (W438F), which contained a phenylalanine in place of the tryptophan, was produced by site-directed mutagenesis, expressed, and purified. Catalase and peroxidase activities were measured via UV-Vis spectrophotometry, and catalase activity was also monitored by oxygen production. We observed a threefold increase in catalase activity by the variant as compared to wild-type KatG. Additionally, W438F displayed a threefold decrease in peroxidase activity. These results are consistent with

the possibility that off-pathway electron transfer could occur by this route, as the phenylalanine substitution would obstruct this oxidizable passage and cause a diminished requirement for the peroxidatic rescue event. However, oxygen production data also revealed stimulation of catalase activity by peroxidatic electron donors at pH 5, and further investigation is needed to understand this pathway.

INTRODUCTION

The enzyme catalase-peroxidase (KatG) is found in a wide range of lower eukaryotes and bacteria, including *Mycobacterium tuberculosis*. KatG from *M. tuberculosis* (MtKatG) has received the most attention because it is required for the activation of the frontline antitubercular agent isoniazid. An alarming trend in tuberculosis has been the increasing prevalence of multi- and extensively drug-resistant strains (World Health Organization, 2013). Isoniazid is one of the most widely used treatments against tuberculosis, but over 70% of the

M. tuberculosis strains resistant to isoniazid are the result of mutations to the KatG gene (Jagielski et al., 2013). In all organisms that carry it, the primary function of KatG is to degrade hydrogen peroxide (H_2O_2). Due to its potential to damage cellular components and create free radicals, H_2O_2 must be removed by all organisms that live in an aerobic environment. Pathogens in particular require a mechanism to decompose H_2O_2 because this compound is a central player in host immune responses. KatGs are found in a number of human and plant pathogens, and they are often associated with other events and virulence factors (Bandyopadhyay & Steinman, 2000; Brunder et al., 1996; Garcia et al., 1999).

Throughout biology there are two principal mechanisms for H_2O_2 decomposition, catalase and peroxidase. In a typical catalase reaction, one unit of H_2O_2 is reduced to H_2O , followed by the oxidation of a second unit of H_2O_2 to produce molecular oxygen (O_2) (Reaction 1). The first step of the peroxidase pathway similarly

involves the reduction of H_2O_2 , but in the second step an exogenous electron donor is oxidized instead (Reaction 2).

Reaction 1:



Reaction 2:



Interestingly, there is almost no overlap between these two pathways. That is, enzymes with robust catalase activity are uniformly poor as peroxidases and *vice versa*. KatG stands as the lone exception as it is capable of both activities.

After intense investigation, it is clear that KatG carries out its catalase activity by a mechanism distinct from typical monofunctional catalases, but this mechanism and its interplay with the enzyme's peroxidase mechanism remain elusive (Njuma et al., 2014). However, each mechanism yet proposed predicts mutual antagonism between KatG's catalytic and peroxidatic mechanisms. That is, peroxidatic electron donors should inhibit KatG catalase activity. Contrary to these predictions, we have previously shown that peroxidatic electron donors can stimulate catalase activity by an order of magnitude (Ndontsa et al., 2012).

KatG is a heme protein, and although its mechanism is not yet understood completely, it is known that a series of highly reactive and oxidizing intermediates is involved, including ferryl iron states (i.e., $\text{Fe}^{\text{IV}}=\text{O}$) as well as

heme- and protein-based free radicals (Njuma et al., 2014). KatG has been shown to contain a novel structure where the side chains of a tryptophan (W), a tyrosine (Y), and a methionine (M) are covalently linked to produce a MYW adduct (Yamada et al., 2002). The MYW adduct appears to function as a redox-cycling cofactor in KatG, alternating between its fully covalent (reduced) and free radical (oxidized) states. Due to these highly reactive and oxidizing intermediates, there exists a possibility for off-pathway electron transfer, where one of these compounds incorrectly oxidizes another part of the protein. Having improperly gained an electron, the enzymatic intermediate would become functionally inactive and unable to continue its cycle, resulting in the loss of activity. However, a peroxidatic electron

may be able to return this catalase-inactive intermediate to the resting ferric form to once again participate in active turnover. In this manner, the peroxidatic donor would serve to "rescue" the enzyme, resulting in the observed stimulation of catalase activity. Peroxidase activity itself, then, could actually be considered a manifestation of misdirected electron transfer that occurs during catalytic turnover (Ndontsa et al., 2012).

One potential route for misdirected electron transfer would be tryptophan 438 (W438). This residue is located near the surface of the protein, allowing for access to exogenous electron donors (Figure 1). W438 is also in close proximity to arginine 418 (R418), which is known to undergo a pH-dependent conformational shift that could potentially permit increased off-pathway electron

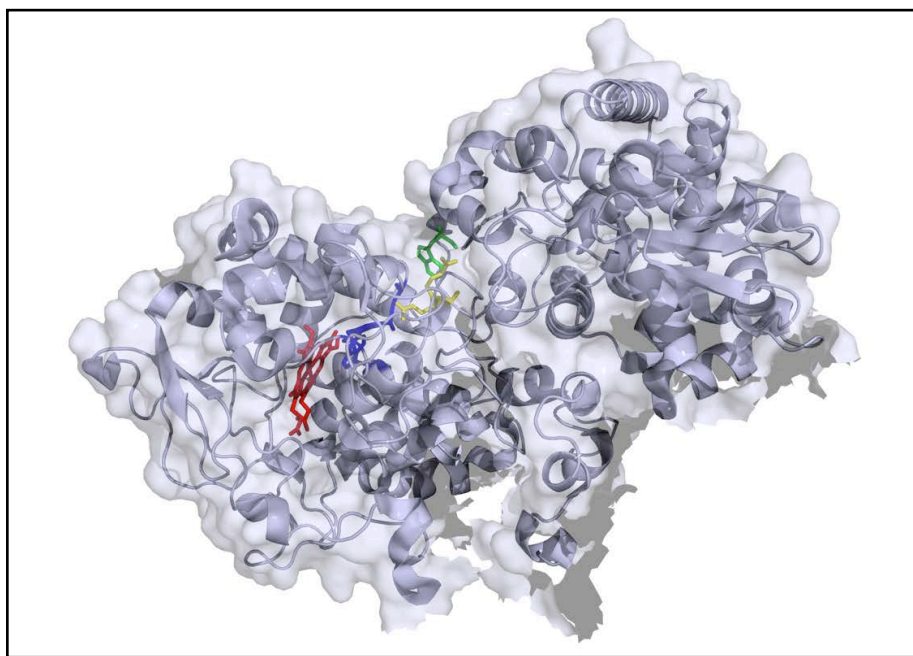
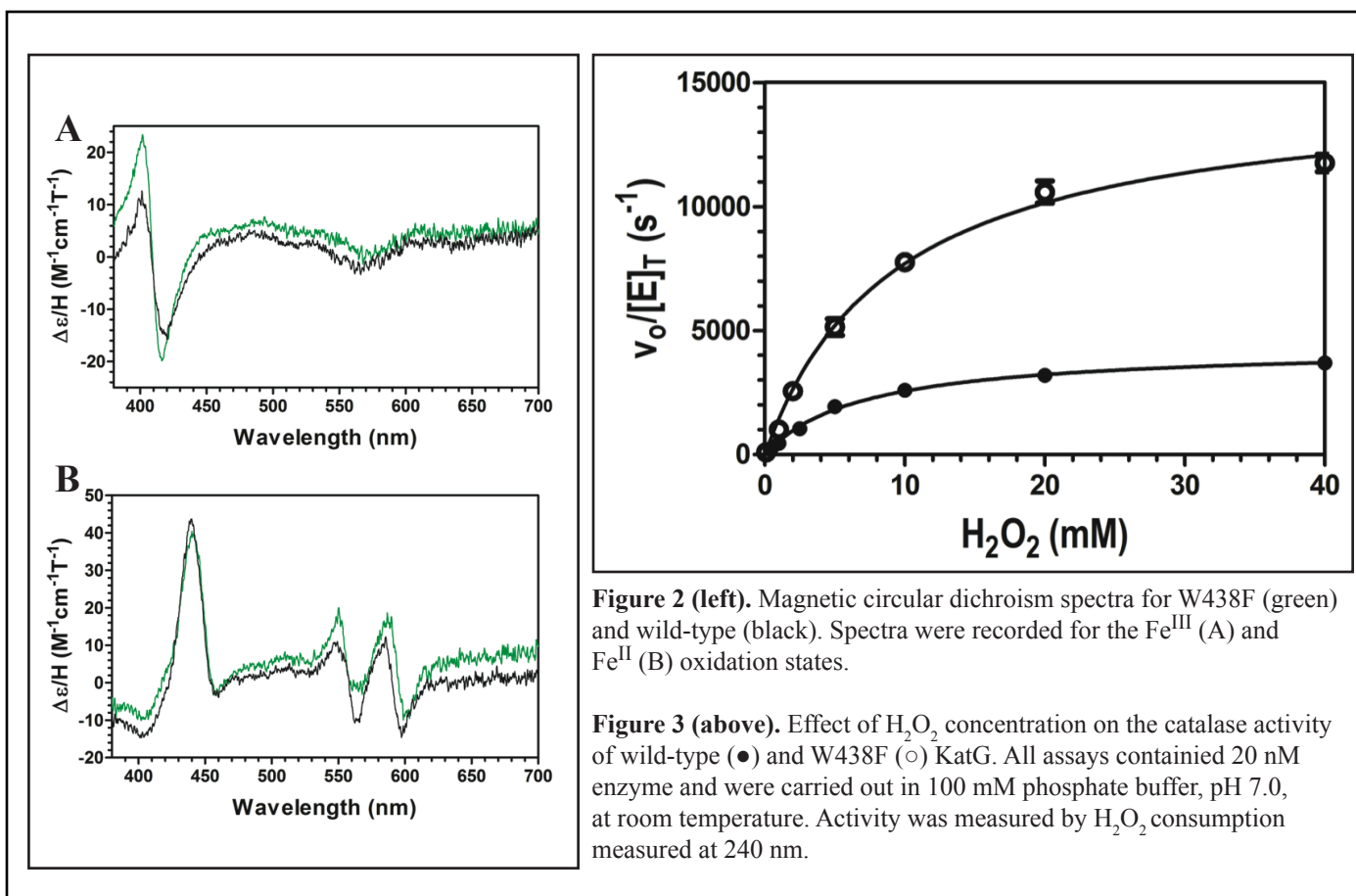


Figure 1. Single subunit of MtKatG. The W438 is shown in green, R418 in yellow, the MYW adduct in blue, and the heme is shown in red. PDB accession number 2CCA (Zhao et al. 2006).



transfer (Carpena et al., 2006; Zhao et al., 2012). To evaluate W438 as an off-pathway electron transfer route, we used site-directed mutagenesis to replace W438 with phenylalanine (F), producing W438F KatG. By replacing oxidizable tryptophan with a non-oxidizable phenylalanine, this route for electron transfer would be blocked. As a result, fewer inactive intermediates would accumulate and require rescue by peroxidatic electron donors. As such, the W438F KatG variant would be expected to exhibit increased catalase and decreased peroxidase activity as compared to the wild-type enzyme.

EXPERIMENTAL METHODS

Mutagenesis, Expression, and Purification of the W438F Variant

All materials were purchased as described previously (Ndontsa et al., 2012). Site-directed mutagenesis also followed the procedure outlined in prior reports (Wang & Goodwin, 2013). The primers TTCAAGATCCGGTCCCTGCG & CAGGGTCTGCTTGGGGAC, which contained a phenylalanine codon replacing that of the tryptophan, were used to introduce the mutation. Plasmids were screened by restriction digests using BamHI and HindIII. Candidate plasmids were sent to Davis

Sequencing for sequence analysis, where it was confirmed that the only substitution occurred at the 438 site. Expression of the W438F variant was carried out using C41 [DE3] cells bearing the pHPEX3 plasmid (Varnado & Goodwin, 2004) as previously described for wild-type *MtKatG* (Ndontsa et al., 2012). Briefly, Luria-Bertani medium was supplemented with ampicillin (100 µg/mL) and tetracycline (20 µg/mL). Cultures (1 L) were grown to mid-log phase (OD₆₀₀ 0.4-0.6), at which point expression was induced by addition of 1 mM isopropyl-β-D-thiogalactopyranoside (IPTG). Hemin (8 µM) was also added at the time of induction to ensure that the protein expressed would include its heme prosthetic group.

At four hours post-induction, cells were harvested by centrifugation and cell pellets stored at -80°C until purification. Analyses of the expression revealed that W438F KatG was expressed in a soluble form. Therefore, purification of the protein was carried out by nickel affinity and anion-exchange chromatography as previously described for the wild-type enzyme (Ndontsa et al., 2012).

Magnetic Circular Dichroism (MCD)

All spectra were obtained using 15 μM enzyme in 50 mM phosphate, pH 7.0, 50 mM NaCl. Spectra were measured using a Jasco J-810 spectropolarimeter (Tokyo, Japan) using a 1.4 Tesla magnetic cell holder. The ferrous state was obtained by the addition of sodium dithionite.

Peroxidase and Catalase Activity Assays

Peroxidase activity was measured by monitoring the production of 2,2'-azino-bis(3-ethylbenzothiazoline-6-sulfonate) (ABTS) radical over time at 417 nm ($\epsilon_{417} = 34.7 \text{ mM}^{-1} \text{ cm}^{-1}$) (Scott et al., 1993). Initial velocities were determined for a range of H_2O_2 concentrations while enzyme (20 nM) and ABTS (0.1 mM) concentrations were held constant. Apparent kinetic parameters were determined by non-linear least squares fitting of the initial velocities to the Michaelis-Menten equation. All assays were carried out at ambient temperature in 50 mM acetate, pH 5.0 using

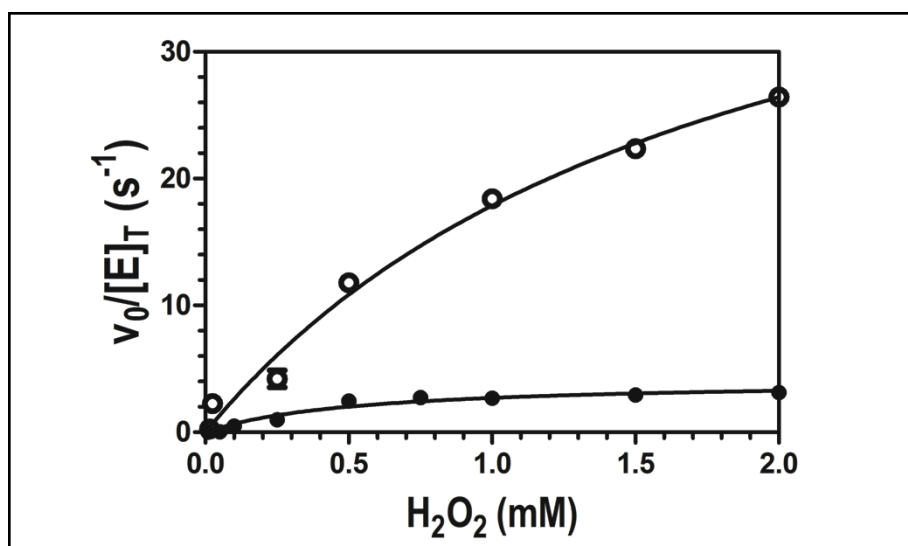


Figure 4. Effect of H_2O_2 concentration on the peroxidase activity of wild-type enzyme (\circ) and W438F (\bullet) KatG. All assays contained 20 nM enzyme and 0.1 mM ABTS, and were carried out in 50 mM acetate, pH 5.0, at room temperature. Activity was measured by ABTS oxidation monitored at 417 nm.

a UV-1601 spectrophotometer (Shimadzu, Columbia, MD).

Catalase activity was measured by two methods. The first monitored the decrease in H_2O_2 spectrophotometrically at 240 nm ($\epsilon_{240} = 39.4 \text{ M}^{-1} \text{ cm}^{-1}$) (Nelson & Kiesow, 1972). All assays contained 20 nM enzyme and were carried out at room temperature in 100 mM phosphate, pH 7.0. The second monitored O_2 production by Clark-type O_2 -sensitive electrode. Sodium dithionite and N_2 were used to calibrate the instrument and initially establish zero O_2 in the reaction chamber. All reactions were carried out at room temperature with either 2 or 5 nM enzyme in either 50 mM acetate, pH 5.0 or 100 mM phosphate buffer, pH 7.0. A 20-second baseline was obtained for each assay mixture prior to the addition of H_2O_2 . H_2O_2 was then added and O_2 production monitored.

RESULTS AND DISCUSSION

The W438F KatG variant was expressed in a soluble form and purified. Because the protein contains heme, a UV-Vis spectrum for the enzyme-bound heme was taken and used to verify the purity of the enzyme. The spectrum for the heme was virtually identical to that of wild type KatG, and the ratio of heme absorbance to general protein absorbance (A_{408}/A_{280}) was consistent with a highly purified preparation of the enzyme (data not shown). To further evaluate the heme environment and thus the structural integrity of the enzyme, magnetic circular dichroism (MCD) was employed. Spectra for the Fe^{III} and Fe^{II} states of W438F KatG showed that the protein contained heme with its iron in a high-spin state, and these spectra were nearly superimposable on

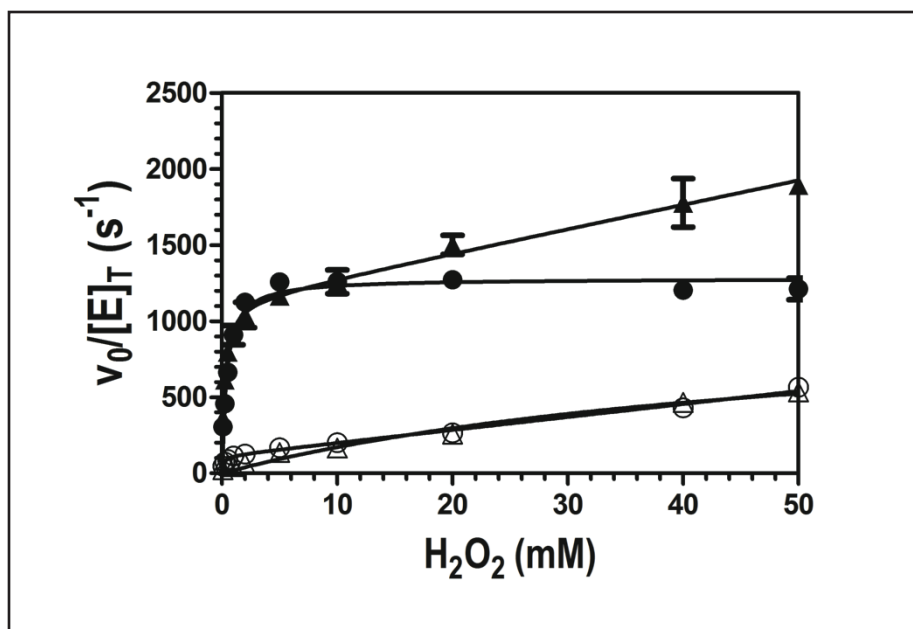


Figure 5. Effect of the electron donor ABTS on catalase activity at pH 5.0. Activity was monitored by measuring O_2 production for W438F in the presence (\blacktriangle) and absence (\triangle) of 0.1 mM ABTS. The same was carried out wild type in the presence (\bullet) and absence (\circ) of 0.1 mM ABTS. All W438F reactions contained 2 nM enzyme, and wild-type KatG reactions contained 5 nM enzyme. All assays were carried out in 50 mM acetate buffer, pH 5.0, at room temperature.

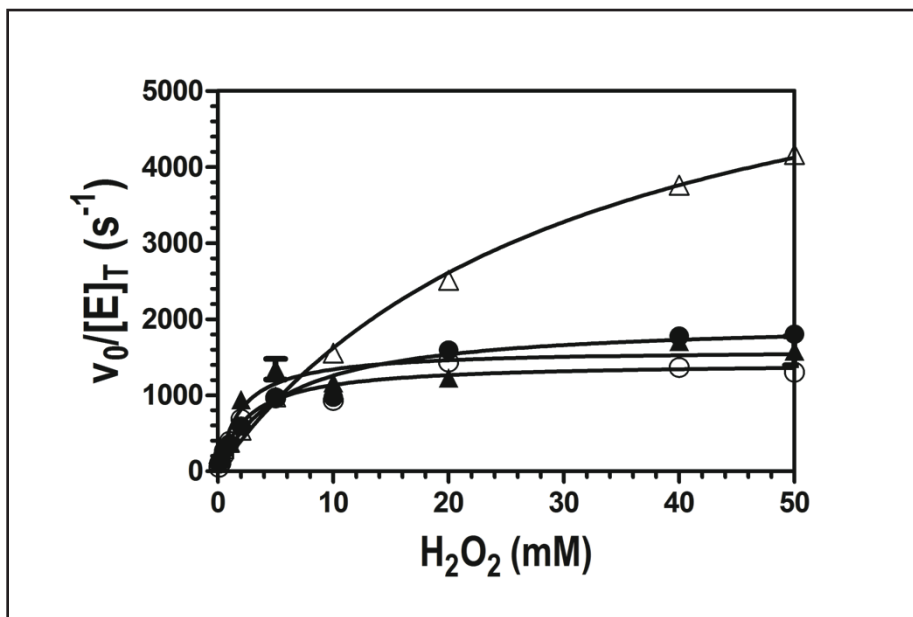


Figure 6. Effect of the electron donor ABTS on catalase activity at pH 7.0. Activity was monitored by measuring O_2 production for W438F in the presence (\blacktriangle) and absence (\triangle) of 0.1 mM ABTS. The same was carried out wild type in the presence (\bullet) and absence (\circ) of 0.1 mM ABTS. All W438F reactions contained 2 nM enzyme, and wild-type KatG reactions contained 5 nM enzyme. All assays were carried out in 100 mM phosphate, pH 7.0, at room temperature.

those of wild-type KatG (Figure 2). All of these results pointed to the robust expression of a properly folded KatG indicating the W438F substitution had not produced a global disruption of the KatG structure.

The variant showed about a threefold increase in catalase activity as compared to the wild-type enzyme (Figure 3). The effect of H_2O_2 concentration on catalase activity showed a catalytic efficiency with respect to H_2O_2 (i.e., k_{cat}/K_M) of $1.6 \times 10^6 M^{-1}s^{-1}$ for the variant *versus* $6.2 \times 10^5 M^{-1}s^{-1}$ for the wild type. In terms of the maximum catalytic output of the enzyme (i.e., k_{cat}), W438F exhibited $1.5 \times 10^4 s^{-1}$ *versus* $4.4 \times 10^3 s^{-1}$ for the wild-type.

In contrast, peroxidase activity diminished threefold as a result of the phenylalanine substitution (Figure 4). In particular, the wild type displayed a k_{cat}/K_M with respect to H_2O_2 of $2.8 \times 10^4 M^{-1}s^{-1}$, significantly higher than that of W438F, $7.9 \times 10^3 M^{-1}s^{-1}$. The difference was even more striking in k_{cat} , with a value of $4.123 s^{-1}$ obtained for the variant, as opposed to $50.72 s^{-1}$ for the wild type. These findings are in keeping with the original hypothesis, which predicted increased catalase activity by the variant as a result of decreased off-pathway electron transfer. Similarly, peroxidase activity was predicted to decrease due to a diminished need for the peroxidatic rescue mechanism.

Catalase activity was also monitored by O_2 production, allowing for measurement of catalase activity even in the presence of a peroxidatic electron donor. The overwhelming absorbance of these compounds where H_2O_2 consumption is typically measured prohibits the use of the spectrophotometric method for these experiments. Previous data have shown that optimal unassisted catalase activity occurs at pH 7, while maximal peroxidase activity and electron donor stimulated catalase activity occur at approximately pH 5 (Moore et al., 2008). Accordingly, the rate of O_2 production by the enzyme was monitored at these two pH values to determine the effects of pH and an electron donor on the catalase activity of wild-type and W438F KatG.

At pH 5, the variant and wild type alike showed substantial stimulation upon addition of an electron donor (Figure 5). However, there appears to be little difference in enzymatic activity between the wild type and W438F in either situation. Interestingly, the behavior of both the wild type and W438F slightly deviated from standard Michaelis-Menten kinetics, in a similar manner but under different conditions. Both enzymes displayed an initial hyperbolic response in activity, which became linear at higher concentrations of H_2O_2 . This behavior was displayed by the wild type at pH 5 in the absence of electron donors, but by W438F at pH 5 only when electron donors were present. In contrast, at pH 7 the addition of electron donor

inhibited W438F catalase activity (Figure 6). In the absence of an electron donor at pH 7, W438F displayed a greater rate of O_2 production (i.e., catalase activity) than the wild type enzyme. Without the complications of off-pathway transfer, we would expect similar inhibition by electron donor as the result of peroxidase activity competing with catalase activity. However, the pH 5 data show that catalase activity by the variant was enhanced by the electron donor.

The data obtained thus far from the W438F variant have illuminated a novel aspect of the overlap between the catalytic and peroxidatic mechanisms of KatG. This variant exhibits increased catalase activity and decreased peroxidase activity as compared to the wild-type enzyme. If indeed the W438 residue is a route of off-pathway electron transfer, the presence of phenylalanine in place of tryptophan would prevent its oxidation by ferryl iron, the MYW adduct radical, or similarly reactive intermediates. With decreased electron transfer, fewer catalase-inactive intermediates would accrue and there would be a diminished need for peroxidatic rescue events. Concomitantly, as a result of lesser accumulation of inactive intermediates, the enzyme would be able to complete and then repeat its catalytic cycle more easily and efficiently. As such, these data support the original hypothesis.

Nevertheless, further evaluation is needed to determine the extent of the effects of pH and electron donors. In addition to more steady-

state kinetic analyses, techniques such as stopped-flow spectrometry and rapid freeze-quench electron paramagnetic resonance should be employed to examine the effects of the W438F substitution. These methods will allow an in-depth examination of which heme, MYW adduct, and protein radical intermediates predominate during and following H_2O_2 decomposition. The high frequency of oxidizable amino acids in the structure of KatG suggests that the process of off-pathway electron transfer may involve multiple residues. Therefore, other amino acids ought to be evaluated to understand this multipartite pathway. One notable candidate is tyrosine 113 (Y113), which is immediately adjacent to W438 and in close proximity to R418 within the KatG structure. With this in mind, we will continue to focus our efforts on investigating these routes to better understand the dynamic interplay between the catalytic and peroxidatic mechanisms of KatG.

ACKNOWLEDGMENTS

Ethan McCurdy was supported as an Auburn University Undergraduate Research Fellow, and Lauren Barr was supported as a Marks Family Research Scholar. We also wish to thank our lab colleagues, both current and former, who have been of extensive help in advancing this project.

REFERENCES

[Click here to view references at the end of the journal.](#)

Password Storage in Databases: Best Practices

Robert Sanek

ABSTRACT

In the past few years, security breaches of the networks of large online companies have exposed millions of user passwords. Though typically stored in an incomprehensible ‘hashed’ format, researchers (and bad actors) can recover the original, plaintext passwords from leaks by applying well-known cracking techniques. When this occurs, the original, single-company data breach increases in scope; no longer are accounts exclusively relevant to the source company insecure, but since users frequently use the same email/password combinations on multiple websites, attackers are able to gain access to accounts on services not directly affected by a security inconsistency. Such spillover effects can affect any website that uses a user account system.

Generally, the companies exploited have employed either insufficient or imperfect protections of user data, either by storing passwords in plaintext, using hashing algorithms not meant for password storage, or by applying poorly-selected encryption to passwords.

In this review, we introduce the question of user authentication and discuss common password storage techniques. An examination of common hashing algorithms used in password storage follows. We close with possible mitigation measures users can utilize in order to minimize the effect a data breach has on their online presence as a whole.

INTRODUCTION

When a company decides it wants to provide more user customization on a website, it has a few options. One is to use cookies, which can track user behavior over different browsing sessions and can store information over extended periods of time. However, cookies are ephemeral (clients can erase them), unreliable (they do not persist over different browsers), and cannot be trusted (they are stored client-side; a user can modify cookies to whatever they want). Even with these drawbacks, cookies are a popular way to provide simple customization on a website.

However, when an online property wants a more robust system with

many capabilities, they turn to the concept of users. A user can then customize a website according to his or her pleasure, and data between different users is separated for privacy. The question then becomes, “How can I identify and authenticate an individual user?”

Overwhelmingly, website operators have chosen to utilize the concept of a password associated with a user account or email address. This works reasonably well at keeping out unwanted users and validating legitimate ones. Over time, however, numerous drawbacks to this system have been discovered.

One such problem is user password memory. If there are only a handful of passwords a user is expected to remember, this is tenable. But as websites become more numerous and users gain in the amount of accounts they must maintain, it becomes difficult to keep track of the different username/password combinations a person has used. Users counter this by re-using passwords across services. This is a legitimate approach, but becomes problematic if an account on any service is compromised; now, all

accounts on services that share credentials with the initial breach can be accessed.

Additionally, passwords that are easy to remember are generally weak passwords. Passwords based on English words, words relating to the specific website in question, and proper nouns are particularly poor choices. Length also has much to do with the strength of a password, and longer passwords are more difficult to remember. In the end, the only true 'secure' password is a long, randomly-generated string of characters. These types of passwords are the most difficult to remember.

Another problem deals with password storage and validation. How should a website operator validate a user when logging in? Generally, this is done through some comparison of the given password to the password that is found in the database (which was saved at account creation). Unfortunately, storing passwords in plaintext is not good security practice, so methods have been developed that try to mitigate the impact of a password breach. The different options available and the ones companies ultimately choose are detailed here.

PASSWORD STORAGE

There are many ways to store passwords in an online database. The leaks provided here exemplify typical storage schemes companies utilize. Unfortunately, none of them are considered safe and none conform to currently-accepted best

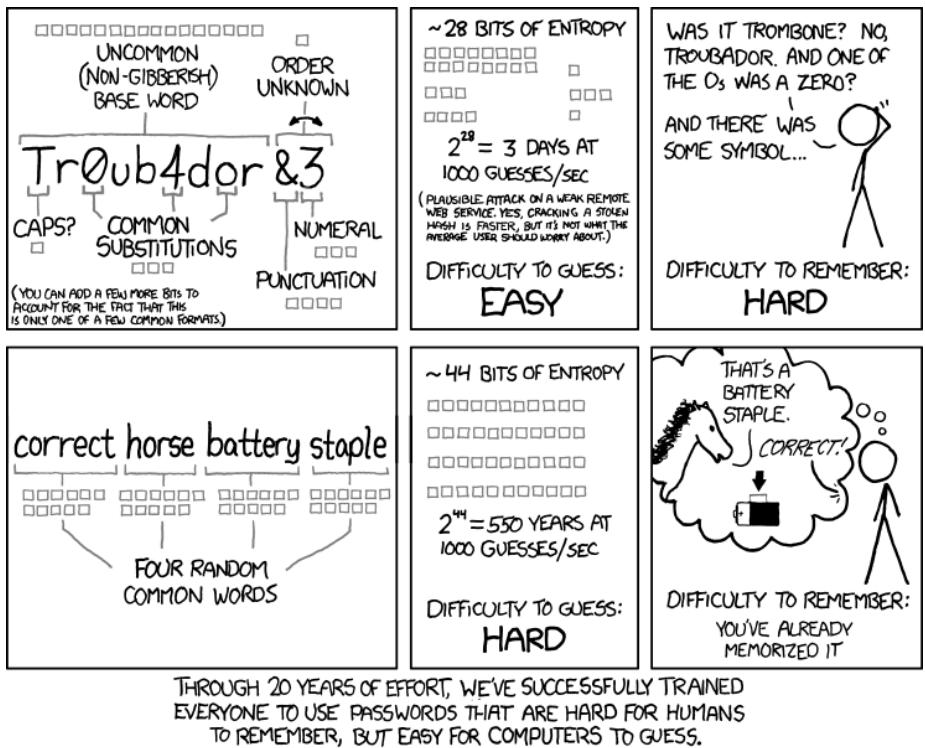


Figure. Password Strength (Munroe 2011).

practices. Below, an examination of the various techniques is given.

PLAINTEXT

Storage of passwords in plaintext is exactly what it sounds like – the password for each user is stored in the database with no encryption, hashing, or transformations of any kind. This means that if the database is ever leaked, the passwords will be exposed without any additional work. Additionally, anyone that has access to the database can see what password each individual user has selected for this site. In a system that adheres to best practices, this should not be possible.

Validation is performed with a simple comparison of the attempted string with the stored password string. If they match, the user is authenticated.

This is by far the worst option for storing passwords. No company should be using this storage scheme because it puts users at a high risk and forces them not only to trust the company's database security but also the database administrators themselves. Since the passwords are viewable by anyone with access to the database tables, a rogue administrator could steal passwords and misuse them.

HASHED PASSWORDS

In this storage scheme, a password is put through a one-way hash function before being stored in the database. In general, a hash function is an algorithm that maps data of a variable length to data of a fixed length ("Cryptographic hash function," 2013). Different inputs to the hash function should always produce differing hash values, and

the same input to the hash function should consistently produce the same value.

Hash functions are frequently used for simple data verification. For example, when a user is downloading a file from a server, the website administrator will provide a hash value for that file. When the download is complete, the user can run the local file through the same hash function to see if it produces a value that matches the one posted. If the values match, then the download completed successfully and no modification of the file has been detected. However, if the values do not match, the user has downloaded a file that is in some way different from the one that the website administrator has posted. This could mean that the download did not complete successfully, or, if it did, that the website has been compromised and the true file has been replaced by an alternative one.

This same concept applied to passwords forms the next level of password storage. There are many different hashing functions, and selection of a correct hashing function is critical to the secure storage of passwords.

Typically, hash functions are designed to be as fast and simple as possible – since they are used for things such as data validation (as in the example above), a faster algorithm means less resource usage and a better user experience. Functions of this nature include MD5 and SHA-1, two common algorithms that are used for storage of hashed passwords.

Unfortunately, when applied to password hashing, the algorithm that is chosen should be one designed to be slow, not fast. The reason has to do with what happens when a data breach does occur. When a cracker gets access to a list of millions of hashed user passwords, the next goal is to recover the plaintext version of these passwords. However, hash functions are meant to be one-way; their output does not suggest anything about the original input. This means that the attacker must continually “guess” various passwords, running them through the hash function each time and then comparing the value to the list of hashed passwords. If two hashes match up, the plaintext version of the password corresponds to the one the attacker just used to create this hash value. Additionally, since the same string will always hash to the same value, users with the same password hash will also have the same originating password. Through billions of attempts and comparisons, an attacker can eventually expect to recover 80-95% of such a list, depending on how persistent the attack is and what password policy the website in question had in place.

It is obvious why a slower algorithm is preferred to a faster one: if the amount of time it takes to compute a specific hash value is increased, the amount of guesses an attacker can try in a given amount of time is lowered. This is why different hashing algorithms have different applications – some should be optimized for speed, but some should not.

With hashes, a user is authenticated by comparing hash values. The user enters the password, the system passes the password through the chosen hashing algorithm, and compares it to the hash stored in the database. If they match, this user has provided a valid password.

Hashing also shields users from prying database administrators. Since the hash value does not reveal anything about the original plaintext password, a person with access to the database would have to employ a similar password-cracking strategy to recover a user’s original password.

HASHED AND SALTED PASSWORDS

A step up from simple password hashing is the current best-practice, salting and then hashing. This approach is similar to hashing-only, but includes adding a cryptographic “salt” to the password before passing it through a hash function. Typically, this involves concatenating a random string to the beginning or end of the original password. This string is stored alongside the username in the database in plaintext.

Salting a password does not provide any additional security on a per-user basis, since the salt is known and will be leaked along with the hashed password in a data breach. However, it increases the amount of time an attacker has to dedicate to cracking the entire database. Since each hashed password now includes random additional characters, the attacker cannot simply compare his guess to the entire list and crack

multiple passwords at once, as he was able to with hashing-only. In other words, if two users share the same password, they will not hash to the same value, unlike with simple hashing (assuming that the salt is unique).

Since the salt is known and should be unique, one approach that has been considered is simply using the username as the salt. This way, the salt will always be unique (since two users can't have the same username) and the benefits of using a salt will (apparently) still apply. This is almost true, and using this system is better than hashing-only, but is not without drawbacks.

Firstly, one of the main attacks on passwords hashed through any hashing algorithm are so-called pre-computed "rainbow tables". A rainbow table is a table that contains pre-computed hashes for specific inputs. This means that the password cracker can now use a rainbow table to compare the leaked hashes he has received and find the plaintext passwords without additional computations. Salting is meant to prevent this; now, rainbow tables cannot be pre-computed for common passwords because the salt changes the password itself.

Using a username as the salt, however, makes rainbow tables again effective. For almost all websites, there are common usernames like "admin" or "root". Rainbow tables can be computed using this as the salt and the same attack can be mounted on these users.

Additionally, if a user has the same username across multiple websites, the database will have the same hash value computed if they are using the username as the salt, the user re-uses their password, and the same hashing algorithm is used for computation. This is a very specific case, but nevertheless is a possible result of not using random salts. Salts should be chosen from a truly random space to provide the most benefit.

HASHING ALGORITHM SELECTION

As was mentioned previously, selection of which specific hashing algorithm is used is a central concern if a company decides to utilize password hashing. Since any one-way hashing algorithm will 'work' in practice, companies can get away with selecting ones that are not ideal for password storage. Most often, companies fail to select correct hashing algorithms due to ignorance of best practices or due to the difficulty of changing an authentication system once it is set up. When a company is young, the focus likely is not on password security. As the business grows, companies may be hesitant to change authentication systems because they will inconvenience users at no immediate benefit. Ideally, best practices would be followed from the beginning of a company's life and updated upon obsolescence. An examination of a few popular and ideal algorithms follows.

Insecure Algorithms

An arbitrarily-chosen hash function is likely to be insecure. Here, two common functions in use today are discussed, MD5 and SHA-1. Neither should be used for storing password hashes.

MD5

MD5 is a message-digest algorithm that takes an arbitrary-length input and produces a 128-bit output (Pornin, 2011). Designed in 1991 by Ron Rivest (Rivest, 1992), it is an update to MD4, an earlier hash function. MD5 is widely utilized and is oftentimes used as the only hashing function that protects plaintext passwords. Since its introduction, MD5 has shown to be vulnerable to collisions (different inputs can result in the same hash value), among a host of other issues. In fact, the CMU Software Engineering Institute considers it "cryptographically broken and unsuitable for further use."

Although these problems are troubling, the greatest weakness for password storage is MD5's speed. Two ATI Radeon 7970 graphics cards can compute over 23 billion MD5 hashes per second. As mentioned, the more hashes that can be computed per second, the easier it will be to crack a list of passwords.

MD5 should never be used to store hashed passwords, even if salted. The only passwords that resist cracking with this algorithm are extremely long, random-character passwords, which are not typical.

SHA-1

SHA-1 (secure hash function 1) was designed by the United States National Security Agency in 1995 as a successor to SHA-0 (“Federal Information Processing Standards,” 2002). It produces a 160-bit output to a variable-length input. SHA-1 is the most widely used of the SHA family of hash functions, but attacks have been found (Biham et al., 2005) and NIST now recommends that federal agencies utilize SHA-2, its successor.

SHA-1 is also frequently used for password hashing, and is only slightly better than MD5. The same graphics cards as mentioned before can compute over 8 billion hashes of SHA-1 per second, roughly 1/3 of the speed of MD5. This is still an unacceptably high rate of hashing for passwords, however. SHA-1, when applied to passwords, suffers the same vulnerabilities that any fast hash function does. As such, it should not be used.

Secure Algorithms

There are currently a few algorithms accepted as best practices. The focus here is on PBKDF2 and bcrypt, which are both key derivation functions designed to be slow (and, therefore, more secure).

PBKDF2

The Password-Based Key Derivation Function 2 was introduced by RSA Laboratories in 2000, meant to replace PBKDF1 (Kaliski, 2000). It produces a variable-length key and is widely implemented as part of programming language libraries.

PBKDF2 relies on an underlying hash function (such as MD5 or SHA-1) and a salt value to compute a derived key. It continually applies the hashing function, with a variable length of iterations.

PBKDF2 is secure because of the iterations it includes. Instead of passing a password through one iteration of MD5, PBKDF2 passes it through the algorithm at least 1000 times. This means that the amount of iterations that an attacker can perform per second fall precipitously.

bcrypt

Designed by Niels Provos and David Mazieres in 1999, bcrypt is a key derivation function that is similar to, but stronger than, PBKDF2 (Provos, 1999). bcrypt is based on the Blowfish cipher, which relies on constant changes to the underlying table structure during key derivation. This means that GPU-based acceleration techniques become less effective, and the speed of guessing is greatly reduced (Pornin, 2011). Current benchmarks place bcrypt on 5,000 to 10,000 on comparable CPU/graphics-card combinations, though speeds of up to 500,000 are possible through specialized set-ups (“John the Ripper benchmarks,” 2013).

Although there are other, more recent algorithms available for secure hash storage, bcrypt and PBKDF2 are two competent choices. Brute-force guessing attacks on passwords stored with these algorithms will be able to crack only the most basic of choices, and other types of attacks will still be very limited by the attacker’s computation power. If a data breach does happen within a

service, these algorithms will allow ample time for the organization to assess the damage and reset affected passwords without having accounts compromised. Additionally, through communication with users and other companies, the usual worrisome spillover effects of password leakage can be corrected.

USER PASSWORD SELECTION

While changes in the way an Internet service stores passwords have the biggest effect on overall password security, an individual user cannot themselves make such change happen. If they wish to utilize a service, they are forced to put their trust in the website’s security architects. As recent data breaches have shown, such trust is, in many cases, misplaced. In the past two years alone, there have been data breaches of tens of universally-recognizable online brands. With an average user utilizing just 5 passwords spread across 26 online accounts (Waugh, 2012), a simple back-of-the-envelope calculation suggests that hackers can expect to access 4 or 5 accounts on different websites whenever a breach happens. This is unacceptable, as improved password selection on the part of users can mitigate all but the most egregious of password storage mistakes by web developers.

Recommendations are given in increasing difficulty and/or decreasing importance. Users would be well-served in a data breach by implementing many of these suggestions.

PASSWORD REUSE

To begin with, there should be no re-use of passwords across online services. With each password re-use, the vector for attack for hackers increases, and they become more likely to breach an account. In the worst case, a user uses just one password for all websites. In the best case, there is no repetition of any password on any website. At the very least, unique passwords should be used for websites of high importance, such as for online banking accounts.

This ensures that if a breach happens at a relatively insignificant service, such as a news website, its negative effects do not spill over to more important accounts. Since smaller services are also more likely to have poor password-storage techniques, using the same password for two accounts of varying importance is not a good idea.

PASSWORD LENGTH AND CHARACTER SPACE

The most frequent way passwords are stored are with a weak hashing algorithm, such as MD5 or SHA1. Even with best-practice password storage techniques, particularly weak password selection can cause accounts to be compromised. Though there is a wealth of information online about successful password selection, there are two things that affect password strength: length and character space (for brute-force techniques).

Character space refers to the possible characters that are used within a password: for example, a

password such as “bumper33” is alpha-numerical. Adding a special character will make it resistant to attacks based only on letters and numbers.

In general, the length of a password is its most important feature in brute-force attacks. The difference between the amounts of time it takes to crack MD5 passwords of length 6 versus 8 is immense, whereas cracking a 6-character password that includes only letters and one with letters, numbers, and special characters is comparable.

Dictionary-based attacks, where the password cracker utilizes a dictionary of English words and inserts common substitutions/modifications such as “0” for “o”, are widespread. This is why a password such as “bumper33” is not a good choice: “bumper” is a common English word and the additional “33” is just a small modification. However, even using all lower-case characters with four common words as a password, such as “correcthorsebatterystaple” (Findkle & Saba, 2012), results in much better security. This is primarily due to the length of the password.

Character space also has an impact on password strength, but it is not as great as length. If there is no additional work involved for adding all character types in a password, then using as many different characters as possible (upper case, lower case, numeric, special) offers the best security. Users should strive to utilize the maximum character space that a website’s password policy allows.

PASSWORD STORAGE

Password storage is of huge importance, but best practices are not always easy to implement. In the worst case, a user tries to remember all passwords. This is not a good storage scheme because the brain is not good at remembering multiple unique, long strings. Eventually, users revert to either re-using passwords or utilizing mental shortcuts to achieve quasi-security.

One common compromise is to select a ‘base’ password that is difficult to remember and make slight modifications to it for different websites based upon the website name. This way, all passwords are still unique and the user may retain the ability to ‘remember’ everything, since they are only forced to remember one string of random characters. This can be a reasonable solution for users that do not want to pursue any additional security, but the approach will break down during a targeted attack. If a cracker is not simply using automated tools to try and re-use passwords across services, they can recognize this special string (assuming they get the plaintext password) and base new passwords off of this. This is an unlikely situation, but a possibility nevertheless.

Although many online resources recommend against it, storing passwords on physical paper is not a terrible choice. The vast majority of unauthorized account accesses through stolen passwords are the result of a data breach in a service, which an individual user

has no effect on. The probability of a home burglary (in which the intruder is interested in stealing passwords) is usually much lower than the probability of a password leak. As long as such a list is hidden reasonably well, this type of password storage can prove effective. It is certainly better than password reuse.

Many users utilize the built-in password storage schemes included by browser vendors. Using this service is not a good idea; although this provides for a very good user experience, such passwords can not only be stolen by anyone with physical access to your computer (as with the physical password list), but browser and computer insecurities can expose the same information. And since these passwords are not typically stored in any encrypted fashion, such exploits are not difficult to carry out.

Ideally, a user will keep an encrypted database of passwords and refer to it when a password needs to be retrieved. There are many services available for this storage scheme, the most popular of which is likely KeePass. With KeePass, an encrypted database can be kept on a flash drive which contains all usernames and passwords to each website. Then, when a login screen requires password retrieval, the user can utilize the program to copy the password over. This type of password storage is extremely secure and very unlikely to be exploited by other programs. And since the information is encrypted, even loss of the flash drive will not result in a problem (assuming

the encryption password is strong enough).

But this approach has drawbacks. It is not user-friendly, because it forces the user to go into a different program to retrieve any username or password, a significant step-down for users accustomed to the auto-filling that a browser password management scheme offers. Also, it is inflexible: in situations that the flash drive is unavailable or cannot be used, the user is helpless.

A service that solves these problems with minor trade-offs is LastPass. LastPass is an online password management service that includes extensions for all major browsers. This allows them to have the same auto-filling capability that a native browser implementation does, but also retain the cryptographic strength of storage with encryption that KeePass offers. Also, there are mobile and web apps that offer back-up ways to look up passwords if LastPass is not installed on a computer.

TRULY RANDOM PASSWORDS

The simple truth is that the only truly secure password is a very long, truly random, maximum-character-space password. Using a randomly generated, extended-length password (such as 16 characters) which includes all of the possible characters in its character space is the best possible selection. Using different random passwords for each web service and storing them with either KeePass or LastPass offers a huge improvement in security.

Even with a supercomputer, no cracker could expect to recover random, 16-character length passwords. Of course, if a web service with passwords stored in plaintext experiences a breach, the user's password will be exposed – but such a situation is not truly problematic, since the password makes no indication of a password selection 'style' (as in the common-base technique described earlier) and provides no additional information about the user. At worst, the individual account that was leaked will be breached – but in this case, the company in question has made so many mistakes that no password selection strategy could save the user.

OTHER NOTES

Finally, users should be suspect of services that ask to “connect” to other accounts by providing passwords. A breach in one service could now affect any of the other connected services. Although some websites may claim not to store these passwords, always assume that this is untrue and that they are indeed retaining the information.

ACKNOWLEDGMENTS

Thanks to Ars Technica for providing the spark to pique my interest in password security.

REFERENCES

[Click here to view references at the end of the journal.](#)

Research Highlights

Gasification of Southeastern Woody Biomass for the Production of Transportation Liquid Fuels

Ryan Baker and Phillip Cross

With the rapid development in countries like India and China, the demand for energy and petroleum products will continue to grow. If this demand is not met in a responsible manner, it could result in irreversible climate change. This has sparked research and development of alternative energy and renewable sources to replace or substitute petroleum-based fuels and products. In theory, utilizing renewable resources creates a carbon cycle of emission and sequestration rather than the introduction of “locked carbon” associated with earthen bound fossil fuels. Gasification is a promising technology for this effort; it can convert carbon trapped in biomass by sequestration into fuels and chemicals. Gasification uses low levels of oxygen to partially combust biomass, converting about 70% mass into carbon monoxide, hydrogen, methane, and carbon dioxide. The production of these combined gases, known as syngas, can be burned directly as an energy source or processed further to produce gasoline and other petroleum products such as waxes and plastics. What challenges this process is finding a way to supply enough biomass to meet the growing demand, operate the reactor efficiently, and create clean syngas.

Using a bench-scale bubbling

fluidized bed gasification unit, we compare syngas and contaminants (i.e., ammonia, sulfur dioxide, hydrogen sulfide, and tar) production of different, readily available woody biomasses from the southeastern United States such as pine, eucalyptus, and hybrid poplar. Each biomass is gasified under different parameters such as reaction temperature, feed rate, and oxygen to fuel ratio to improve our understanding of optimal reactor conditions for producing better quality syngas. Each run is analyzed using the collected steady state gas composition data. These data sets are then modeled as a continuous process enabling mass and energy balances to be performed showing that these three types of woody biomass (e.g., pine, hybrid poplar and eucalyptus) will produce very similar syngas.

A difficulty that was not foreseen with these experiments was the major difference in feed rate between different biomass types. The gasifier’s feeding system is comprised of a biomass holding hopper with bottom alternating screws rotating at a set speed of 200 RPMs (revolution per minute), feeding the biomass into a horizontal spinning auger that delivers the biomass into the reactor. It is believed that variation in feed rate is due to the fibrous nature of the material and high moisture

content. Eucalyptus was particularly difficult, while pine, hammer-milled and sieved (through 1/32” screen size) to the same size as eucalyptus, flowed more easily providing the fastest feed rate. An investigation is on-going in another group in Biosystems Engineering Department, to understand the feeding behavior with different biomass.

In conclusion, pine and eucalyptus are viable feedstocks which can supplement the demand for renewable sources of carbon while hybrid poplar is being evaluated. Gasification operation has been improved by better understanding the specific nature of each type of biomass. A still precedent issue that is the focus of our future work is reducing the levels of contamination of “tar”.

Statement of Research Advisor:

Ryan’s research project focuses on understanding the quality of syngas from different biomass types and at different ages. Ryan has developed a protocol for measuring syngas and contaminants using a bench-scale gasifier. His project is funded by the National Institute of Food and Agriculture of U.S. Department of Agriculture (NIFA-USDA).
- *Sushil Adhikari, Biosystems Engineering*

Enactment as Rhetorical Strategy in America's Most Effective Literary Journalism

Gabrielle Bates Stahlman

This project attempts to discern features that culturally significant works of literary journalism have in common. The process involves conducting rhetorical analyses of three New Yorker articles published in the post-WWII era on behalf of victims of injustice. As the creative nonfiction genre becomes increasingly en vogue, the demand for scholarly criticism on creative nonfiction and its subgenres, such as literary journalism, grows as well. My rhetorical analysis of three groundbreaking works of literary journalism contributes to what Lee Gutkind, the “godfather of creative nonfiction” himself, has claimed is a lack of scholarship pertaining to the genre.

The three samples—“Hiroshima” by John Hersey, “Silent Spring” by Rachel Carson, and “A Letter from a Region in my Mind” by James Baldwin—were all published during the New Yorker’s “golden age,” during which the subscription rate doubled, New York City became a hub of international cultural leadership, and the educated middle class in America grew immensely. These articles have also endured the test of time; they are cited as being among the most important works of creative nonfiction ever published and remain in circulation today. Locating mid-century World

Almanacs allowed me to narrow the scope of my investigation and justify the time period and publication from which I procured my samples.

Borrowing from the rhetoric of inquiry theory exemplified by James Boyd White, I read and annotated each work with a close eye for how language worked to reveal authorial intention. I sought commonalities that could be investigated in other works of literary journalism in the future. Visual mapping allowed me to see overlapping strategies such as enactment, in which the language structures physically reflect the actions and effects being described. Enactment functions within each of the samples at the sentence level and in the pieces’ overall structures. By unpacking specific examples of enactment in “Hiroshima,” “Silent Spring,” and “A Letter from a Region in My Mind,” I was able to argue for enactment as a strategy that may contribute to the cultural resonance and rhetorical effectiveness of a literary journalism article.

To make a more definitive case for enactment as a unifying strategy at play among culturally significant works of literary journalism, one would need a much larger sample size. In addition, instances in which the physical structure of a sentence

or article contradicts or complicates the author’s meaning, rather than enacts it, would provide an important counterpoint for my preliminary investigation. Moving forward, I am interested in the possibility of investigating enactment through the lens of cognitive science, forming an interdisciplinary partnership to research how the physical structures of language affect how the brain processes the semantic meanings of that language. This would open up the topic to apply to all literary arts—including poetry and fiction—and potentially unearth biological roots of how and why certain units of language affect us more strongly than others.

Statement of Research Advisor:

Gabby had to read secondary scholarship about American magazine culture and the genre of creative nonfiction in order to design her study with a sample of articles that was appropriate. She utilized an established method of analysis to demonstrate a common rhetorical feature that lays the ground work for further studies and opens new possibilities for linking cognitive processing with rhetorical choices made by authors.
- Margaret J. Marshall, English

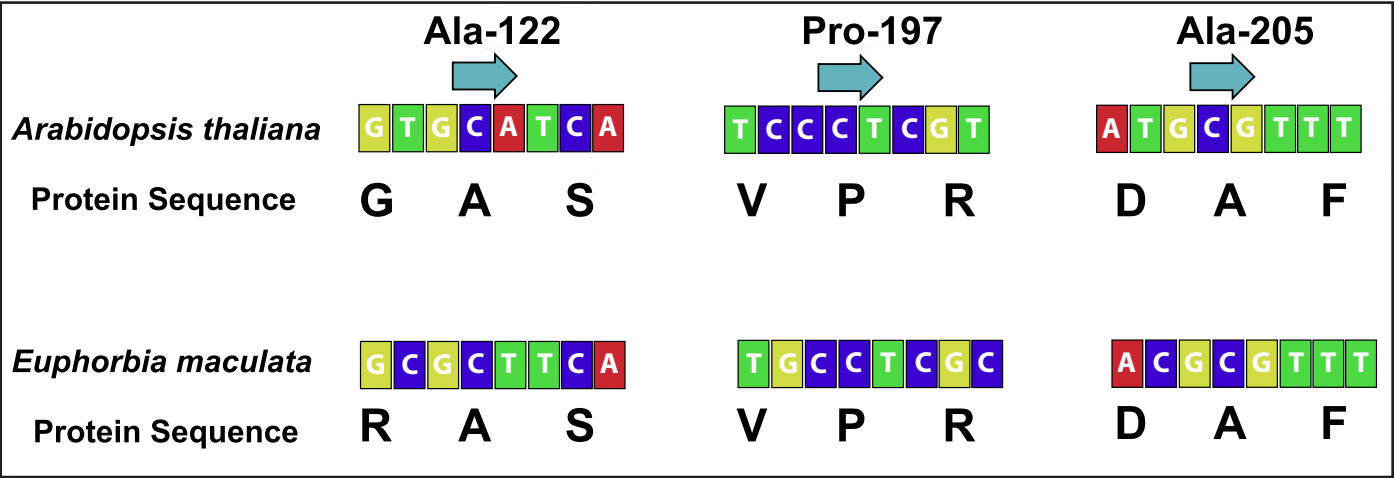
Identifying the Mechanism of Resistance to ALS-Inhibiting Herbicides in *Euphorbia maculata* (L.)

Tyler B. Miller, Shu Chen, and Patrick McCullough

Spotted spurge (*Euphorbia maculata*) is a problematic weed commonly found in golf course putting greens and sports fields. Acetolactate synthase (ALS) inhibitors are widely used for control. The University of Georgia has discovered a spotted spurge population resistant to metsulfuron, a herbicide commonly used to control spurge. ALS is critical in the biosynthesis pathway of three branch-chained amino acids: valine, leucine, and isoleucine (Ray, 1984; Umbarger, 1978). These amino acids are essential for the plant to grow and function properly. Resistance to ALS inhibitors is usually caused by mutations in ALS encoding gene sequences. Mutations are changes in the genome of the plant that alter how that plant functions. Mutations can be identified through sequencing of the susceptible and resistant populations to determine if a substitution occurred.

DNA was extracted for sequencing to determine if a mutation had occurred in the resistant spurge population. Three common methods were used in the DNA extraction: CTAB extraction, Omega BioTek e.z.n.a DNA Kit, and a Qiagen DNA Plant mini kit. Extraction followed the protocol given in the kits. For CTAB DNA extraction, a modified procedure was used based on the procedure proposed by Porebski et al. (1997).
Extracted DNA was used in a polymerase chain reaction (PCR) to amplify the ALS gene (approximately 2,000bp long) of spotted spurge in both the susceptible and resistant populations. This amplification allows for a more simple method of sequencing the genome. Phusion DNA Polymerase is used for PCR following the reaction mixture and thermal cycling conditions as

suggested by the protocol. PCR Primers were designed through Primer3 and ordered from Eurofins genomics. Some of the primers utilized were designed by previous research (Duran Prado, 2004). Upon successful amplification, the PCR product was run through a 1% agarose gel electrophoresis. The desired fragment was extracted using a Qiagen Gel Extraction Kit. This fragment (DNA concentration must be > 25ng/μL) was sent to the Auburn University Genomics and Sequencing Lab for capillary sequencing with the same forward and reverse primer pair used in PCR. The obtained nucleotide sequences and the translated protein sequences were then aligned with the *Arabidopsis thaliana* ALS gene in CLC Genomic Workbench 6.0 (Figure).
DNA extraction techniques had to be modified after several failures



Figure, Miller. Sanger Sequencing Alignment.

due to the high polysaccharide content of the milky, latex sap that is found in spotted spurge. Of all designed primers, only 2 pairs have proven to amplify portions of the ALS gene. Figure 1 shows sections of the alignment of the nucleotide sequence and the translated protein sequence for both spotted spurge and *A. thaliana* to identify if a substitution was present in the amino acid sequence. The sites highlighted in this figure (Ala-122, Pro-197, Ala-205) illustrate the most common mutation sites that confer resistance. The alignment revealed no mutations in the resistance conferring codons.

Future research will focus on amplifying the remaining portions of the ALS gene. Currently, there is interest in having the transcriptome of the two spurge biotypes sequenced through Next Generation Sequencing. This will allow for a side-by-side comparison of the gene expression in the two populations to deduce if a greater/lesser ALS gene expression could contribute to the resistance. With resistance being a major concern for sustainable agriculture in the future, being able to identify the true cause of this resistance is the building block of research that can allow for future generations to overcome herbicidal resistance altogether.

Statement of Research Advisor:

Identification of resistance-endowing mutations is critical for the development of management practices to control herbicide resistant weeds. Depending on the mutation location, all herbicides chemically related to metsulfuron may also be ineffective. Such would greatly limit possible control options, but such knowledge would prevent frivolous use of herbicides that are no longer effective.
—*J. Scott McElroy, Crop, Soil, and Environmental Science*

Battleground Texas: Media Framing of the 2014 Texas Gubernatorial Race

Rachel M. Pipan

In the year 2014, female governors still made up less than a fourth of all state governors, and while the number of women serving in Congress continued to increase, only around 20 percent of Congress is female. Previous research has already shown that women are less likely to be recruited for office and are less likely to run. Our research sought to determine whether media representation of female political candidates influenced how female candidates were perceived by the public. Our hypothesis is that how media “frame” candidates in certain ways would influence public opinion and would negatively impact a

female candidate’s chances of winning her race. This research question is crucial to our society, as equal political representation has eluded us despite strides made in achieving equal pay and position in other institutions.

We decided to focus on the media coverage surrounding the 2014 Texas gubernatorial race for a few reasons; first, this race in particular was gaining nationwide attention. Second, the race had no incumbent candidate. Finally, it was between a male and a female candidate with notable appearance (a petite, blond female Democrat and a white male Republican using a

wheelchair.) One of our research questions specifically focused on appearance and how frequently appearance was mentioned by the media in race coverage – would the female candidate’s appearance be mentioned more than the male candidate?

To research this topic, we pulled a random sample of newspaper articles from four periods around the Texas gubernatorial race. The first period focused on the female candidate, Wendy Davis, only, as she had gained nationwide attention for her 11-hour filibuster against Texas Senate Bill 5. The following three periods focused

on both Wendy Davis and her opponent Greg Abbott. Each period had a random sampling of 100 articles, and each article was coded twice by the researchers. Each researcher had to answer 36 questions about the article and how each candidate was portrayed in terms of personality traits and political issues, as well as mentions of appearance and likelihood of winning the race. Our hypothesis was that the female candidate would rank higher on typically “female” personality traits, like warmth and people skills, while the male candidate would rank higher on “male” traits such as good leadership skills and toughness. We also hypothesized that the media would primarily report the female candidate’s expertise on “female” issues like healthcare and education, while

the coverage of the male candidate would focus on “male” issues like crime and infrastructure.

We are still compiling the results of our article coding. Next, we will find and report any statistical correlations using MANOVA in SPSS and draw our conclusions. Within the next month and a half, Dr. Susan Waters will write the methods and results section, and Rachel and Dr. Waters will write the discussion section together. We will submit our research paper to both an undergraduate and national conference for presentation in the next few months, as well as to a national journal for publication.

We hope our research will elucidate new patterns in male vs. female political campaigns, as well as denote emerging trends in modern elections. From a public relations

standpoint, we hope our research will help campaign strategists for female political candidates create a more effective media relations strategy.

Statement of Research Advisor:

It has been my pleasure to work with Rachel Pipan on her research project. She is extremely competent and confident in her written work and has the passion to continue pursuing social justice for women in the workplace. Rachel is well on her way to possibly becoming a top public affairs specialist, research specialist, media relations specialist or political analyst within the public relations field. I am very proud of her and her accomplishments!
- Susan Waters, Public Relations

From Dahrar to Déorwine: Examining Tolkien’s Interpretation of Sound Symbolism

Matthew Pollock

The philologist J.R.R. Tolkien, whose decades spent teaching real world languages at Oxford won him much less popular fame than the fictional languages and world he created in *The Lord of the Rings*, had a clear philosophy on language. He saw the proper “construction of sounds” as creating “word-music,” and certain other combinations as truly repugnant (Tolkien, 218). Through an experimental analysis of four Tolkien-created languages,

Germanic-influenced Rohirric and Dwarvish and Tolkien-created Orcish and Entish, this investigation examined the way that readers interpreted invented words and also the means by which sound influences individual interpretations of language, part of the concept of sound symbolism.

Studied by both psychologists and linguists, sound symbolism examines phonemes (sounds), attempting to determine their

meaning. In numerous studies, for example, participants have been shown pointed and rounded images and given two or more created words; individuals overwhelmingly match words like takete with the pointed image and those like maluma with the rounded (Holland, 111). Despite copious studies, the mechanisms through which this symbolism functions are still not fully agreed upon or understood.

Table, Pollock. Percentage for each selection from total dataset with *neutrals* removed.

| Language | Musical | Harsh |
|----------|---------|-------|
| Entish | 84.1% | 15.9% |
| Orcish | 1.5% | 98.5% |
| Rohirric | 70.6% | 29.4% |
| Dwarvish | 70.7% | 29.3% |

Survey data was gathered from 73 Auburn University students, asking them to respond to ten words as neutral, musical, or harsh and explain “why” they found them that way. The neutrals were then disposed of, their connected “why” answers indicating that they had been treated as non-responses, and the remaining results were tabulated (Table). The Germanic-based languages Rohirric and Dwarvish were less decisively classified than the Tolkien-created Entish and Orcish. Participants’ characterization of the Tolkien-created languages aligned with the attributes of the textual characters; the evil Orcs’ language, Orcish, was regarded as harsh, while the benign Ents’ tongue, Entish, was classified as musical.

The qualitative results gathered from responses to the “why” question were compiled and compared to a corpus of the four

languages represented in *The Lord of the Rings*. Fricatives (sounds created with a narrowed mouth, e.g. [s] or [f]) were remarked in the Orcish data as making words harsh and were therefore sought out across the corpus. Entish, having no fricatives, stood out from the others based on this characteristic.

The reason that this English speech community found Entish to be melodic speaks to a larger linguistic issue. In the final stages of this investigation, the reasons behind this interpretation were analyzed to determine how Tolkien employed sound symbolism to effectively advance the narrative. Combining the experimental linguistic approach with a literary one, unprecedented in Tolkien scholarship, generated quantifiable data which have provided actual rather than theoretical reactions of a speech community.

Statement of Research Advisor:

Matthew’s research seeks to explain in linguistic categories what Tolkien tried to do creatively, to establish a link between aural aesthetics and cultural identity. His research challenges us to think beyond the obvious, that Tolkien invented a ‘bad-sounding’ language for ‘bad’ people and a ‘good-sounding’ language for ‘good’ people, but instead Matthew asks how we as English-language readers are made to respond to alien cultures only on the basis of the attractiveness that their languages may or may not appear to hold for us.
- Craig Bertolet, *English*

Maternal Diet and Its Impact on the Gut and Milk Microbiota

Nikki Wyatt

At birth, mammalian young enter a dangerous environment characterized by parasites and pathogens to which they must develop a dynamic immune system to survive. The incipient community of microbes that take residence in the offspring gut is believed to play a pivotal role in training immune function (Smith, McCoy, and Macpherson, 2007). Among the most important founders of this community are microbes that reside in a mother's milk (Donnet-Hughes et al., 2010, Perez et al., 2007). It has recently been shown that the microbes found in a mother's milk are derived, at least in part, from her gut (Perez et al., 2007), and gut microbial diversity is sensitive to variation in the maternal diet (David et al., 2014). Yet it remains unknown if and how maternal diet impacts the community of microbes in milk. The goal of this study is to determine if maternal protein intake impacts gut and milk microbial diversity in the wild-derived house mice (*Mus musculus*).

For this study, females and their mates were randomly assigned to one of two dietary treatment groups, high protein diet (20% crude protein) and low protein diet (10% crude protein). These diets were isocaloric and offered ad libitum. The females of each group were mated and milk

was collected for analysis upon peak lactation. The bacterial DNA in each sample was then isolated. Bacterial DNA was sent to a commercial lab for 16S rRNA sequencing. The 16S rRNA sequencing of microbes in milk samples from female mice consuming the high protein diet showed 63.85% relative abundance of Proteobacteria, 29.5% of Firmicutes, and 6.07% of Actinobacteria. The sequencing of microbes in milk samples from female mice consuming the low protein diet showed a higher relative abundance of Proteobacteria (68.9%), and a lower relative abundance of Firmicutes (25.4%) and Actinobacteria (4.77%). Both Proteobacteria and Firmicutes are prominent phyla in human milk (Ward, Hosid, Ioshikhes, & Altosaar, 2013). Proteobacteria have been shown to be of high abundance in human mammary tissue (Urbaniak et al., 2014), whereas Firmicutes are abundant in the gastrointestinal tract (Ward et al., 2013). Thus, it is likely that the Firmicutes in the mouse milk are derived from the mother's gut. It is possible that the differences in the relative abundance of Firmicutes in milk reflect differences in their relative abundance in the mother's GI tract (Ward et al., 2013). Actinobacteria shows mostly

proteolytic activity in milk (Hantsis-Zacharov & Halpern, 2007). As the protein content of mouse milk has been shown to be elevated in mice consuming a 20% vs a 10% protein diet (Derrickson & Lowas, 2007), it is possible that the enhanced Actinobacteria play a role in the protein digestion in the neonate (Hantsis-Zacharov & Halpern, 2007). Additional milk samples and gut content samples are currently being analyzed. Future statistical analyses will evaluate differences in both milk and gut microbial diversity between the two diet groups at the level of species.

Statement of Research Advisor:

Nikki played a leading role in maintaining the mice for her study, collecting milk and gut contents samples, extracting bacterial DNA, and she is now in the process of learning bioinformatics to complete her analyses. The impact of protein intake on milk microbiota had not been examined previously. Her research will make an important contribution to our understanding of the role that a mother's diet plays in shaping the phenotype of her offspring.
-Wendy R. Hood, Biological Sciences

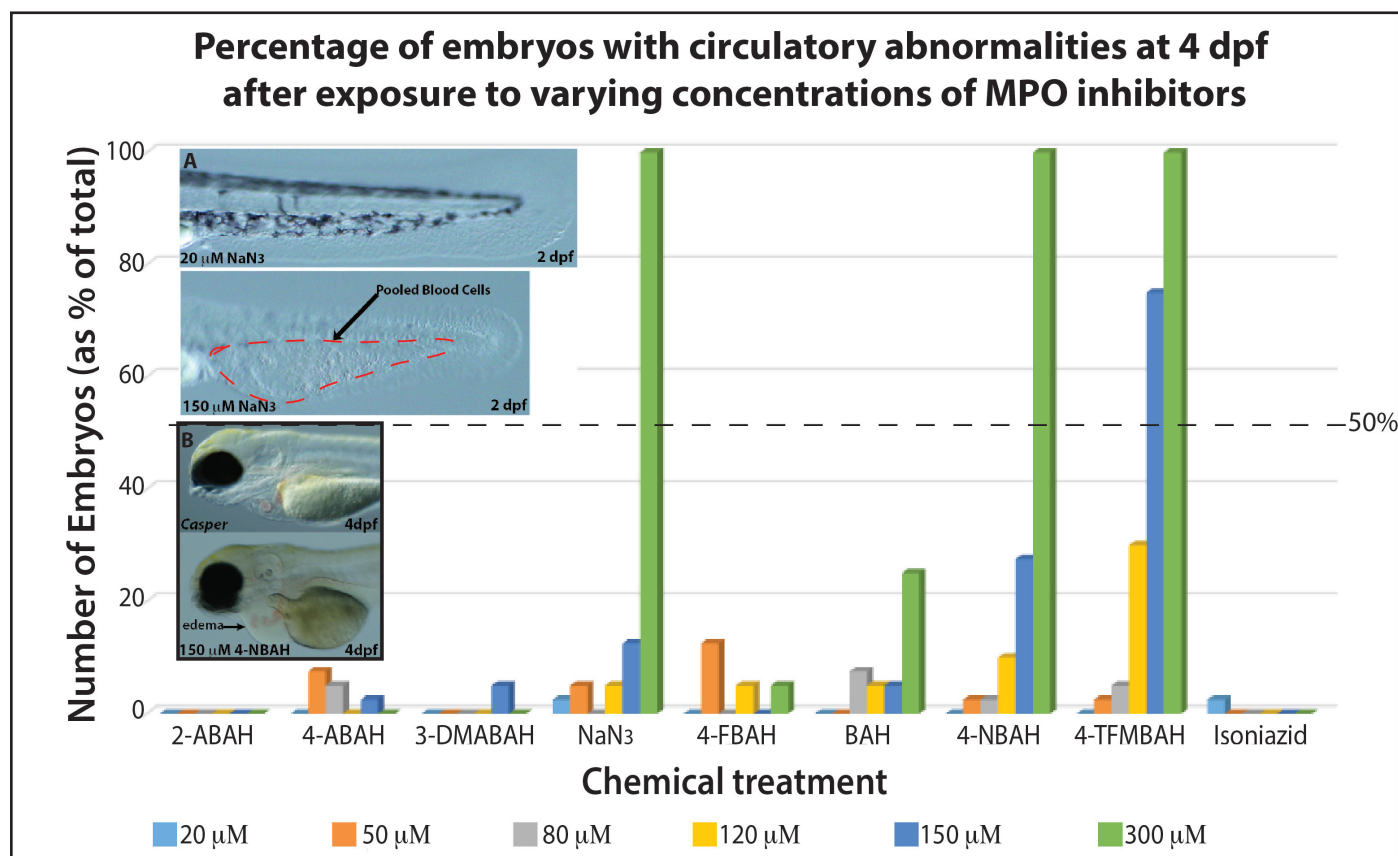
Zebrafish Toxicity Screen of Novel Myeloperoxidase Inhibitors

Andrew Wilkins and Jeff Daniel

Myeloperoxidase (MPO) is produced by a subset of immune cells to stimulate the breakdown of hydrogen peroxide and the formation of the powerful oxidant hypochlorous acid (HOCL) at sites of inflammation in the body. HOCL, the active component of bleach, helps the body battle infections by triggering deleterious modifications of proteins and

DNA of engulfed pathogens. However, during chronic diseases with associated inflammation, like rheumatoid arthritis, atherosclerosis, and certain cancers, elevated circulating MPO levels cause collateral damage to the host. As such, there is a need for developing safe ways to abrogate these unwanted MPO effects.

The goal of our research was to conduct in vivo safety screening of benzoic acid hydrazine (BAH) analogs, recently shown to inhibit MPO in vitro. Here, we use the zebrafish as our model for vertebrate development and organ function due to their ability to produce large numbers of rapidly developing, visibly transparent offspring with each weekly mating.



These properties allow us to closely monitor the effects of treatments before, during, and after organ development within the first five days after fertilization. In addition, zebrafish share a remarkable degree of genetic similarity to humans, having similar genes to at least 70 percent of all human protein-coding genes. Thus, the data generated from this study is likely predictive of potential adverse effects in humans.

We screened nine BAH analogs (2-ABAH, 4-ABAH, 3-DMABAH, NaN₃, 4-FBAH, BAH, 4-NBAH, 4-TFMBAH, and isoniazid) for effects detrimental to proper organ development. Initially, 6 concentrations of each analog were added to groups of 40 embryos six hours post-fertilization, at which time gastrulation had just begun. In a second assay, we measured toxic effects on cardiac function by adding the compounds to embryos at 2 days post-fertilization, after the heart was developed. In both techniques wild-type (AB) and pigmentation mutant (Casper) embryos were observed for 5 days and grown under normal conditions, except

that 0.4% DMSO was added to aid in chemical absorption.

If any, the primary defects observed after treatment during early development were pericardial edema and pooling of blood cells in the tail region, hereafter referred to as circulatory abnormalities (see Figure). Our studies found treatment with 300 μ M of NaN₃, 4-NBAH, and 4-TFMBAH caused circulatory abnormalities in all embryos, with these defects appearing less frequently as dosage was lowered. Both NaN₃ and 4-NBAH have an estimated EC₅₀ of 150-300 μ M, while the estimated EC₅₀ of 4-TFMBAH is 120-150 μ M. For all other chemicals, fewer than 25% were affected with doses up to 300 μ M. In our assay for effects on cardiac function, we found circulatory abnormalities only with NaN₃ and 4-TFMBAH treatments at doses of 80-300 μ M (not shown).

Our results suggest that 2-ABAH, 4-ABAH, 3-DMABAH, 4-FBAH, BAH, and isoniazid cause little to no developmental or organ toxicity when administered at dosages of 300 μ M and below, thus making

them ideal candidates for further in vivo testing of MPO-inhibitory function.

Our immediate future plans include LC₅₀ determination for the above drugs and screening a new panel of 60 small molecule MPO inhibitors. Additionally, we will use transgenic zebrafish lines with either fluorescent neutrophils or blood vessels to study the impact of MPO inhibition on normal inflammation and circulation, respectively.

Statement of Research Advisor:

Andrew's toxicity analysis of these compounds is part of a drug discovery process that allows us to reduce the number of potential drugs prior to further animal testing, thus lessening the number of mice or other species required. Discovery of new therapeutics for detrimental effects of the inflammatory process may prove useful in treatment of patients with rheumatoid arthritis, cancer, and cardiovascular disease.
- Jennifer Panizzi, *Anatomy, Physiology, and Pharmacology*

Depth Estimation with a Plenoptic Camera

William Roberts

The Advanced Flow Diagnostics Laboratory (AFDL) at Auburn University has recently built a novel device called a plenoptic camera. This device is constructed like a conventional DSLR camera with an array of

microlenses mounted in front of the sensor chip. Light passes through the microlenses in a way that allows the camera to capture both the location and angle at which light rays impact the image sensor. Because of

this, the photographer captures the complete four-dimensional light field with a single exposure and can change the viewing perspective using image processing after the image has been taken. It is then possible to

estimate the distance of an object from the camera. The human brain perceives depth in exactly this way – interpreting depth by comparing the perspective of each eye. Traditionally, optical depth estimation is performed in stereo, using two cameras, but this requires extensive calibration and high financial cost. Instead of only two lines of sight, the plenoptic camera inherently records many (over 100) with a single snapshot – providing far more perspectives for comparison. This could significantly reduce the complexity, size, and expense of current systems used for range-finding applications. Furthermore, the plenoptic camera is a passive sensor, unlike LIDAR and structured light sensors which must emit a signal to calculate depth. This makes the plenoptic camera less prone to detection in military applications.

This research focused on the development of an image processing algorithm that uniquely exploits plenoptic

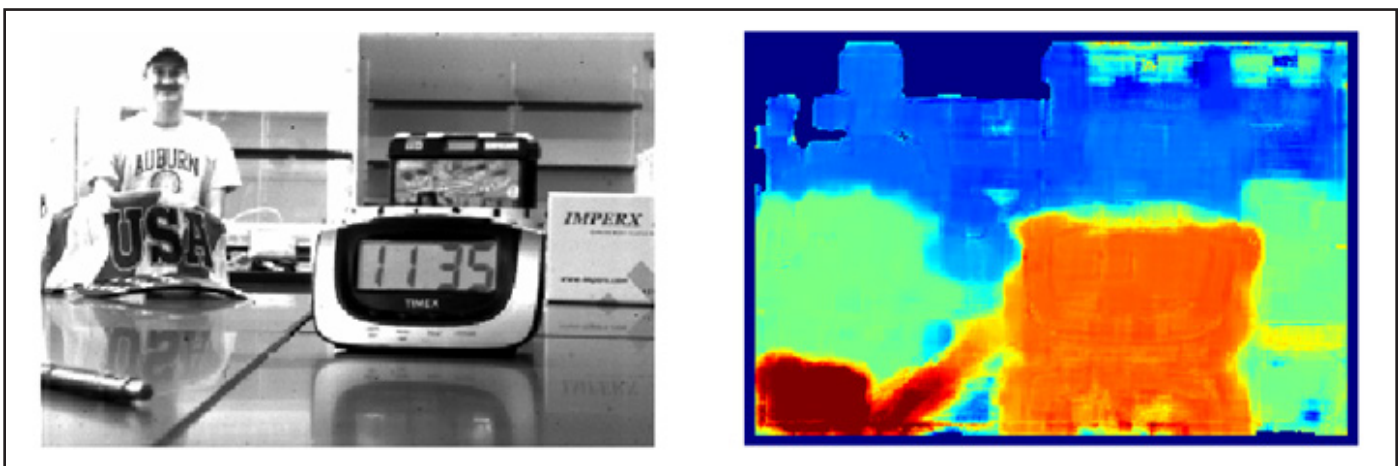
image data to compute a depth-map of the scene. In the finished algorithm, features in a perspective image are compared to a template image and the apparent motion, or “disparity”, of that feature is estimated. A number called a “confidence coefficient” is assigned to that feature to indicate the probability that the disparity calculation is correct. The algorithm proceeds in this way through every possible perspective of the scene until a great many perspective images have been processed. When disparity estimates have been calculated on every image, they are averaged together. Disparity estimates with high confidence are given more weight than estimates with low confidence during the averaging process. Using the principles of geometric optics, the disparity estimates can be converted into a depth map, as in the example image shown in the figure. The image on the left is a sample perspective image generated by the camera. On the right is a depth map showing near

and far objects after processing.

The algorithm was tested with the plenoptic camera on a small static image target placed at several distances in front of a featureless background. Depth was recovered to within five percent error, validating the algorithm. Future work will focus on computational efficiency so that plenoptic cameras can be used for range-finding applications such as UAV navigation and obstacle avoidance.

Statement of Research Advisor:

Due to the fundamental way that they record 3D information about a scene, plenoptic cameras have the potential to supplant traditional cameras in a large number of applications and settings. William’s work exploits the unique nature of these cameras to produce 3D images and is critical in advancing the capabilities of these cameras.
- Brian Thurow, Aerospace Engineering



Figure, Roberts. Sample plenoptic image with depth map, illustrating near (red) and far (blue). Note issues with accurately interpreting reflections and the edges of objects.

The Influence of a Rider with a Disability on the Equine Walk

Ellen Rankins

Therapists and instructors in Equine Assisted Activities and Therapies (EAAT) use the horse as a therapy tool or to provide an activity for riders that find it difficult to participate in other activities and sports. Due to the physical limitations of the participants in EAAT, horses used within this field are subjected to unique stresses that are not seen in other equine disciplines. It is possible that these stresses placed upon EAAT horses can affect their health

and soundness and, therefore, their usefulness. The horse and rider system is a complex and integrated one and changes in one part of the system can easily produce consequences in the rest of the system. Based on this information, the following question arises: Does a rider with limitations (as seen in a therapeutic riding setting) affect the motion pattern of a horse at a walk as compared to the same horse ridden by a rider without limitations? To answer

this question, three riders with similar riding experience, body weight, and build rode the same set of four horses on the same day. Two of the riders were able-bodied and the other rider had a physical limitation. Prior to the day of the video capture, riders participated in two riding lessons to familiarize themselves with the facilities and horses. The day of the filming, the horses were fitted with reflective markers on their hooves to facilitate tracking their movement in the videos. All filming utilized high speed video capture. Each of the four horses was filmed being ridden by each of the three riders and also while being led with no rider. Each rider rode the horse both while being led and while off lead or independently. Each condition (i.e. led with no rider or ridden) was filmed three times to ensure a more accurate measurement of the horse's gait. Following filming, variables of stride length, step length, stance width, stance phase duration of each leg, swing phase duration of each leg, and stride duration were measured for each horse and condition pair. The videos are currently being analyzed with results forthcoming. The results of the study will provide a better understanding of the interaction that takes place between the horse and rider in



Figure, Rankins. This picture shows one of the horse and rider combinations during the data capture. The video camera in the foreground is recording the sagittal or side view of the horse and rider. There is a second video camera in front of the horse that cannot be seen from this angle recording the frontal view.

EAAT. This understanding will facilitate the creation of practices that protect the horses used in these programs and ensure their soundness and health resulting in a more effective interaction between horse and rider.

Statement of Research Advisor:

Biomechanics research with horses and riders has primarily focused on how skilled and experienced riders affect the horse's movement. Very little has been done with inexperienced riders, let alone riders with disabilities,

to examine how they may affect the horse's movement. Though we have always assumed there is an influence, documenting and verifying the differences is the first step in quantifying the unique stressors experienced by horses used in EAAT.

- Elizabeth Wagner, Department of Animal Sciences

Validation of Canine TRAIL in Canine Tumor Cells

Paulina Platten and Maninder Sandey

Cancer in dogs shares several important characteristics with human cancers, including microscopic appearance, biological behavior, tumor genetics, inter-individual and intra-tumoral heterogeneity, and metastasis to relevant distant sites. Each year, approximately 4 million new cancer cases are diagnosed in the dog population. Thus, we not only need to design better therapeutics to treat canine cancers, but this vast pool of cancer patients can also be used to better understand the biology of cancer and to evaluate new drugs and approaches to treat cancer, be it canine or human. Gene therapy is a promising therapeutic approach that offers several advantages over traditional cancer therapies, including selective targeting of cancer cells and minimal other side effects. Tumor necrosis factor-related apoptosis-inducing ligand (TRAIL) is a type II transmembrane protein that interacts with cell surface receptors (DR4 and DR5) and induces cell death, or apoptosis, in a variety of tumor cells. Several studies have

also shown that TRAIL does not induce apoptosis in normal cells, thus highlighting its potential as a cancer therapeutic. The goal of this study was to clone, express canine TRAIL, and to determine the tumor killing potential of canine TRAIL in a wide variety of canine tumor cells.

The extracellular domain of canine TRAIL was cloned and tagged at its amino terminus with the signal peptide from the canine immunoglobulin (Ig) kappa-chain. This peptide targets the protein for efficient secretion from the cell. The construct was cloned into a mammalian expression plasmid containing the cytomegalovirus (CMV) promoter for high-level constitutive expression. A reverse orientation clone was used as a negative control. The recombinant plasmids were transfected into human embryonic kidney (HEK 293) cells. Cell lysates and supernatants were isolated, resolved on SDS polyacrylamide gel electrophoresis, blotted onto a membrane, and the membrane was

probed with Anti-Human TRAIL antibody in a Western blot. The recombinant plasmids were also transfected into CMT28 (canine mammary tumor), CML10 (canine melanoma), and NCF cells (Normal canine fibroblasts). After 72hrs, transfected cells were assayed with a cell proliferation assay (MTT) to determine the growth inhibitory effects of canine TRAIL.

The extracellular domain of the canine TRAIL was successfully cloned into the pDC311 plasmid. The orientation of TRAIL in the recombinant plasmids was confirmed by sequencing, restriction enzyme digestion, and agarose gel electrophoresis. Western blot analysis confirmed that canine TRAIL was expressed in cell lysates and also actively secreted into the culture supernatant, showing that the signal peptide was functional. We then transfected various canine normal and cancer cell types and performed proliferation assays to determine whether the cells were undergoing apoptosis.

Although transfection efficiencies were low, both canine mammary adenocarcinoma (CMT 28) and melanoma (CML 10) cells showed some cell death while normal canine fibroblasts (NCF), which were used as a control, did not. Additional canine and human tumors such as osteosarcoma will be tested in the future.

Based on the cells that we have tested so far, we have been successful in validating that the canine TRAIL molecule inhibits growth of canine cancer cells.

However, due to low transfection efficiency, we have cloned extracellular domain of canine TRAIL into an adenoviral plasmid (pAdenoX adenoviral system) that we expect to show much higher rates of gene transfer. This replication deficient vector expressing canine TRAIL will be further used to characterize its biological properties.

Statement of Research Advisor:

Paulina had to learn several new

techniques in order to perform the experiments she has described, including restriction endonuclease digestion, mammalian cell culture, transfection, and assays for cell proliferation. Through these techniques, she was able to show that we had cloned the canine TRAIL gene, that the TRAIL protein was expressed and secreted, and that the protein was able to inhibit tumor cell growth while not affecting normal cells.
- Bruce F. Smith, Scott-Ritchey Research Center

Gold-Lipid Nanocomposites for Cancer Drug Delivery and Detection

Connor Dobson

Chemotherapy drugs are toxic agents that are effective at killing cancer cells, but are also harmful to healthy cells. Stealth liposomes are nanoscale particles consisting of an aqueous core and a hydrophobic shell composed of the same lipids found in the body; they are surrounded by a polymer called poly-(ethylene glycol) that delays their removal from the body by the immune system. Liposomes have been used as an effective strategy for improving drug delivery and limiting non-target toxicity (side effects), but are still prone to several disadvantages. It is difficult to control the release of the drug payload from liposomes. It is also somewhat challenging to track the biodistribution of liposomes in animals and humans.

We hypothesize nanocomposite systems, consisting of gold nanoparticles encapsulated within liposomes, may be used to improve drug delivery to tumors while also permitting non-invasive imaging. As part of this research, we have studied the synthesis and conjugation of gold nanoparticles in order to control their surface properties. We evaluated potential synthesis procedures based on several criteria, including the size, shape, stability, and optical properties of the particles produced by each method. For our desired application, we desired very small particles that could be readily conjugated with various drugs or targeting and imaging agents. We determined that a reduction of gold chloride solution with sodium borohydride, performed

in a solvent system composed of water and methanol, is the most suitable method for creating gold nanoparticles that are of use for the overall goal of the project. We demonstrated that this method could produce 2-nanometer gold clusters surrounded by a layer of a natural peptide called glutathione. The particles are stable in water, which is an essential feature because the human body is primarily an aqueous environment. We have also begun to explore the conjugation of a model drug called paclitaxel to the gold nanoparticles. Paclitaxel is a highly effective chemotherapy drug whose clinical use is limited by its poor solubility in water. Our aim is to bind paclitaxel to the gold nanoparticles (which are stable in water) in such a way that it is only

released to act once it is inside cancer cells.

Future work will focus on conjugating targeting peptides to the surface of the composites, which would enhance their delivery to cancerous cells while reducing side effects resulting from non-target delivery. Simultaneous imaging could be performed by conjugating a fluorescent probe to the gold nanoparticles or into the lipid shell of the liposomes, allowing the composites to be tracked both in cell cultures and in humans or animals. It has also been demonstrated that gold

nanoparticles themselves can be imaged in both cells and animals using a wide array of techniques, further increasing the flexibility of these nanocomposites for cancer imaging and diagnosis. Our gold-lipidic nanocomposites could also one day be used as a two-stage drug delivery system to diagnose and treat diseases of the brain, which are still quite challenging due to the tight barrier separating the brain from the blood.

Statement of Research Advisor:

The goal of Connor's research

has been the development of nanoparticle composite systems that exploit the favorable attributes of lipid-based delivery with the benefits of solid gold nanoparticles. Connor has synthesized gold nanoclusters (~2 nm) and is working to attach and improve the stability and release kinetics of paclitaxel, a clinically approved chemotherapeutic agent. Overall, Connors's research will aid in overcoming challenges associated with detection and treatment of cancer.
- Robert Arnold, Harrison School of Pharmacy

Development of a Functional Assay to Detect Inhibitors of Plasmodium Falciparum Glutathione Reductase Utilizing Liquid Chromatography-mass Spectrometry

Lexi Burkard, Alexis Scheuermann, and Johayra Simithy

Malaria has and continues to be a prominent health issue around the world. Transmitted via the bites of infected mosquitoes, it causes uncomfortable symptoms that, left untreated, can lead to death. Increasing worldwide drug resistance has been observed to the current antimalarial drugs. Therefore, there is a great need for the development of antimalarial drugs that can effectively kill these new strains.

Plasmodium falciparum causes the most deadly form of malaria. Like most other organisms, it has a sophisticated antioxidant system, a part of which includes glutathione

reductase (GR). GR works by recycling toxic glutathione disulfide (GSSG or oxidized glutathione) to glutathione (GSH or reduced glutathione), a form the parasite can use. Research has shown that inhibition of this enzyme in *P. falciparum* impedes parasite growth. In addition, it has been confirmed that *P. falciparum* glutathione reductase (PfGR) is not identical to human GR. Thus, PfGR is an excellent target for antimalarial drug development.

We have developed an enzyme inhibitory activity assay that measures the functional activity of the enzyme monitoring end

product of the reaction by liquid chromatography mass spectrometry (LC-MS) to identify inhibitors of PfGR. Using recombinant 0.02 μM PfGR enzyme in a buffer containing 100 mM $\text{K}_2\text{PO}_4\text{H}$, 200 mM KCl, and 1 mM EDTA adjusted to pH 6.9 at 25°C and substrates 1,4-naphthoquinone, 4-nitro-2,1,3-benzothiadiazole, and methylene blue ranging from 0-400 μM in DMSO as reference compounds, we quantified the concentration of GSH produced compared to a control to determine the inhibitory effect of these compounds. The reaction time totaled at 10 minutes

followed by centrifugation for 20 minutes to separate the enzyme from the product and remaining substrate. The product-substrate supernatant was what we analyzed. Our inhibitory results coincide with that presented in literature: 1,4-naphthoquinone, 4-nitro-2,1,3-benzothiadiazole, and methylene blue inhibit PfGR with IC₅₀ values of 2.71, 8.38, and 19.23 μ M, respectively (IC₅₀ – half the maximal inhibitory concentration). Good precision for this assay was exhibited by low values of intraday and interday coefficient of variation (CV) (3.1% and 2.4%, respectively). Figure 1 shows the dose response curves for the three compounds in order as listed here. Figure 2 shows the extracted ion chromatogram (EIC) for GSH and

GSSG for 1,4-naphthoquinone and the control reactions.

Thus, we have developed and validated a functional LC-MS assay that allows for quick and reliable screening for inhibitors of PfGR. This assay could be used to determine structure activity relationship similarities among new and existing PfGR inhibitors and has the potential to be used with more complex mixtures. We expect to use the assay for the discovery of new inhibitors of PfGR in future antimalarial drug studies. This would allow us to surpass what current antimalarial drugs can do for people suffering from malaria, effectively battling the new resistant parasites that cause this disease.

Statement of Research Advisor:

Lexi reviewed papers from the literature about methods for biological evaluation of antimalarials. Additionally, she was trained on the use of the LC-MS instrument to carry out the project. Her study was focused on the development of the LC-MS based PfGR inhibitory assay that represents a new assay added to our drug discovery program to serve as a counter screening assay for selective *P. falciparum* thioredoxin reductase (PfTrxR) inhibitors.
- Angela I. Calderón, Harrison School of Pharmacy

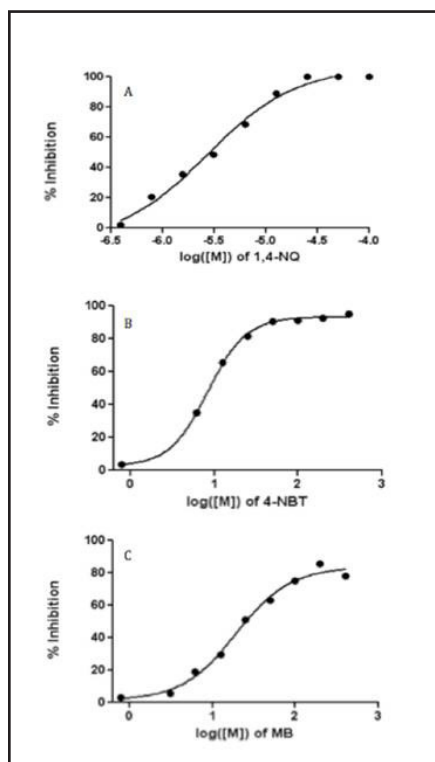


Figure 1, Burkard. Dose response curves of compounds 1 (A), 2 (B), and 3 (C).

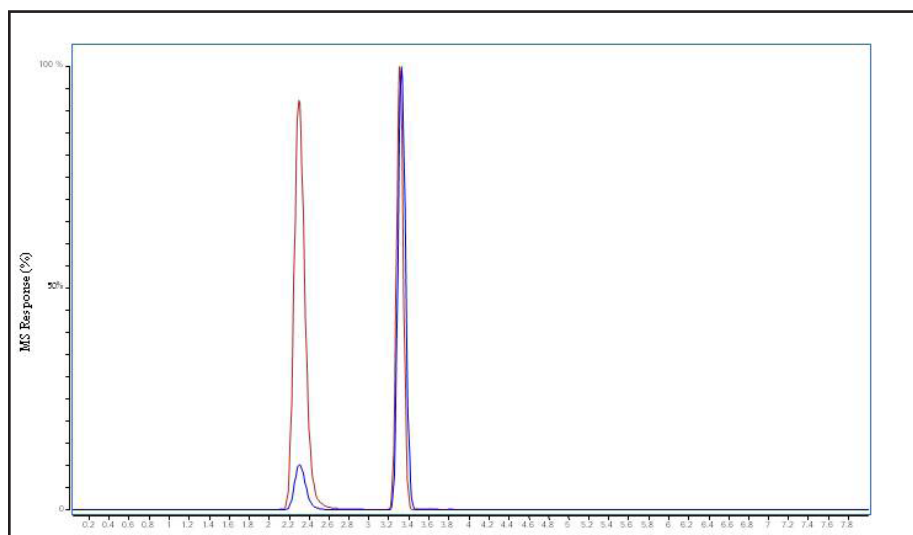


Figure 2, Burkard. Overlapped EIC chromatogram showing LC/MS screening of test compound 1 incubated with 0.02 μ M PfGR tested at 0, 0.1953125, 0.390625, 0.78125, 1.5625, 3.125, 6.25, 12.5, 25, 50, and 100 μ M. The blue line represents the reaction using the test compound. The red line represents a control reaction. The peaks on the left show product formation (GSH, m/z = 308.0911 [M+H]⁺). The peaks on the right show unused reactant in a saturated solution (GSSG, m/z = 307.5883 [M+H]²⁺).

Analyzing the Catalytic Role of a Conserved Active Site Residue in Cysteine Dioxygenase

Abigail K. Bartlett

Understanding the mechanisms of sulfur-metabolizing enzymes is important due to their vital role in the human body. Cysteine dioxygenase (CDO) is an iron-dependent enzyme that oxidizes cysteine to form cysteine sulfinic acid. This product serves as a branchpoint for the synthesis of taurine or pyruvate. CDO ensures that these two important compounds are produced in sufficient quantities to maintain metabolic function; it also prevents cysteine from reaching cytotoxic levels in the cell. The enzyme's active site is unique from others in its family due to the presence of a thioether crosslink between Cys93 and Tyr157. Results from prior research suggest that crosslinked CDO has increased cysteine oxidation activity compared to noncrosslinked CDO. Therefore, it is believed that the crosslink may play a critical role in catalysis. The involvement of neighboring amino acid residues in both crosslinking and oxidation activities may help explain the correlation. My project is specifically focused on evaluating the possible role of His155, a histidine residue near the crosslink region. Because histidine residues can be directly involved in catalytic events, this residue is thought to contribute to cysteine oxidation and may also participate in forming the crosslink before catalysis begins.

To date, my project has yielded further insight into the overall role of His155 in cysteine oxidation and crosslink formation. I have worked with the H155A variant, in which the histidine residue was substituted with alanine, which cannot participate in catalysis due to its structure. The research has included a variety of experiments intended to observe the effects of the alanine replacement on enzyme activity. The enzyme was expressed in *E. coli* and purified using ion exchange chromatography. I observed the overall folded shape of the variant with circular dichroism; purified H155A CDO showed similar secondary structural features as the wild-type enzyme. Because the crosslink makes CDO more compact, it is possible to identify the presence of the crosslink using gel electrophoresis. I incubated the variant in vitro with varying concentrations of L-cysteine and used electrophoresis to evaluate the results. The H155A variant can form the crosslink to some degree when exposed to L-cysteine, but shows less formation than wild-type CDO. I also used an oxygen electrode to determine the steady-state kinetic parameters of the enzyme; the variant does not oxidize cysteine as efficiently as wild-type CDO. These results indicate that His155 may be involved in forming the

crosslink – the variant cannot form the crosslink as efficiently and is not as catalytically active as the wild type.

The research focus of the group continues in several interesting directions. Further assays are being performed to analyze how H155A CDO behaves when exposed to L-cysteine analogs such as D-cysteine and cysteamine. In addition, a H155R CDO variant that replaces histidine with arginine is being constructed. The common characteristics between histidine and arginine, such as their size and basicity, make the substitution conservative – however, arginine has a much higher pKa, which will allow us to test the effect of reduced proton abstraction efficiency on the enzyme's overall function.

Statement of Research Advisor:

Abby's work has focused on evaluating the mechanistic properties of CDO, a mammalian enzyme involved in cysteine catabolism and linked to several disease states. The results from her studies have enhanced our overall understanding regarding a metabolic reaction critical to maintaining cellular function.
- Holly Ellis, *Chemistry and Biochemistry*

Factors Influencing the Frequency and Composition of Mammalian Carnivore Road Mortality

Forrest Cortes

Road mortality has been implicated as the most important transportation-related influence on wildlife populations (Grilo et al. 2012; Bateman and Fleming 2012). Some studies point to road mortality as a critical factor leading to localized extinction events of species such as the Eurasian badger (Lankester et al., 1991). As human expansion into rural areas continues and transportation networks grow, these effects will become more pronounced.

However, despite the strong evidence linking roadways to negative impacts on wildlife, knowledge about the distribution and composition of road mortality incidents is incomplete for many regions and landscapes. While studies have been conducted internationally and in some parts of the United States, there have been no studies that analyze the factors that influence road mortality in the pine-dominated landscapes of the Southeastern United States. Therefore the purpose of this study is to determine the species composition and distribution of mammalian carnivore road mortality in East-Central Alabama and to correlate mortality data with other data variables including speed limit, traffic volume, and distance to nearest vegetation.

In this study, we investigated the variables that contribute to the mortality of carnivores on the road. We drove predetermined routes along 2-lane and 4-lane roadways and counted roadkill carcasses within the shoulders of the road. Carcasses were identified to species, and geographic coordinates of carcass locations were loaded into GIS software for analysis.

Virginia opossum (*Didelphis virginiana*) and raccoon (*Procyon lotor*) carcasses made up approximately 80% of roadkill incidents on our sampled routes. Other recorded species included the nine-banded armadillo (*Dasypus novemcinctus*), gray fox (*Urocyon cinereoargenteus*), striped skunk (*Mephitis mephitis*), coyote (*Canis latrans*), and bobcat (*Lynx rufus*). Additionally, our results suggest that road kill sites were significantly closer to vegetation than randomly generated points. Specifically, our results indicate that with each 10-meter increase in distance toward vegetation, a site was 1.24 times as likely to be a road kill site; however, this research is still in progress. With data collection complete, we are in the process of analyzing the correlation of road mortality to speed limit, and traffic volume.

Results of this study may be used to better plan roadway expansions to mitigate wildlife-vehicle collisions. Utilization of results from the current study and those of other road mortality studies, may help planners to develop better ways to protect drivers, reduce costly vehicle damage, and minimize harm to proximate wildlife populations when expanding and creating roadways.

Statement of Research Advisor:

Forrest's project required him to drive roads to collect new data on the locations of road-killed mortality, extract data on the characteristics of road-kill and random sites using Google Earth, and collect existing data on road characteristics of sites from government agencies. The results of his study can be used to make recommendations for minimizing road-kill of carnivores here in Alabama, and potentially elsewhere.
- Todd D. Steury, Forestry and Wildlife

Water in Oil Microemulsion for Nanocomposite Particles and Its Application in Oral Drug Delivery

Colton Martinez and Xin Fan

The method of administering a drug orally has many benefits including noninvasiveness, painlessness, and ease of self-medication. However, while this method is typically preferable in drug administration, there are complications that limit the usage of oral drug delivery. These include complications such as chemical incompatibility within the drug particle and a lack of drug distribution in the blood stream through oral delivery. In an effort to remedy the complications found with oral drug delivery, nanocomposite particles, synthesized from silica and the polysaccharide alginate, are to be used to enhance the range of drugs that can be effectively administered orally.

Silica and alginate were chosen as the two primary components of the nanocomposite due to properties that each would contribute to the stability and chemical compatibility of the particle. Alginate provides mucoadhesive properties that prolong the drug residence time in the gastrointestinal tract as well as provide a means for controlled drug release. Silica provides the stability of the nanocomposite in the acidic environment of the stomach as well as a surface that can be easily modified for further specific targeted drug delivery.

These composite nanoparticles are synthesized using the sol-gel reaction occurring in a water in oil microemulsion. The microemulsion utilizes the thermodynamic stability created between the water and oil phases and the surface-active agent, the surfactant. The micelles that are formed serve as platforms for the encapsulation of the polysaccharide as the silica precursor, tetraethyl-orthosilicate (TEOS), undergoes condensation reactions to produce a silica network. Trials with differing weight ratios of alginate have produced monodisperse particles of nanosize diameter when viewed on a transmission electron microscope (TEM).

With the current alginate nanocomposite, drug uptake and release can be modeled using a fluorescent dye, Rhodamine-B, to simulate a drug. This fluorescent dye can be added to the microemulsion process and integrated into the nanocomposite utilizing the same sol-gel reaction. The drug release and uptake can then be measured using a dialysis tube and spectrofluorometer. Once the uptake and release of the simulated drug can be controlled using the nanocomposite, actual drugs are to be tested for potential use with the nanocomposite. The surface properties of the particles can also be modified through

silica reactions to help provide the particles with more specific targeting.

The results produced from the completed experiments show that a nanocomposite particle can be made from silica and alginate. Further testing is required to tune the drug uptake and release properties of the particles. Once the properties of the nanocomposite are fully determined, drugs can be explored for compatibility in an effort to enhance the administration of drugs orally.

Statement of Research Advisor:

Colton has assisted in the development of nanoparticles that are comprised of an inorganic and organic component, mixed on the nanoscale (i.e. a nanocomposite). This is not a trivial task and the results show promise for the development of novel drug formulations.
- *Allan E. David, Chemical Engineering*

The Effects of Auditory Training on Elderly Hearing Impaired Listeners with Cognitive Decline

Dianna Tingle and Caitlyn Piper

The purpose of this study was to determine if Elderly Hearing Impaired (EHI) listeners with and without cognitive decline show improvement in cognitive and auditory working memory tests after auditory training. Very little research has been conducted to study EHI listeners with and without cognitive decline and learning-induced plasticity on auditory function. As the rate of cognitive decline in the aging population in the United States increases, it becomes more urgent to find ways to assist these individuals's ability to function on a daily basis.

In this pilot study, specific listening tasks designed to improve peripheral and central auditory functioning in aging individuals with hearing loss and cognitive decline were used. Four subjects between the ages of 65 to 80 with bilateral sensorineural hearing loss who were previously diagnosed with moderate cognitive decline were tested for the pilot stage of this study. These subjects were recruited from the Arbor Springs Health and Rehabilitation Center in Opelika, Alabama. The degree of hearing loss was measured using a portable audiometer and a baseline was established for both auditory and cognitive tasks using Angel Sound™ software and several working memory

tasks. Each subject was trained according to his or her preliminary results using Angel Sound™ software over a four-week period (ten sessions).

Results during the post-intervention stage demonstrated that the auditory and cognitive training significantly impacted auditory working memory tests and somewhat impacted consonant recognition tests. This showed that auditory training does impact cognitive functioning over time. The results of the study support the view that the central auditory nervous system can be trained by means of specific listening tasks and may even have an impact on cognitive processing. This research is still in progress; the same testing methods and procedures are in use, but the subjects are different. Testing continues to solidify the previous conclusion regarding the improvement of cognitive functioning with auditory training.

This work shows that simple, thirty minute training sessions conducted twice a week can significantly impact the cognitive functioning and overall quality of life of these EHI patients. The Angel Sound™ software is free and simple to use, which would allow for easy utilization by health care workers working with these patients.

Statement of Research Advisor:

Dianna Tingle has completed her project titled, "The Effects of Auditory Training on Elderly Hearing Impaired Listeners with Cognitive Decline." Her research will be published in a peer-reviewed scientific journal. Research continues on the key topic relating to plasticity effects.

- Sridhar Krishnamurti,
Communication Disorders

Research Highlight References:

Please note references for all Research Highlights are available in our digital edition at: www.auburn.edu/undgres/currentvolume.php.

About the Authors



Katharyn Brennan is a recent Auburn graduate who received her B.S. in Animal Sciences from the College of Agriculture. While at Auburn, she was involved in research at the State Diagnostic Lab, and later joined Dr. Bartol's lab to work on the canine uterine development research study under the direction of Dr. Wilborn. She served as a College of Agriculture Ambassador for three semesters and volunteered with the Lee County Humane Society for three years. Currently, she works at the Mayo Clinic in Jacksonville, Florida, in the field of Ovarian Cancer Research and will attend medical school beginning in the Fall of 2015.

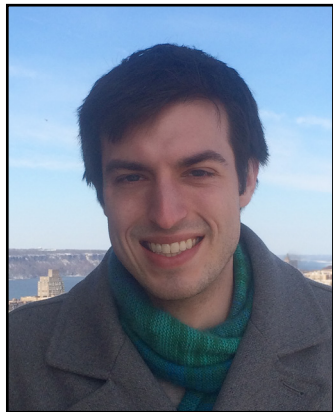


Andrew Clark is a senior at Auburn University pursuing a degree in Microbial Biology. His studies at Auburn led him to develop an interest in pathobiology. In Fall 2013, he began working as an undergraduate researcher in the lab of Dr. Peter Panizzi in the Harrison School of Pharmacy. With the help of the Auburn Cellular and Molecular Biology Fellowship and the Auburn Undergraduate Research Fellowship, he has studied the pathogenesis of *Staphylococcus aureus* infections and explored the development of novel methods of pathogen detection. He plans to enter medical school next fall and eventually hopes to work as a physician in academic medicine.



Ala Mansour is a senior pursuing two degrees in Biomedical Sciences and Health Services Administration. In addition to her veterinary biomedical research through the Auburn University Research Initiative in Cancer, she has also interned for two months at the Helmholtz Centre for Infection Research in Germany. She has given presentations and prepared her Honors Thesis on her research of multidrug resistance in canine and human lymphoid tumor cells. Fueled by her interests in medicine and healthcare, Ala is preparing to apply for medical school where she hopes to specialize in medical oncology and public health.

About the Authors



Ethan McCurdy began his research as an undergraduate at Auburn University. During this time, he worked in the laboratory of Douglas Goodwin, investigating the catalytic mechanism of the enzyme catalase-peroxidase, prominently known for its role in *Mycobacterium tuberculosis*. He majored in chemistry and graduated *summa cum laude* in 2014. During his senior year, he was awarded the Dean's Undergraduate Research Award for the College of Science and Mathematics. After graduating, Ethan began his PhD studies in the Department of Biochemistry and Molecular Biophysics at Columbia University, where he has begun to study the common signaling pathways that underlie neurodegenerative disorders such as Alzheimer's Disease and amyotrophic lateral sclerosis.



Robert Sanek has been interested in computing ever since learning HTML at age 13. Since then, he has started multiple profitable online businesses, assembled computers for local schools, and interned at SAIC in Huntsville, Ala. and Conductor in New York, N.Y. More recently, Robert worked with Dr. Orlando Acevedo on a parallelized program for modeling molecular interactions (MCGPU). Within technology, he is most excited about opportunities in investing, peer-to-peer networking, and decentralized trust. Robert will be graduating in May 2015 with a degree in Software Engineering and a minor in Finance; after graduation, he hopes to work at a leading software firm.

Call for Submissions

AUJUS

Auburn University Journal of Undergraduate Scholarship

WHAT?

The *Auburn University Journal of Undergraduate Scholarship (AUJUS)* is currently accepting submissions of full-length articles and short research highlights from Auburn University undergraduate students.

WHEN?

Articles may be submitted for review at any time during the year and will be published online as they are accepted.

To be considered for publication in the 2016 print version, articles and highlights must have completed the review and revision phases and been accepted by January 15, 2016.

Please note the review and revision process typically takes from 4 to 12 weeks from the time of submission until a final acceptance decision is made.

How?

More information about how to submit an article or highlight can be found by visiting www.auburn.edu/aujus or by emailing undgres@auburn.edu.



AUBURN
UNIVERSITY



AUBURN
UNIVERSITY

AUJUS

Auburn University Journal of Undergraduate Scholarship

Undergraduate Research
201 Cater Hall
Auburn, AL 36849

Research Article References

Medroxyprogesterone Acetate Reduced Cellular Proliferation of the Luminal and Glandular Epithelium in the Developing Canine Uterus

Katharyn Brennan, Robyn Wilborn, Meghan Davolt, Anne Wiley, Dori Miller, Paul Cooke, Aime Johnson, Bruce Smith, and Frank Bartol

Bartol, F. F., Wiley, A. A., Floyd, J. G., Ott, T. L., Bazer, F. W., Gray, C. A., & Spencer, T. E. (1999). Uterine differentiation as a foundation for subsequent fertility. *J Reprod Fertil Suppl*, 54, 287-302.

Beijerink, N. J., Bhatti, S. F. M., Okkens, A. C., Dieleman, S. J., Mol, J. A., Duchateau, L., Kooistra, H. S. (2007). Adenohypophyseal function in bitches treated with medroxyprogesterone acetate. *Domestic Animal Endocrinology*, 32(2), 63-78.

Cooke, P. S., Borsdorf, D. C., Ekman, G. C., Doty, K. F., Clark, S. G., Dziuk, P. J., & Bartol, F. F. (2012). Uterine gland development begins postnatally and is accompanied by estrogen and progesterone receptor expression in the dog. *Theriogenology*, 78(8), 1787-1795.

Cooke, P. S., Ekman, G. C., Kaur, J., Davila, J., Bagchi, I. C., Clark, S. G., Bartol, F. F. (2012). Brief Exposure to Progesterone During a Critical Neonatal Window Prevents Uterine Gland Formation in Mice. *Biology of Reproduction*, 86(3), 63, 61-10.

Fournier, A. K., & Geller, E. S. (2005). Behavior Analysis of Companion-Animal Overpopulation: A Conceptualization of the Problem and Suggestions for Intervention. *Behavior & Social Issues; Spring/Summer 2004*, 13(1), 51.

Gray, C. A., Bartol, F. F., Tarleton, B. J., Wiley, A. A., Johnson, G. A., Bazer, F. W., & Spencer, T. E. (2001). Developmental Biology of Uterine Glands. *Biology of Reproduction*, 65(5), 1311-1323.

Kutzler, M., & Wood, A. (2006). Non-surgical methods of contraception and sterilization. *Theriogenology*, 66(3), 514-525.

Olson, P. & Moulton, C. (1993). Pet (dog and cat) overpopulation. *Journal of Reproduction and Fertility*, 2013(47), 433-438.

Selman, P. J., Wolfswinkel, J., & Mol, J. A. (1996). Binding specificity of medroxyprogesterone acetate and proligestone for the progesterone and glucocorticoid receptor in the dog. *Steroids*, 61(3), 133-137.

Smith, D., Enever, R., Dey, M., Latta, D., & Weierstall, R. (1993). Pharmacokinetics and bioavailability of medroxyprogesterone acetate in the dog and the rat. *Biopharm Drug Dispos*, 14(4), 341-355.

Von Berky, A. G., & Townsend, W. L. (1993). The relationship between the prevalence of uterine lesions and the use of medroxyprogesterone acetate for canine population control. *Aust Vet J*, 70(7), 249-250.

Detection of Pathogens from Biopsy by Use of Sortase Activity

Andrew Clark, Jiansheng Huang, and Peter Panizzi

Baddour, L.M., Wilson, W.R., Bayer, A.S., Fowler Jr., V.G., Bolger, A.F., Levison, M.E., ... Taubert, K.A. (2005). Infective endocarditis: diagnosis, antimicrobial therapy, and management of complications: a statement for healthcare professionals from the Committee on Rheumatic Fever, Endocarditis, and Kawasaki Disease, Council on Cardiovascular Disease in the Young, and the Councils on Clinical Cardiology, Stroke, and Cardiovascular Surgery and Anesthesia, American Heart Association: endorsed by the Infectious Diseases Society of America. *Circulation*. 111(23), 394-434.

Bor, D.H., Woolhandler, S., Nardin, R., Bruschi, J., Himmelstein, D.U. (2013) Infective Endocarditis in the U.S., 1998–2009: A Nationwide Study. *PLoS ONE* 8(3), e60033. doi:10.1371/journal.pone.0060033

Cabell, C.H. & Fowler, V.G. (2004). Repeated echocardiography after the diagnosis of endocarditis: too much of a good thing? *Heart*. 90(9), 975-976.

Dantes, R. (2013). National Burden of Invasive Methicillin-Resistant *Staphylococcus aureus* Infections, United States, 2011. *Jama Internal Medicine*. 173(21), 1970-1978.

Kobashigawa, Y. (2009). Attachment of an NMR-invisible solubility enhancement tag using a sortase-mediated protein ligation method. *Journal of Biomolecular NMR*. 43(3), 145-50.

Maresso, A.W. & Schneewind, O. (2008). Sortase as a target of anti-infective therapy. *Pharmacology Reviews*. 60(1), 128-41.

Mazmanian, S.K. (2002). An iron-regulated sortase anchors a class of surface protein during *Staphylococcus aureus* pathogenesis. *Proceedings of the National Academy of Sciences USA*. 99(4), 2293-8.

Naik, M.T. (2006). *Staphylococcus aureus* Sortase A transpeptidase - Calcium promotes sorting signal binding by altering the mobility and structure of an active site loop. *Journal of Biological Chemistry*. 281(3), 1817-1826.

Pace, C.N. (1995). How to Measure and Predict the Molar Absorption-Coefficient of a Protein. *Protein Science*. 4(11), 2411-2423.

Panizzi, P. (2011). In vivo detection of *Staphylococcus aureus* endocarditis by targeting pathogen-specific prothrombin activation. *Nature Medicine*. 17(9), 1142-6.

Panizzi, P., Stone, J.R., and Nahrendorf, M. (2014). Endocarditis and molecular imaging. *Journal of Nuclear Cardiology*. 21(3), 486-495.

Spirig, T., Weiner, E.M., and Clubb, R.T. (2011). Sortase enzymes in Gram-positive bacteria. *Molecular Microbiology*. 82(5), 1044-59.

Stamatas, G.N., Southall, M., and Kollias, N. (2006). In vivo monitoring of cutaneous edema using spectral imaging in the visible and near infrared. *Journal of Investigative Dermatology*. 126(8), 1753-1760.

Diindolylmethane Inhibits the Activity of P-glycoprotein in 17-71 Canine B-Cell Lymphoid Tumor Cells

Ala Mansour, Kodye Abbott, Patrick Flannery, Elaine Coleman, Amit Tiwari, and Satyanarayana Pondugula

-
- Anderton, M. J., Manson, M. M., Verschoyle, R., Gescher, A., Steward, W. P., Williams, M. L., and Mager, D. E. (2004a). Physiological modeling of formulated and crystalline 3,3'-diindolylmethane pharmacokinetics following oral administration in mice. *Drug Metabolism & Disposition*, 32, 632-638.
- Anderton, M. J., Manson, M. M., Verschoyle, R. D., Gescher, A., Lamb, J. H., Farmer, P. B., . . . Williams, M. L. (2004b). Pharmacokinetics and tissue disposition of indole-3-carbinol and its acid condensation products after oral administration to mice. *Clinical Cancer Research*, 10, 5233-5241.
- Auborn, K. J. (2002). Therapy for recurrent respiratory papillomatosis. *Antiviral Therapy*, 7, 1-9.
- Azmi, A. S., Ahmad, A., Banerjee, S., Rangnekar, V. M., Mohammad, R. M., and Sarkar, F. H. (2008). Chemoprevention of pancreatic cancer: characterization of Par-4 and its modulation by 3,3' diindolylmethane (DIM). *Pharmaceutical Research*, 25, 2117-2124.
- Baer, M. R., George, S. L., Dodge, R. K., O'Loughlin, K. L., Minderman, H., Caligiuri, M. A., . . . Larson, R. A. (2002). Phase 3 study of the multidrug resistance modulator PSC-833 in previously untreated patients 60 years of age and older with acute myeloid leukemia: Cancer and Leukemia Group B Study 9720. *Blood*, 100, 1224-1232.
- Banco, B., Grieco, V., Servida, F., and Giudice, C. (2011). Sudden death in a dog after doxorubicin chemotherapy. *Veterinary Pathology*, 48, 1035-1037.
- Biersack, B., and Schobert, R. (2012). Indole compounds against breast cancer: recent developments. *Current Drug Targets*, 13, 1705-1719.
- Bonnesen, C., Eggleston, I. M., and Hayes, J. D. (2001). Dietary indoles and isothiocyanates that are generated from cruciferous vegetables can both stimulate apoptosis and confer protection against DNA damage in human colon cell lines. *Cancer Research*, 61, 6120-6130.
- Borst, P., Evers, R., Kool, M., and Wijnholds, J. (2000). A family of drug transporters: the multidrug resistance-associated proteins. *Journal of the National Cancer Institute*, 92, 1295-1302.
- Chen, D., Banerjee, S., Cui, Q. C., Kong, D., Sarkar, F. H., and Dou, Q. P. (2012). Activation of AMP-activated protein kinase by 3,3'-Diindolylmethane (DIM) is associated with human prostate cancer cell death in vitro and in vivo. *PloS One*, 7, e47186.
- Chen, T. (2010). Overcoming drug resistance by regulating nuclear receptors. *Advanced Drug Delivery Review*, 62, 1257-1264.
- Daenen, S., van der Holt, B., Verhoef, G. E., Lowenberg, B., Wijermans, P. W., Huijgens, P. C., . . . Sonneveld, P. (2004). Addition of cyclosporin A to the combination of mitoxantrone and etoposide to overcome resistance to chemotherapy in refractory or relapsing acute myeloid leukaemia: a randomised phase II trial from HOVON, the Dutch-Belgian Haemato-Oncology Working Group for adults. *Leukemia Research*, 28, 1057-1067.
- Dano, K. (1973). Active outward transport of daunomycin in resistant Ehrlich ascites tumor cells. *Biochimica et Biophysica Acta*, 323, 466-483.
- Dervisis, N. G., Dominguez, P. A., Sarbu, L., Newman, R. G., Cadile, C. D., Swanson, C. N., and Kitchell, B. E. (2007). Efficacy of temozolomide or dacarbazine in combination with an anthracycline for rescue chemotherapy in dogs with lymphoma. *Journal of the American Veterinary Medical Association*, 231, 563-569.

- Fahey, C. E., Milner, R. J., Barabas, K., Lurie, D., Kow, K., Parfitt, S., . . . Clemente, M. (2011). Evaluation of the University of Florida lomustine, vincristine, procarbazine, and prednisone chemotherapy protocol for the treatment of relapsed lymphoma in dogs: 33 cases. (2003-2009). *Journal of the American Veterinary Medical Association*, 239, 209-215.
- Fan, S., Meng, Q., Saha, T., Sarkar, F. H., and Rosen, E. M. (2009). Low concentrations of diindolylmethane, a metabolite of indole-3-carbinol, protect against oxidative stress in a BRCA1-dependent manner. *Cancer Research*, 69, 6083-6091.
- Fan, T. M. (2003). Lymphoma updates. *The Veterinary Clinics of North America: Small Animal Practice*, 33, 455-471.
- Flory, A. B., Rassnick, K. M., Al-Sarraf, R., Bailey, D. B., Balkman, C. E., Kiselow, M. A., and Autio, K. (2008). Combination of CCNU and DTIC chemotherapy for treatment of resistant lymphoma in dogs. *Journal of Veterinary Internal Medicine / American College of Veterinary Internal Medicine*, 22, 164-171.
- Fox, E., and Bates, S. E. (2007). Tariquidar (XR9576): a P-glycoprotein drug efflux pump inhibitor. *Expert Review of Anticancer Therapy*, 7, 447-459.
- Gelsomino, G., Corsetto, P. A., Campia, I., Montorfano, G., Kopecka, J., Castella, B., . . . Riganti, C. (2013). Omega 3 fatty acids chemosensitize multidrug resistant colon cancer cells by down-regulating cholesterol synthesis and altering detergent resistant membranes composition. *Molecular Cancer*, 12, 137.
- Greger, D. L., Gropp, F., Morel, C., Sauter, S., and Blum, J. W. (2006). Nuclear receptor and target gene mRNA abundance in duodenum and colon of dogs with chronic enteropathies. *Domestic Animal Endocrinology*, 31, 327-339.
- Griessmayr, P. C., Payne, S. E., Winter, J. E., Barber, L. G., and Shofer, F. S. (2009). Dacarbazine as single-agent therapy for relapsed lymphoma in dogs. *Journal of Veterinary Internal Medicine / American College of Veterinary Internal Medicine*, 23, 1227-1231.
- Gropp, F. N., Greger, D. L., Morel, C., Sauter, S., and Blum, J. W. (2006). Nuclear receptor and nuclear receptor target gene messenger ribonucleic acid levels at different sites of the gastrointestinal tract and in liver of healthy dogs. *Journal of Animal Science*, 84, 2684-2691.
- Harmsen, S., Meijerman, I., Febus, C. L., Maas-Bakker, R. F., Beijnen, J. H., and Schellens, J. H. (2010). PXR-mediated induction of P-glycoprotein by anticancer drugs in a human colon adenocarcinoma-derived cell line. *Cancer Chemotherapy and Pharmacology*, 66, 765-771.
- Ishikawa, Y., Nagai, J., Okada, Y., Sato, K., Yumoto, R., and Takano, M. (2010). Function and expression of ATP-binding cassette transporters in cultured human Y79 retinoblastoma cells. *Biological & Pharmaceutical Bulletin*, 33, 504-511.
- Jamadar-Shroff, V., Papich, M. G., and Suter, S. E. (2009). Soy-derived isoflavones inhibit the growth of canine lymphoid cell lines. *Clinical Cancer Research*, 15, 1269-1276.
- Keller, R. P., Altermatt, H. J., Nooter, K., Poschmann, G., Laissue, J. A., Bollinger, P., and Hiestand, P. C. (1992). SDZ PSC 833, a non-immunosuppressive cyclosporine: its potency in overcoming P-glycoprotein-mediated multidrug resistance of murine leukemia. *International Journal of Cancer / Journal International du Cancer*, 50, 593-597.
- Kojima, K., Fujino, Y., Goto-Koshino, Y., Ohno, K., and Tsujimoto, H. (2013). Analyses on Activation of NF-kappaB and Effect of Bortezomib in Canine Neoplastic Lymphoid Cell Lines. *The Journal of Veterinary Medical Science / the Japanese Society of Veterinary Science*, 75, 727-731.
- Kolitz, J. E., George, S. L., Dodge, R. K., Hurd, D. D., Powell, B. L., Allen, S. L., . . . Cancer and Leukemia Group B. (2004). Dose escalation studies of cytarabine, daunorubicin, and etoposide with and without multidrug resistance modulation with PSC-833 in untreated adults with acute myeloid leukemia younger than 60 years: final induction results of Cancer and Leukemia Group B Study 9621. *Journal of Clinical Oncology*, 22, 4290-4301.

- Kuan, C. Y., Walker, T. H., Luo, P. G., and Chen, C. F. (2011). Long-chain polyunsaturated fatty acids promote paclitaxel cytotoxicity via inhibition of the MDR1 gene in the human colon cancer Caco-2 cell line. *Journal of the American College of Nutrition*, 30, 265-273.
- Lee, J. J., Hughes, C. S., Fine, R. L., and Page, R. L. (1996). P-glycoprotein expression in canine lymphoma: a relevant, intermediate model of multidrug resistance. *Cancer*, 77, 1892-1898.
- Lori, J. C., Stein, T. J., and Thamm, D. H. (2010). Doxorubicin and cyclophosphamide for the treatment of canine lymphoma: a randomized, placebo-controlled study. *Veterinary and Comparative Oncology*, 8, 188-195.
- Lymphoma. (n. d.). *National Canine Cancer Foundation*. Retrieved from <http://www.wearethecure.org/lymphoma>
- MacDonald, V. (2009). Chemotherapy: managing side effects and safe handling. *The Canadian Veterinary Journal / La Revue Veterinaire Canadienne*, 50, 665-668.
- Marzac, C., Garrido, E., Tang, R., Fava, F., Hirsch, P., De Benedictis, C., . . . Legrand, O. (2011). ATP Binding Cassette transporters associated with chemoresistance: transcriptional profiling in extreme cohorts and their prognostic impact in a cohort of 281 acute myeloid leukemia patients. *Haematologica*, 96, 1293-1301.
- Matsuda, A., Tanaka, A., Muto, S., Ohmori, K., Furusaka, T., Jung, K., . . . Matsuda, H. (2010). A novel NF-kappaB inhibitor improves glucocorticoid sensitivity of canine neoplastic lymphoid cells by up-regulating expression of glucocorticoid receptors. *Research in Veterinary Science*, 89, 378-382.
- Meuten, J. D. (Ed.) (2002). Tumors in domestic animals (4th ed.). Ames, Iowa: Iowa State Press.
- Moiseeva, E. P., Almeida, G. M., Jones, G. D., and Manson, M. M. (2007). Extended treatment with physiologic concentrations of dietary phytochemicals results in altered gene expression, reduced growth, and apoptosis of cancer cells. *Molecular Cancer Therapeutics*, 6, 3071-3079.
- Moore, A. S., Leveille, C. R., Reimann, K. A., Shu, H., and Arias, I. M. (1995). The expression of P-glycoprotein in canine lymphoma and its association with multidrug resistance. *Cancer Investigation*, 13, 475-479.
- Moore, A. S., London, C. A., Wood, C. A., Williams, L. E., Cotter, S. M., L'Heureux, D. A., and Frimberger, A. E. (1999). Lomustine (CCNU) for the treatment of resistant lymphoma in dogs. *Journal of Veterinary Internal Medicine / American College of Veterinary Internal Medicine*, 13, 395-398.
- Northrup, N. C., Gieger, T. L., Kosarek, C. E., Saba, C. F., LeRoy, B. E., Wall, T. M., . . . Keys, D. A. (2009). Mechlorethamine, procarbazine and prednisone for the treatment of resistant lymphoma in dogs. *Veterinary and Comparative Oncology*, 7, 38-44.
- Okamura N., Sakaeda, T., Okumura, K. (2004). Pharmacogenomics of MDR and MRP subfamilies. *Personalized Medicine*, 1, 85-104.
- Pondugula, S. R., and Mani, S. (2013). Pregnane xenobiotic receptor in cancer pathogenesis and therapeutic response. *Cancer Letters*, 328, 1-9.
- Pondugula, S. R., Tong, A. A., Wu, J., Cui, J., and Chen, T. (2010). Protein phosphatase 2Cbeta1 regulates human pregnane X receptor-mediated CYP3A4 gene expression in HepG2 liver carcinoma cells. *Drug Metabolism and Disposition*, 38, 1411-1416.
- Rahman, M. M., Veigas, J. M., Williams, P. J., and Fernandes, G. (2013). DHA is a more potent inhibitor of breast cancer metastasis to bone and related osteolysis than EPA. *Breast Cancer Research and Treatment*, 141, 341-352.
- Rassnick, K. M., Mauldin, G. E., Al-Sarraf, R., Mauldin, G. N., Moore, A. S., and Mooney, S. C. (2002). MOPP chemotherapy for treatment of resistant lymphoma in dogs: a retrospective study of 117 cases (1989-2000). *Journal of Veterinary Internal Medicine / American College of Veterinary Internal Medicine*, 16, 576-580.

- Rebhun, R. B., Kent, M. S., Borrofska, S. A., Frazier, S., Skorupski, K., and Rodriguez, C. O. (2011). CHOP chemotherapy for the treatment of canine multicentric T-cell lymphoma. *Veterinary and Comparative Oncology*, 9, 38-44.
- Reed, G. A., Arneson, D. W., Putnam, W. C., Smith, H. J., Gray, J. C., Sullivan, D. K., . . . Hurwitz, A. (2006). Single-dose and multiple-dose administration of indole-3-carbinol to women: pharmacokinetics based on 3,3'-diindolylmethane. *Cancer Epidemiology, Biomarkers & Prevention : a Publication of the American Association for Cancer Research, cosponsored by the American Society of Preventive Oncology*, 15, 2477-2481.
- Reed, G. A., Sunega, J. M., Sullivan, D. K., Gray, J. C., Mayo, M. S., Crowell, J. A., and Hurwitz, A. (2008). Single-dose pharmacokinetics and tolerability of absorption-enhanced 3,3'-diindolylmethane in healthy subjects. *Cancer Epidemiology, Biomarkers & Prevention : a Publication of the American Association for Cancer Research, cosponsored by the American Society of Preventive Oncology*, 17, 2619-2624.
- Ruslander, D. A., Gebhard, D. H., Tompkins, M. B., Grindem, C. B., and Page, R. L. (1997). Immunophenotypic characterization of canine lymphoproliferative disorders. *In Vivo*, 11, 169-172.
- Sharom, F. J. (2008). ABC multidrug transporters: structure, function and role in chemoresistance. *Pharmacogenomics*, 9, 105-127.
- Sodani, K., Patel, A., Kathawala, R. J., and Chen, Z. (2012). Multidrug resistance associated proteins in multidrug resistance. *Chinese Journal of Cancer*, 31, 58-72.
- Spande, T. (1979). Hydroxyindoles, Indoles, Alcohols and Indolethiols. In W. J. Houlihan (Ed.), *Indoles* (pp. 1-355) New York, NY: John Wiley & Sons, Inc.
- Steingold, S. F., Sharp, N. J., McGahan, M. C., Hughes, C. S., Dunn, S. E., and Page, R. L. (1998). Characterization of canine MDR1 mRNA: its abundance in drug resistant cell lines and in vivo. *Anticancer Research*, 18, 393-400.
- Stresser, D. M., Williams, D. E., Griffin, D. A., and Bailey, G. S. (1995). Mechanisms of tumor modulation by indole-3-carbinol. Disposition and excretion in male Fischer 344 rats. *Drug Metabolism and Disposition*, 23, 965-975.
- Thomas, H., and Coley, H. M. (2003). Overcoming multidrug resistance in cancer: an update on the clinical strategy of inhibiting p-glycoprotein. *Cancer Control : Journal of the Moffitt Cancer Center*, 10, 159-165.
- Tsuruo, T., Iida, H., Tsukagoshi, S., and Sakurai, Y. (1981). Overcoming of vincristine resistance in P388 leukemia in vivo and in vitro through enhanced cytotoxicity of vincristine and vinblastine by verapamil. *Cancer Research*, 41, 1967-1972.
- Uozurmi, K., Nakaichi, M., Yamamoto, Y., Une, S., and Taura, Y. (2005). Development of multidrug resistance in a canine lymphoma cell line. *Research in Veterinary Science*, 78, 217-224.
- Wiatrak, B. J. (2003). Overview of recurrent respiratory papillomatosis. *Current Opinion in Otolaryngology & Head and Neck Surgery*, 11, 433-441.
- Zandvliet, M., Teske, E., Chapuis, T., Fink-Gremmels, J., and Schrickx, J. A. (2013). Masitinib reverses doxorubicin resistance in canine lymphoid cells by inhibiting the function of P-glycoprotein. *Journal of Veterinary Pharmacology and Therapeutics*, 36, 583-587.

Evaluating the Novel Role of Tryptophan 438 in Active Turnover of *Mycobacterium tuberculosis* Catalase-Peroxidase

Ethan McCurdy, Lauren Barr, Olive Njuma, Elizabeth Ndontsa, and Douglas Goodwin

Bandyopadhyay, P. & Steinman, H.M. (2000). Catalase-peroxidases of *Legionella pneumophila*: Cloning of the *kata* gene and studies of KatA function. *Journal of Bacteriology*, 182 (23), 6679-6686.

Brunner, W., Schmidt, H., & Karch, H. (1996). KatP, a novel catalase-peroxidase encoded by the large plasmid of enterohaemorrhagic *Escherichia coli* O157:H7. *Microbiology*, 142 (11), 3305-3315.

Carpena, X., Wiseman, B., Deemagarn, T., Herguedas, B., Ivancich, A., Singh, R., Loewen, P.C., & Fita, I. (2006). Roles for Arg426 and Trp111 in the modulation of NADH oxidase activity of the catalase-peroxidase KatG from *Burkholderia pseudomallei* inferred from pH-induced structural changes. *Biochemistry*, 45, 5171-5179.

Garcia, E., Nedialkov, Y.A., Elliott, J., Motin, V.L., & Brubaker, R.R. (1999). Molecular characterization of KatY (Antigen 5), a thermoregulated chromosomally encoded catalase-peroxidase of *Yersinia pestis*. *Journal of Bacteriology*, 181 (10), 3114-3122.

Jagielski, T., Grzeszczuk, M., Kaminski, M., Roeske, K., Napiorkowska, A., Stachowiak, R., Augustynowicz-Kopec, E., Zwolska, Z., & Bielecki, J. (2013). Identification and analysis of mutations in the *katG* gene in multidrug-resistant *Mycobacterium tuberculosis* clinical isolates. *Pneumonologia i Alergologia Polska*, 81, 298-307.

Moore, R.L., Powell, L.J., & Goodwin, D.C. (2008). The kinetic properties producing the perfunctory pH profiles of catalase-peroxidases. *Biochimica et Biophysica Acta*, 1784 (6), 900-907.

Ndontsa, E.N., Moore, R.L., & Goodwin, D.C. (2012). Stimulation of KatG catalase activity by peroxidatic electron donors. *Archives of Biochemistry and Biophysics*, 525 (2), 215-222.

Nelson, D.P., & Kiesow, L.A. (1972). Enthalpy of decomposition of hydrogen peroxide by catalase at 25° C (with molar extinction coefficients of H₂O₂ solutions in the UV). *Analytical Biochemistry*, 49 (2), 474-478.

Njuma, O.J., Ndontsa, E.N., & Goodwin, D.C. (2014). Catalase in peroxidase clothing: Interdependent cooperation of two cofactors in the catalytic versatility of KatG. *Archives of Biochemistry and Biophysics*, 544, 27-39.

Scott, S.L., Chen, W.-J., Bakac, A., & Espenson, J.H. (1993). Spectroscopic parameters, electrode potentials, acid ionization constants, and electron exchange rates of the 2,2'-azinobis(3-ethylbenzothiazoline-6-sulfonate) radicals and ions. *Journal of Physical Chemistry*, 97 (25), 6710-6714.

Varnado, C.L., & Goodwin, D.C. (2004). System for the expression of recombinant hemoproteins in *Escherichia coli*. *Protein Expression and Purification*, 35 (1), 76-83.

Wang, Y. & Goodwin, D.C. (2013). Integral role of the I'-helix in the function of the "inactive" C-terminal domain of catalase-peroxidase (KatG). *Biochimica et Biophysica Acta*, 1834 (1), 362-371.

World Health Organization (2013). Global tuberculosis report 2013.

Yamada, Y., Fujiwara, T., Sato, T., Igarashi, N., & Tanaka, N. (2002). The 2.0 Å crystal structure of catalase-peroxidase from *Haloarcula marismortui*. *Nature Structural Biology*, 9 (9), 691-695.

Zhao, X., Yu, H., Yu, S., Wang, F., Sacchettini, J.C., & Magliozzo, R. S. (2006). Hydrogen peroxide-mediated isoniazid activation catalyzed by *Mycobacterium tuberculosis* catalase-peroxidase (KatG) and its S315T mutant. *Biochemistry*, 45, 4131-4140.

Zhao, X., Khajo, A., Jarrett, S., Suarez, J., Levitsky, Y., Burger, R. M., Jarzecki, A. A., & Magliozzo, R. S. (2012). Specific function of the Met-Tyr-Trp adduct radical and residues Arg-418 and Asp-137 in the atypical catalase reaction of catalase-peroxidase KatG. *Journal of Biological Chemistry*, 287 (44), 37057-37065.

Password Storage in Databases: Best Practices

Robert Sanek

Biham, E., Chen, R., Joux, A., Carribault, P., Lemuet, C., & Jalby, W. (2005, January 1). Collisions of SHA-0 and Reduced SHA-1. *Advances in Cryptology – EUROCRYPT 2005*, 3494 (2005), 36-57.

Cryptographic hash function. (n.d.). In *Wikipedia*. Retrieved December 3, 2013 from https://en.wikipedia.org/wiki/Cryptographic_hash_function

Federal Information Processing Standards (2002, August 1). Publication 180-2.

Findkle, J. & Saba, J (2012, June 6). LinkedIn suffers data breach - security experts. Retrieved December 3, 2013 from <http://in.reuters.com/article/2012/06/06/linkedin-breach-idINDEE8550EN20120606>

John the Ripper benchmarks. (2013, December 3). Retrieved December 3, 2013 from <http://openwall.info/wiki/john/benchmarks>

Kaliski, B. (2000, September 1). PKCS #5: Password-Based Cryptography Specification. Retrieved December 3, 2013 from <http://www.ietf.org/rfc/rfc2898.txt>

Munroe, R. (2011, August 1). Password Strength. Retrieved January 23, 2015.

Pornin, T. (2011, August 19). Do any security experts recommend bcrypt for password storage? Retrieved December 3, 2013 from <http://security.stackexchange.com/q/4781>

Provos, N., & Mazieres, D. (1999, June 6). A Future-Adaptable Password Scheme. *Proceedings of 1999 USENIX Annual Technical Conference*.

Rivest, R. (1992, April 1). The MD5 message digest algorithm.

Waugh, R. (2012, July 16). No wonder hackers have it easy: Most of us now have 26 different online accounts - but only five passwords. Retrieved December 3, 2013 from <http://www.dailymail.co.uk/sciencetech/article-2174274/No-wonder-hackers-easy-Most-26-different-online-accounts--passwords.html>

Research Highlights References

Enactment as Rhetorical Strategy in America's Most Effective Literary Journalism

Gabrielle Bates Stahlman

White, James B. (2002). Human Dignity and the Claim of Meaning: Athenian Tragic Drama and Supreme Court Opinions. *Journal of Supreme Court History*, 27 (1): 45-64.

Gutkind, Lee. (1997). *The Art of Creative Nonfiction: Writing and Selling the Literature of Reality*. New York: Wiley. 8.

Factors Influencing the Frequency and Composition of Mammalian Carnivore Road Mortality

Forrest Cortes

Bateman, P.W., and Fleming, P.A., 2012. Big city life: carnivores in urban environments. *J. Zoology* 287, 1-23.

Grilo, C., Ascensao, F., Bernardo, J., Costa, M., Leitao, I., Lourenco, R., Matos, H., Pinheiro, P., Reto, D., Revilla, E., Santos-Reis, M., and Sousa J., 2012. Individual spatial responses towards roads: implications for mortality risk. *PLoS ONE* 7(9).

Lankester, K., Van Apeldoorn, R., Meelis, E., Verboom, J., 1991. Management perspectives for populations of the Eurasian badger (*Meles meles*) in a fragmented landscape. *J. Appl. Ecology* 28, 561-573.

Identifying the Mechanism of Resistance to ALS-Inhibiting Herbicides in *Euphorbia maculate* (L.)

Tyler B. Miller, Shu Chen, and Patrick McCullough

Duran Prado, M., De Prado, R., & Franco, A. R. (2004). Design and optimization of degenerated universal primers for the cloning of the plant acetolactate synthase conserved domains. *Weed Science*, 52, 487-491.

Porebski S., Bailey, L., & Baum, B.(1997, March). Modification of a CTAB DNA extraction protocol for plants. *Plant Molecular Biology Reporter*, 15(1), 8-15. Retrieved from <http://link.springer.com/article/10.1007/BF02772108>.

Ray, T. B. (1984). Site of Action of Chlorsulfuron. *Plant Physiology*, 75(3), 827-831.

Umbarger, H E. (1978). Amino acid biosynthesis and its regulation. *Annual Review of Biochemistry*, 47, 532-606.

From Dahrar to Déorwine: Examining Tolkien's Interpretation of Sound Symbolism

Matthew Pollock

Holland, Morris, and Michael Wertheimer. "Some Physiognomic Aspects Of Naming, Or, Maluma And Takete Revisited." *Perceptual And Motor Skills* 19 (1964): 111-17. Ammons Scientific LTD. Web. 28 Nov. 2014.

Tolkien, J. R. R., "A Secret Vice." *The Monster and the Critics and Other Essays*. Ed. Christopher Tolkien, pp. 198-223. London: George Allen and Unwin, 1983. Print.

Maternal Diet and Its Impact on the Gut and Milk Microbiota

Nikki Wyatt

David, L. A., Maurice, C. F., Carmody, R. N., Gootenberg, D. B., Button, J. E., Wolfe, B. E., . . .

Turnbaugh, P. J. (2014). Diet rapidly and reproducibly alters the human gut microbiome. *Nature*, 505, 559-563. doi:10.1038/nature12820

Derrickson, E. M., & Lowas, S. R. (2007). The effects of dietary protein levels on milk protein levels and postnatal growth in laboratory mice (*Mus musculus*). *Journal of Mammalogy*, 88 (6), 1475-1481. <http://dx.doi.org/10.1644/06-MAMM-A-253R2.1>

Donnet-Hughes, A., Perez, P. F., Doré, J., Leclerc, M., Levenez, F., Benyacoub, J., . . . E.J., S (2010). Potential role of the intestinal microbiota of the mother in neonatal immune education. *Proceedings of the Nutrition Society*, 69(3), 407-415. doi:10.1017/S0029665110001898

Hantsis-Zacharov, E., & Halpern, M (2007). Culturable psychrotrophic bacterial communities in raw milk and their Proteolytic and lipolytic traits. *Applied and Environmental Microbiology*, 73(22), 7162-7168. doi:10.1128/AEM.00866-07

Perez, P.F., Dore, J., Leclerc, M., Levenez, F., Benyacoub, J., Serrant, P., . . . Donnet-Hughes, A. (2007). Bacterial imprinting of the neonatal immune system: lessons from maternal cells? *Pediatrics*, 119(3), e724-e732. doi:10.1542/peds.2006-1649

Smith, K., McCoy, K. D., & Macpherson, A. J. (2007). Use of axenic animals in studying the adaptation of mammals to their commensal intestinal microbiota. *Seminars in Immunology*, 19(2), 59-69. doi:10.1016/j.smim.2006.10.002

Urbaniak, C., Cummings, J., Brackstone, M., Jean, M. M., Gloor, G. B., Baban, C. K., . . . Reid, G. (2014). Microbiota of human breast tissue. *Applied and Environmental Microbiology*, 80, 3007-3014. doi:10.1128/AEM.00242-14

Ward, T., Hosid, S., Ioshikhes, I., & Altosaar, I. (2013). Human milk metagenome: a functional capacity analysis. *BMC Microbiology*, 13, 116. doi:10.1186/1471-2180-13-116